Microplastic in subsurface water in the South Pacific Ocean

An investigation of particle number, size, polymer type, and shape of microplastics

By

Madelen Hegrestad

Master of Science in Marine Biology

Department of Biological Sciences

University of Bergen

Spring 2023

Supervisors: Alessio Gomiero (NORCE), Bjørn Einar Grøsvik (Institute of Marine Research), and Odd André Karlsen (Department of Biological Sciences, University of Bergen)

Acknowledgments

First, I would like to thank my supervisors Bjørn Einar Grøsvik at IMR, Alessio Gomiero at NORCE, and Odd Andre Karlsen at UiB for their support and guidance throughout this project. Delays in the data post-processing have been a test of patience for me, but you have always been positive and motivating.

Thanks to André Marcel Bienfait and Mats Huserbråten for helping me with the instrumental analysis, Agnethe Hertzberg for assisting me at the laboratory with all the unexpected challenges that comes up when working on a new method, and Vidar Lien for helping me with the oceanographic models.

Thanks to Crown Prince Haakon for showing interest in microplastic research and letting me discuss my thesis. Thanks to the staff at Statsraad Lehmkuhl for always helping us when we had challenges with the microplastic sampling.

In addition, I would like to thank my partner for putting up with me throughout the process and always supporting me. Thanks to all my classmates for sharing frustrations through the work with our thesis, long coffee breaks, and for making the days at the study hall a little better. Finally, I would like to thank my family for their support in every step of my life.

Bergen, June 2023

Madelen Hegrestad

Abstract

Microplastic (MP) in the world's oceans is a global concern. Studies on MP are frequently published, but there is limited information on MP in the South Pacific Ocean. Here, a seawater filtration unit collected MPs down to 20 μm in size on an 11 000 km transect from Chile to Fiji in the South Pacific Ocean. Data on MP occurrence in this region is important to validate oceanographic models for the transport and fate of MPs. Two different analysis instruments were used for the quantification and characterisation of MPs. Previous studies have emphasised the significant influence of sampling methods on the quantified levels of environmental MP. However, this study goes beyond that and sheds light on the substantial impact of different analysing instruments on both the quantification and characterisation of MPs. The mean MP concentration across the whole transect was 3564 ± 2374 MP m^{-3} using a QCL-IR instrument, while a μ-FTIR instrument found the mean MP concentration to be 166 ± 85 MP m^{-3}. Higher concentrations were found in the South Pacific subtropical gyre. For the first time, MP particles down to 20 μm in size are documented in the South Pacific. The particle size is crucial in determining effects on marine organisms, as higher toxicity is reported for smaller sizes. An overwhelming majority (98%) of all identified MPs were smaller than 300 μm, emphasising the importance of studying this smaller size range. μ-FTIR identified polypropylene (55%) as the dominant polymer, and QCL-IR identified polyethylene (64%) as the dominant polymer, while both instruments identified fragments as the most dominating morphology of the MP particles. The comparison of the two different analysis instruments in this study is a first step towards harmonisation and standardisation of MP monitoring at two laboratories in Norway. Standardised or harmonised quantification of marine MP levels is essential to assess changes over time and evaluate success of plastic waste management.

List of abbreviations

AI	Artificial intelligence
ER	Epoxy resin
EPS	Expanded polystyrene
FTIR	(μ - micro) Fourier transform infrared spectrometers
MP	Microplastic
PA	Polyamide
PC	Polycarbonate
PE	Polyethylene
PEEK	Polyether ether ketone
PES	Polyester
PET	Polyethylene Terephthalate
PP	Polypropylene
PS	Polystyrene
PUR	Polyurethane
PVC	Polyvinyl chloride
SPSG	South Pacific subtropical gyre
QCL – IR	Quantum cascade laser – infrared spectroscopy

Table of Contents

1 Introduction

Marine plastic litter is currently considered one of the most important global environmental issues of our time (Barnes et al., 2009; Cózar et al., 2014). It has been estimated that 19 to 23 million metric tons of plastic waste generated globally in 2016 entered the marine environment. By 2030, it is estimated that annual emissions may reach up to 53 million metric tons (Borrelle et al., 2020). All large plastic items released into the environment will eventually degrade into microplastic (MP) (< 5 mm) due to photochemical and physical processes. MPs are ubiquitous, occurring in all compartments of the ocean worldwide, including remote areas such as the Arctic and Antarctic (Bergmann et al., 2022; Cincinelli et al., 2017; Lusher et al., 2015), and have a variety of adverse environmental effects on marine ecosystems (Van Sebille et al., 2020). It is essential to characterise MPs and track the temporal and geographic distribution of MP in the aquatic environment to evaluate plastic contamination, identify hot spots, and characterise the risk of exposure for marine organisms.

This master project has, for the first time in the South Pacific, monitored MP distribution using a large-volume water pump unit with a filtration device for MP installed at the seawater intake, enabling the identification of plastic particles down to 20 µm in size. Sampling was performed during the One Ocean Expedition, a circumnavigation by the tall ship S/S Statsraad Lehmkuhl from August 2021 to April 2023 with the ambition to create attention and share knowledge about the crucial role of the world's oceans (https://oneoceanexpedition.com/no/one-ocean-expedition). This chapter will highlight the complexities of MP and MP research, as well as the challenges and aims of this study.

1.1 Microplastic Characteristics and Degradation

MPs show a large variety of characteristics, including polymer type, chemicals, size, shape, density and colour, all of which influence their potential threats to the ecosystem (Chubarenko et al., 2016; Lehtiniemi et al., 2018). The market is mainly dominated by six classes of plastic polymers: polyethylene (PE, high and low density), polypropylene (PP), polyvinyl chloride (PVC), polystyrene (PS, including expanded EPS), polyurethane (PUR), and polyethylene terephthalate (PET) (Plastics-Europe, 2022). The plastic particle does not only consist of the polymer itself, but also chemicals, such as polybrominated diphenyl ethers, and plasticizers

(e.g. phthalates) are added to the polymers to enhance their quality of being more durable, lightweight, flexible etc. (Evenset et al., 2009; Rudel et al., 2003). MP is commonly defined as smaller than 5 mm in size to include the conventional virgin plastic pellets with 1 – 5 mm in diameter. Still, some researchers also use a smaller size to define MP (Andrady, 2011). MP is either primary MP (made intentionally, like pellets or microbeads) or secondary MP (fragmented parts of larger objects) (Kershaw, 2015). Their shape is normally classified as fragments, pellets, films, or fibres.

The longevity of plastics is estimated to be hundreds or thousands of years, depending on polymer type, additive composition, and environmental factors (Barnes et al., 2009). Environmental weathering causes the breakdown of plastic due to biological and/or abiotic processes. Abiotic plastic degradation can be caused by factors such as light, temperature, air, water, and mechanical forces. Light (mainly UV-B and UV-A) is considered the most important process that initiates plastic degradation (K. Liu et al., 2019). Organisms can induce biotic degradation of plastics by biting, chewing, or digestive fragmentation (gut enzymatic processes and/or intestinal microbiome) (Cassone et al., 2020; Dawson et al., 2018). Microorganisms forming biofilms can also cause biodegradation. While light degradation is mainly responsible for the initial degradation of plastics floating on the surface of seawater, biodegradation may play a more important role once the plastic surface is covered with a biofilm (Khoironi et al., 2020).

1.2 Impact on Marine Ecosystems

The adverse effects of plastic exposure on marine organisms were recently reviewed by Manzoor et al. (2021). Different trophic-level benthic and pelagic organisms deliberately or unintentionally consume MP, which has been demonstrated in invertebrates, fish, birds, turtles, and mammals (Browne et al., 2013; Chastel et al., 2005; Duncan et al., 2019; Graham & Thompson, 2009; Grøsvik et al., 2022; Neumann et al., 2021; Rebolledo et al., 2013; Setälä et al., 2016). Ingestion is the most likely interaction between marine organisms and MP. Ingestion of MP by lower trophic levels might be a pathway into the food chain (Bhattacharya et al., 2010), potentially also ending up in humans. A study by Farrell and Nelson (2013) investigated the trophic transfer of MP from mussels to crabs, where microspheres were found in hemolymph, stomach, hepatopancreas, ovary, and gills of crabs (*Carcinus maenas*) eating blue mussels exposed to MPs.

Different studies have investigated which characteristics matter more when it comes to toxicity. One characteristic seems to matter more, i.e., the size of the particle (Lehtiniemi et al., 2018; G. Liu et al., 2019; Ma et al., 2019). For instance, the copepod, *Acartia clausi*, can absorb a sizable amount of 7.3 μm MP, but to a lesser extent 20.6- and 30.6 μm MP (Cole et al., 2013). As summarised by Lusher (2015), nanometric-sized plastics can pass through cell membranes and cause significant biological effects such as weight loss, reduced feeding activity, increased phagocytic activity, and transference to the lysosomal (storage) system (Koelmans et al., 2022; Kögel et al., 2020). As particle size decreases, the number of particles reaching and being retained in different organs is shown to increase (Kögel et al., 2020). Some polymers appear more hazardous than others, and these are classified as mutagenic and/or carcinogenic. Some polymers in this classification are PUR, PVC and epoxy resins (ER) (Lithner et al., 2011). Plastic additives may further threaten the aquatic environments, as some are known to be toxic to marine organisms and humans (Browne et al., 2013; Evenset et al., 2009; Rochman et al., 2013). In addition to size, polymer type, and chemical additives, there might be a higher risk for some shapes of MPs. It has been demonstrated that fragments and spheres are more likely to be taken up by organisms than fibres (Gray & Weinstein, 2017).

In addition to posing a direct hazard to marine life, MP can enable the colonisation by invasive species, which can be transported over large distances and might pose a threat to marine ecosystems (Barnes, 2002; Kiessling et al., 2015; Zettler et al., 2013). MP act not only as a vector for biological contamination but also chemical contamination by adsorption of pollutants (e.g., heavy metals, antibiotics, and PAHs) from the environment (Mato et al., 2001). But also here, size matters. MPs with different particle sizes have different adsorption behaviours and load capacities for environmental pollutants (Ma et al., 2019).

1.3 Distribution and Transport of Microplastic in the Ocean

The marine ecosystem is contaminated with plastic through rivers, beaches, maritime activities, illegal dumping at sea, and accidentally lost or carelessly handled garbage (Sheavly & Register, 2007). As Hale et al. (2020) summarises, tire wear particles from roads, textile particles from washing machines, and paint particles are typical MPs that end up in the ocean. Once it enters the sea, there are no limits on where plastic can end up. Plastic can be transported by different scales of ocean currents, horizontal and vertical mixing, biota, extreme weather conditions, ice

formation, tides, and directly by the wind. Biota has a prominent role in moving MPs from the surface to the deep by ingesting it and excreting it in sinking faecal pellets (Van Sebille et al., 2020). Migrating marine organisms could also transport MPs horizontally by ingestion and excretion, and birds could transport MPs to land (Bourdages et al., 2021).

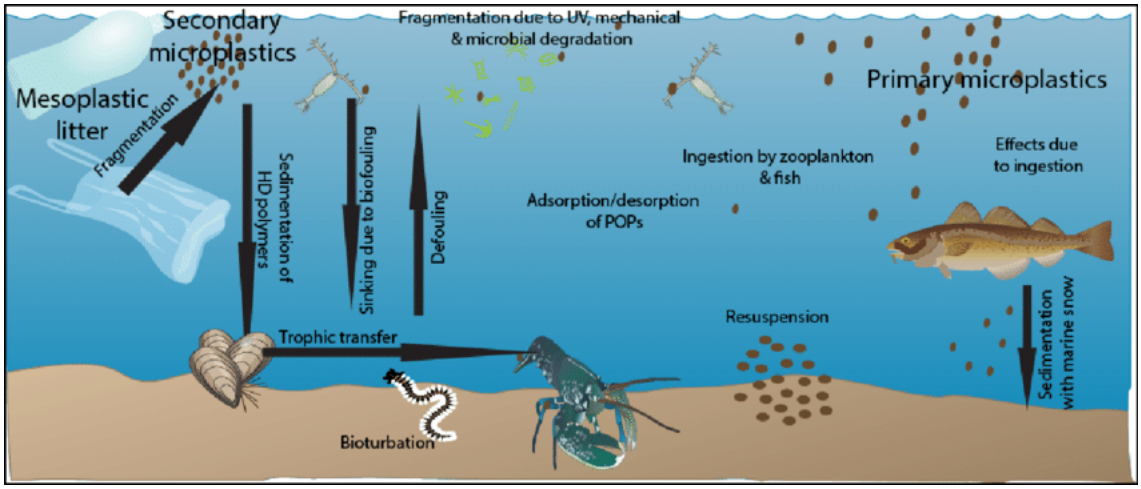

Figure 1: *Biological interactions, potential fate and pathways of microplastics (MPs) (modified by Bråte et al. (2014) from Wright et al. (2013)).*

It is difficult to simulate the transfer of MP since it involves physical, chemical, and biological processes (Andrady, 2011). The characteristics of MPs, which vary greatly and include size, shape, density, and buoyancy, affect their transport (Ballent et al., 2013; Kowalski et al., 2016). PE, PP, and PS, which are the most prevalent plastics in coastal environments, have densities that are comparable to those of seawater (1,03 g/cm^3). These particles float on water and are, therefore, more prone to advection (horizontal movement). The benthic environment is expected to contain high-density MPs such as PVC, polyamide/nylon (PA), polycarbonate (PC) and PET (Hidalgo-Ruz et al., 2012). However, biofilm formation can increase the density and, thus, deposition/sinking, especially for small particles with a larger surface-to-volume ratio (Chubarenko et al., 2016; Semcesen & Wells, 2021).

The global oceanographic currents are important global transport routes of MP that link the population-dense areas to low inhabited sites such as the Artic and the Antarctic (Liu et al., 2021; Lusher, 2015). Plastic accumulation has been confirmed in all five major subtropical gyres on Earth (Van Sebille et al., 2020), areas termed “garbage patches”, which are mainly dominated by plastic pieces in the size of millimetres or micrometres. These gyres are driven by surface winds, generating Ekman drift at the sea surface under the influence of the Earth’s

rotation (Coriolis force), which is directed to the left of the wind in the Southern Hemisphere and the right in the Northern Hemisphere. In the subtropics, Ekman drift is maintaining converging currents in all five subtropical gyres. Surface currents transport floating plastics items that do not experience waves or wind and will accumulate in areas where surface waters converge (Maximenko et al., 2012; Van Sebille et al., 2020). The borders of these accumulation zones are diffuse and changing, they change shape and move with time (van Sebille 2020).

Subtropical gyres accumulate MP particles, but in addition to this, the ocean circulation here also results in oligotrophic water that limits food availability. Due to the convergence and downwelling of surface water, these gyres are referred to as "ocean deserts" because of the low concentration of nutrients (Sigman & Hain, 2012). In fact, the South Pacific subtropical gyre (SPSG) is considered hyper-oligotrophic based on satellite estimates of surface concentrations of chlorophyll A (Ras et al., 2008). Zooplankton is directly dependent on phytoplankton biomass (Sigman & Hain, 2012), and therefore food availability for heterotrophs, including fish, is limited in the SPSG. Despite low average biomass and primary production, 23-29% of total ocean primary productivity worldwide is provided by oligotrophic gyres due to their large areas (Behrenfeld & Falkowski, 1997; Dassow, 2014).

The North Pacific Central Gyre, also known as the "Great Pacific Garbage Patch", is one region that has drawn a lot of attention. While floating plastic fragments have been reported in the subtropical gyres of the northern hemisphere since the early 1970s (Carpenter & Smith Jr, 1972; Hidalgo-Ruz et al., 2012; Law & Thompson, 2014), few studies have reported plastic pollution in the southern hemisphere (Eriksen et al., 2013). The SPSG is the largest subtropical gyre yet one of the least studied ocean regions (Dassow, 2014). Studies on MP in the SPSG show an upward trend in MP concentrations in the gyre's centre (Eriksen et al., 2013; Martinez et al., 2009; Maximenko et al., 2012). The centre of the SPSG is located on the east side of the gyre (**Figure 2**) and is the most oligotrophic marine region known (Morel et al., 2010). The eastern part of the SPSG region is distinct in physical and biological characteristics, as it contains the strongest known productivity gradient in the marine environment, spanning from its hyper-oligotrophic centre to the highly productive coastal Humboldt current system along the South American continental coast. The accumulation zone in the South Pacific is the strongest in terms of intensity and steadiness of the convergence of surface currents, but the concentration of debris appears lower than in the North Pacific (Eriksen et al., 2013; Maximenko et al., 2012). According to higher rates of plastic manufacture, consumption, and

release into the marine environment in the northern hemisphere, northern gyres appear to contain more plastics (Lebreton et al., 2012).

Martinez et al. (2009) demonstrated a three-step process in the drift mechanism of surface marine debris in the South Pacific Ocean. First, the debris drifts to latitudes between 20°S and 40°S, then it is carried eastward by geostrophic currents, and finally, it accumulates in the SPSG's centre. They also demonstrated that all debris reaching the centre remains there. Several studies have identified accumulation zones of surface MP in subtropical gyres, but MP in sub-surface water is less studied (Enders et al., 2015; Pakhomova et al., 2022). Most MP studies in seawater only examine floating items, which is insufficient to paint a whole picture of MP fate in the ocean.

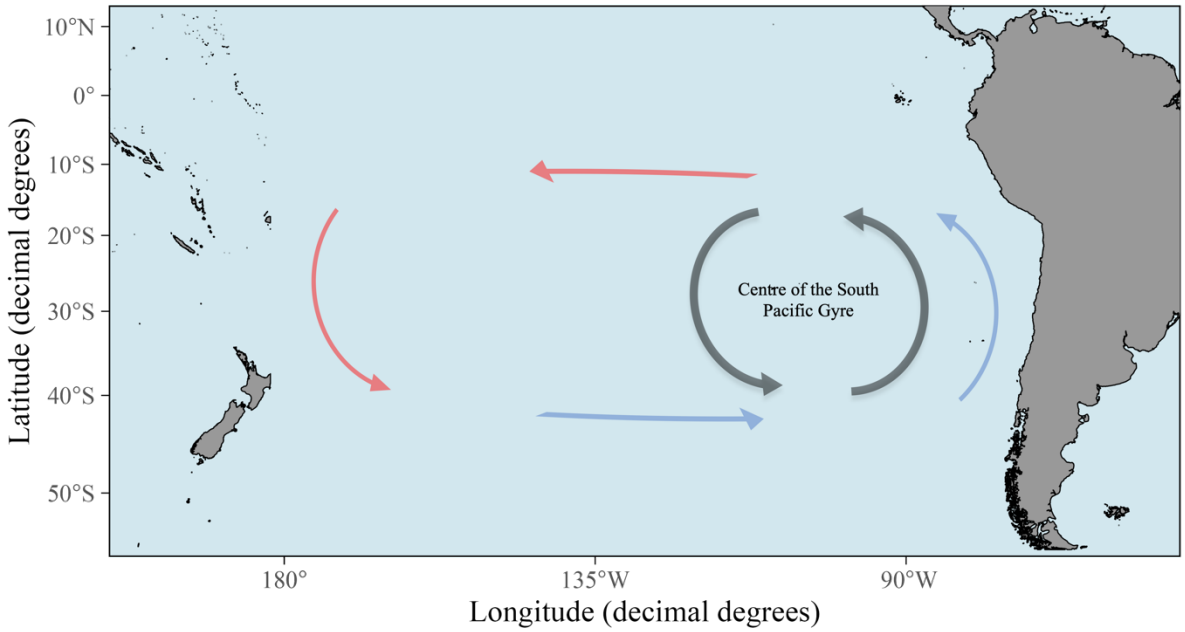

***Figure 2**: Map of the South Pacific gyre showing warm (red arrows) and cold (blue arrows) currents moving counterclockwise. The centre of the South Pacific gyre is located to the west due to the Coriolis force.*

1.4 Microplastic Research

MP pollution is a complex problem that requires open dialogue supported by efficient sharing of high-quality scientific data. Even though the amount of research and data on MP pollution has increased significantly, there is a lack of methodology standardisation and consistency in status reports. To this date, there is no standard analytical protocol for MP quantifications and identification, leading to dissimilarities in methods and less comparability between studies

(Lusher et al., 2021). For instance, studies have reported results in different dimensions, e.g., particles in a known water volume (particles/m^3) or area measurements (particles/km^2). Different dimensions makes the results hard to compare, as it is not possible to compare directly (Lusher, 2015). Global MP researchers should strive to harmonise or standardise methodology to proceed in MP research.

Following a review study of MP sampling techniques by Prata et al. (2019), some suggestions have been made. To achieve representativeness, collection of high volumes (10 – 2000 L) of water may be required, and the volume should always be reported (Prata et al., 2019). The most common methods for sampling MPs are manta trawls and pump filtration. While the Manta trawl can sample larger volumes of water, pump filtration may use lower pore size filters and thereby detect higher concentrations of MP (Schönlau et al., 2020). Because of the differences in the two methods' properties, manta trawl and pump results cannot be compared directly; they are rather complementary than substitutable (Tamminga et al., 2019). Pumping of seawater for MP detection, especially under-way filtering of seawater at the ship's seawater intake, has become a favourable method as data can be collected in a quick, affordable, and interoperable way. Pumping also allows the study of smaller MP, down to 10 μm. Higher levels of quality assurance and control are necessary for research on smaller MP, particularly in terms of documentation of contamination. MP is present in every surrounding, and the primary issue is contamination from the air. Precautions must therefore be made in every step, from sampling to analysis, to reduce contamination.

Including a digestion phase during sampling preparation is strongly advised to eliminate organic matter and improve identification. However, this depends on how much organic matter is present in the sample and the identification method used. Different chemicals could facilitate digestion, but caution should be made. While hydrogen peroxide (H_2O_2) and enzymatic digestion will have little to no breakdown of plastic polymers, acid could potentially destroy plastic polymers (particularly PA and PVC) (Prata et al., 2019). Chemical characterisation of MP by Fourier transform infrared spectroscopy (FTIR) and Raman spectroscopy is recommended for investigating the particle' size distribution, shape, and polymer composition. FTIR and Raman spectroscopy allows high-quality MP quantification, but unfortunately, Raman and, to some extent, FTIR are time-consuming and do not fit into current environmental monitoring routines. In this study, μ-FTIR and a laser-based microscope was used. High-

brightness Quantum Cascade Lasers (QCLs) in IR spectroscopy is a promising technique that may extend the capacity to process larger amounts of samples (Primpke et al., 2020). These advantages are essential to MP research, which often requires rapid analysis of numerous samples.

1.5 This Study

MPs are currently present in every ecosystem on Earth. However, little is known about their temporal and geographic distribution, which is important for evaluating the actual exposure organisms experience and potential adverse effects. Long-term monitoring of MP in the marine environment is also required to verify whether remediation actions are effective, but such data are limited. This study will investigate the distribution and characteristics of MP in the South Pacific Ocean and potentially confirm previously held assumptions about plastic accumulating in subtropical gyres (Eriksen et al., 2013; Van Sebille et al., 2020). Particle number, size, shape (fibre/fragment), and polymer type will be identified from subsurface water in the open ocean of the South Pacific, as well as the main harbours of Tahiti and Fiji.

Since previous studies in the South Pacific used a Manta trawl with a mesh size of 335 µm (Bakir et al., 2020; Eriksen et al., 2013; Gardon et al., 2021), this study will step beyond the current state-of-the-art by focusing on MPs down to 20 µm in size, which has never been done previously in the South Pacific. This smaller size range are of interest as these particles are likely to have the largest impact on ecosystems (Covernton et al., 2019). Several studies that have measured smaller particles than 300 µm confirm that sizes below this are predominant (Conkle et al., 2018; Gomiero, Øysæd, et al., 2019; Haave et al., 2019; Jian et al., 2022).This also indicates that most studies could be underestimating MP contamination.

The populations of the South Pacific islands depend on ocean resources as a source of food and livelihood (Barnett & Adger, 2003). MP can introduce particle stress, chemical additives, adsorbed pollutants, and microorganisms into the food chain, causing a potential risk for marine organisms and humans (Rochman et al., 2013). This study aimed to identify MP exposure to marine organisms at five meters depth and aid in filling the knowledge gap on marine MPs surrounding the South Pacific islands (Varea et al., 2020). To do such assessments, we need comparable and reliable methods. This study used recommended methods for MP sampling (pump-filtration), sample preparation (digestion steps), and analysis (IR microscopy).

Furthermore, these methods were described, and samples were analysed in two different laboratories (at NORCE in Stavanger and the Institute of Marine Research in Bergen) hosting two different analysis instruments (μ-FTIR and QCL-IR, respectively). Results from the two different instruments were compared with the goal of harmonising methodology.

1.5.1 Aim and Objectives

The goal of this study was to investigate abundance and distribution patterns, as well as size distribution, polymer types, and morphology of MPs in the South Pacific. A total of 42 subsurface water samples, sampled at the seawater intake at five meters depth on the tall ship S/S Statsraad Lehmkuhl during the One Ocean Expedition, were used to quantify and identify MPs using recommended approaches.

Three hypotheses are tested in this study:

i. MP concentration is higher at stations close to the SPSG (longitudes 90° to 120°W) and in the island harbours compared to the other stations.
ii. All stations generally have more MP particles in the smallest size category (< 300 μm).
iii. QCL-IR and μ-FTIR with associated software will give comparable MP concentrations and characteristics.

Three objectives are followed in this study:

i. Quantify MP concentration in 14 (x 3 replicates) subsurface water samples along a transect from Chile to Fiji using a high-volume water pump with filter mesh sizes of 10 μm and 300 μm and IR- microscopy.
ii. Use collected data to look for regional trends in MP concentration, size distribution, polymer type, and shape of MPs.
iii. Compare results (MP concentration, sizes, polymer types, and morphology) from two laboratories using QCL-IR and μ-FTIR and two different post-processing approaches for MP analysis.

2 Method

2.1 Study Area

Samples were collected onboard the tall ship Statsraad Lehmkuhl during the "One Ocean Expedition". An expedition from August 2021 to April 2023 with the ambition to create attention and share knowledge about the crucial role of the ocean to help achieve the UN Sustainable Development Goals. A plastic litter project investigating MP sources and transportation routes along the route for the One Ocean Expedition has not been conducted before. MP samples have been collected continuously during the circumnavigation, but this study focuses on 14 stations from the leg from Valparaiso, Chile to Fiji (**Figure 3**) conducted from May 1st to June 26th, 2022. When operating within areas with a research permit, sampling was performed every three days due to time limitations, resulting in 14 stations. Chile to Fiji is an interesting leg concerning MP because it crosses the SPSG, known to accumulate plastics (Eriksen et al., 2013; Van Sebille et al., 2020).

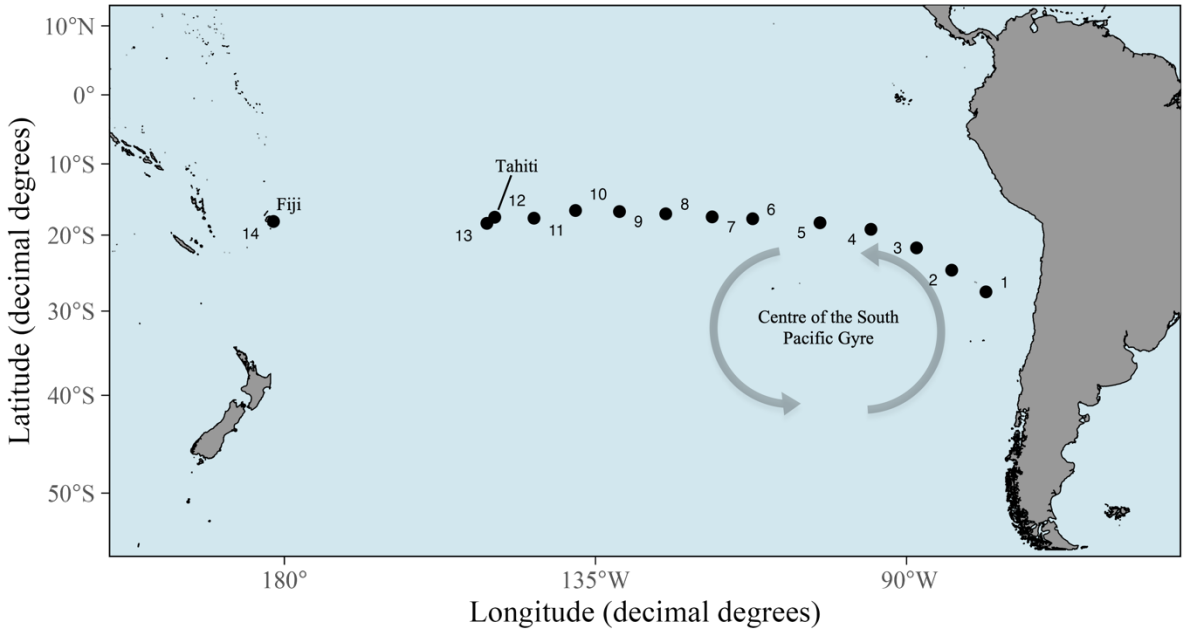

***Figure 3**: Locations of 14 sampling stations in the South Pacific Ocean during the One Ocean Expedition in May – June 2022. All sampling has been conducted in open water, except stations 12 and 14 which were conducted in Papeete and Suva harbour respectively. Three replicates were collected at each of the 14 stations, resulting in a total of 42 samples.*

2.2 Sample Collection

The 107-year-old ship has been equipped with modern instrumentation, such as an *ad hoc* large-volume water pump unit with a filtration device for MP installed at the seawater intake located at a depth of about 5 m on the port side. The two-chamber MP sampling device with displaceable filters was recently developed by NORCE staff and enabled the production of comparable and reliable results. The pump unit conveys a large volume of seawater from five meters depth to a cascade of two stainless steel filters. The filtration unit consists of two interconnected chambers where the top chamber holds the 300 µm mesh size filter, while the bottom chamber accommodates a 10 µm mesh size filter. The pump was set to 7,0 rotations/sec for 60 minutes to filtrate 350 L of seawater. After filtration, the filters were removed from the filter holder unit and placed in pre-cleaned (burned) glass bottles before being sealed with aluminium foil and a plastic lid. On the ship, samples were kept in a dark freezer at -40°C to avoid extra biofilm formation. Three replicates were collected at each sampling location while the ship was in motion, resulting in slightly different coordinates for each replicate.

The ship maintained an average speed of approximately 6 knots throughout the two-month transect, while mainly experiencing calm and sunny weather conditions. From Suva, Fiji, to the MP laboratory at the Institute of Marine Research (IMR) in Bergen, Norway, samples were flown in Styrofoam boxes at room temperature. The samples were thawed by the time they reached Bergen because the transportation process took around three days. The samples were subsequently frozen once again in a freezer set to -40 °C until the analysis.

2.3 Analysis of Microplastics

2.3.1 Sample Preparation

Half of the samples (every second sample) were prepared and analysed at NORCE MP laboratory in Stavanger, while the other half were prepared and analysed at the plastic laboratory of the Institute of Marine Research (IMR) in Bergen. Information about contamination controls and prevention is described in chapter 2.4. An overview of the sample preparation is shown in **Figure 4**.

The two filters from each sample (1x 300 µm + 1x 10 µm) were placed in crystallising dishes with 5% SDS solution and stirred at room temperature for at least 6 hours. The filters were

flushed and removed, and the liquid from both filters was filtered through a 47 mm diameter stainless steel filter of 10 μm mesh size. The filter was placed in a 600 mL beaker and 100 mL acetate buffer solution (pH 4,8) was added. The samples were then ultra-sonicated for 10 minutes before the filter was scraped, flushed, and removed. One mL cellulase enzyme blend and 1 mL Viscozyme were added before the samples were placed in a heating cabinet (between 40 and 50 °C) and incubated for 40 hours.

With the aid of cell lytic enzymes, some organic material had now been dissolved and the liquid was filtered through a 10 μm steel mesh. The filter was placed in the same beaker and sonicated for 10 minutes in 100 mL of H_2O_2 (30%). The filter was scraped and flushed with H_2O_2 and removed. The sample, containing H_2O_2, was kept in a heating cabinet, and the temperature was kept between 40 and 50 °C for at least 5 hours.

Again, the liquid was filtered through a 10 μm steel mesh. If signs of rust, which most probably originated from the pipes of the seawater intake at the ship, some droplets of 0.1 M hydrogen chloride (HCl) were added to dissolve it. The filter was transferred back to the same beaker with 50-100 mL of 50% EtOH and sonicated for 10 minutes before scraping and flushing the filter with 50% EtOH and removing it.

The sample containing 50% EtOH was transferred to an evaporation beaker, and the previous beaker was well flushed with EtOH when empty. The sample was evaporated (45 °C) until 1 mL remained. 4 mL of absolute ethanol (100%) was used to flush the evaporation beaker well, and the sample (now 5 mL) was transferred to a 10 mL vial, sealed with an aluminium cork.

Before analysis, the samples were transferred and filtered onto an anodisc filter (d= 25 mm; 0.02 μm, framed (IMR) and d=10 mm; 0.2 μm; not framed (NORCE), GE Whatman®) for analysis. To remove any remaining rust, the filter was flushed with 37% (12 M) HCl before being quickly rinsed with 50% EtOH. The filters were placed in glass Petri dishes and allowed to dry overnight. The filters were now ready to be analysed.

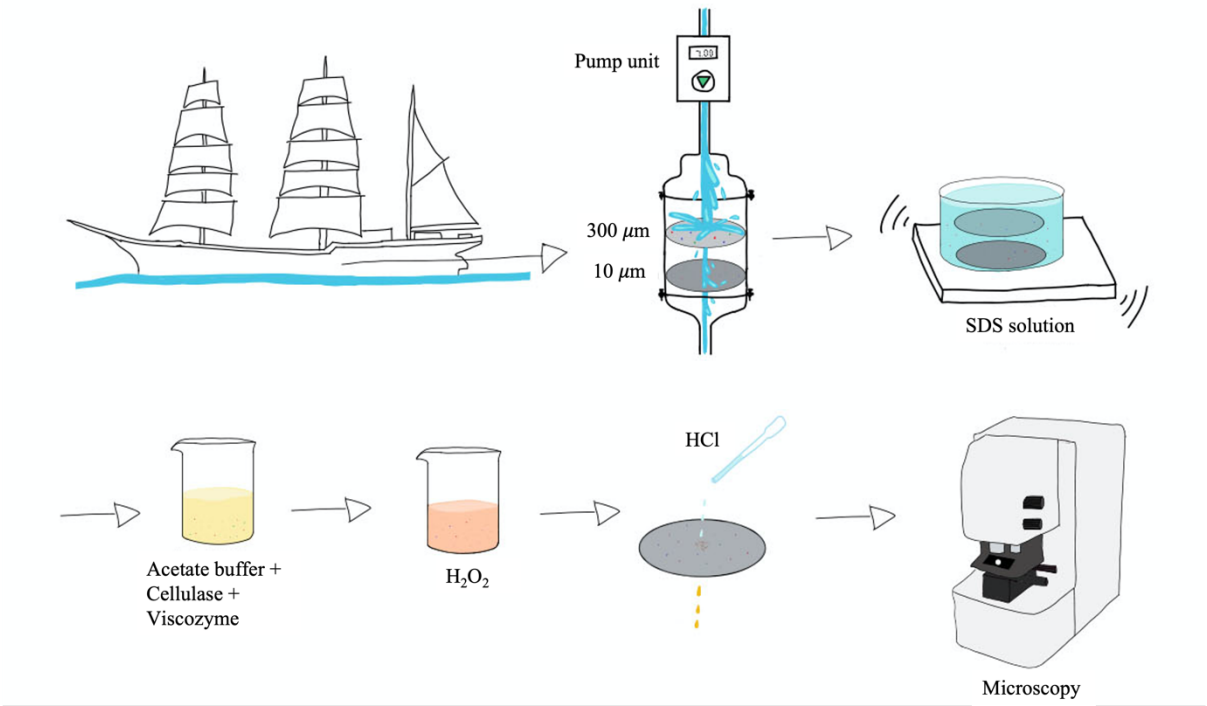

Figure 4: *Schematic overview of sample preparation from sampling onboard S/S Statsraad Lehmkuhl, digestion and chemical treatment, then microscopy.*

2.3.2 IR – Analysis

While the procedure for sample preparation was the same in both laboratories, MP analyses were slightly different using two different microscope-oriented technologies. The even-numbered stations (station 2, 4, 6, 8, 10, 12, and 14) was analysed with µ-FTIR at NORCE, while the odd-numbered stations (station 1, 3, 5, 7, 9, 11, and 13) was analysed with QCL-IR at IMR. Preferably, to compare the two instruments more accurately, the same samples should have been analysed with both instruments. However, this was not practically possible in this study, as MPs on the anodisc filters can easily fall off the filter during transport.

At NORCE, a Nicolet™ iN10 Infrared Microscope (Thermo Scientific™) was used. The FTIR microscope is equipped with arrays of detectors arranged in focal plane array (FPA) geometry. These arrays can contain up to 128 x 128 individual detectors. During acquisition, the FPA detector receives all wavelengths through a Michelson interferometer. This results in the generation of an interferogram, which is then converted into an actual spectrum using a Fourier transform. FTIR microscopes that utilize an FPA are typically equipped with a thermal Globar source of IR photons. The interferometer effectively provides all the desired wavelengths

within a spectral region that typically ranges from 4000 to 500 cm^{-1}, covering the mid-infrared region.

At IMR, a laser-based microscope SPERO QT (DRS Daylight Solutions) was used. This microscopy and imaging platform is based on infrared quantum cascade laser (QCL-IR) technology. QCLs are a type of semiconductor lasers that emit in the mid-to far-infrared range of the electromagnetic spectrum. These lasers operate based on quantum cascade structures, where electrons undergo inter-sub band transitions, resulting in the emission of photons. The electrons tunnel to the subsequent period of the structure, and this process repeats. Unlike IR interferometers, QCLs generate the mid-IR signal wavelength-by-wavelength, providing absolute values for each wavelength. Consequently, the spectrum reconstruction does not require the use of a Fourier transform. However, due to this wavelength-by-wavelength generation, acquiring a large spectral region may take time. To address this, pulsed lasers with millisecond ranges have been developed to compensate for the signal generation mode. QCLs currently cover a relatively limited spectral interval, typically no more than 100-300 cm^{-1}. Therefore, combining and modulating several QCLs is necessary to cover a broader spectral region, like FTIR setups. The software ChemVision, Version 3.3.8 (DRS Daylight Solutions) was used to scan MPs on the SPERO instrument.

In comparison to existing FTIR microscopes that provide similar imaging capabilities, such as those equipped with a large focal-plane array (FPA) detector and a motorised sample stage for capturing extensive sample areas, QCL-IR microscopes offer the potential for significantly higher signal-to-noise (S/N) ratios. This is primarily due to the high-power output and photon flux of QCL lasers. However, it is important to note that QCL-IR microscopes are limited to a shorter spectral interval, typically ranging from 1800 to 830 cm^{-1}.

2.4 Contamination Controls and Contamination Prevention

A passive blank sample was collected during sampling of the first replicate of each sampling site. Pre-filtered milli-Q water (GF/A 0,7 μm) in an amount of 15 mL was added to a pre-cleaned glass container with aluminium foil and a steel lid. The container's cover and foil were removed, and the milli-Q water was constantly exposed to air while the steel filters were exposed to air. MPs identified in this contamination control allows us to estimate the sample's contamination while the filters were exposed to the air in the sampling area at the ship. Blank

samples were stored and transported frozen to the NORCE laboratory. To prevent airborne contamination at the laboratories, sample preparation was carried out in a laminar flow bench whenever possible. When it was not possible to use the laminar flow bench, a passive blank sample containing filtered milli-Q water was kept open the whole time at each batch. In addition to the risk of getting contamination from air in the sample, there is also a risk of losing particles. To avoid this, the original beakers were always flushed well with filtered Milli-Q or ethanol when the sample was transferred. Another action to prevent the loss of particles was the ultrasonication of the filters to release the remaining MPs.

Lab coats (100% cotton) and lab shoes were worn during the preparation procedure. Gloves were worn when working with H_2O_2 and HCl. All reagents and water used during the sample preparation procedure were filtered through a 0.7 µm filter, and all the equipment was muffled at 500°C before use. Samples and equipment were always covered with aluminium foil when practically possible to minimise periods of exposure.

The passive blank samples from the ship and laboratory were filtered directly to the anodisc filter and analysed to estimate contamination from the air. In addition, a procedural blank for each batch was made at each laboratory. These samples were handled the same way as the original samples throughout the whole preparation and analysis procedure. The number of MPs per blank sample has been quantified and presented but not subtracted from each sample.

A recovery test to estimate how many particles were lost during the procedure was not performed in this study. However, the applied method was preliminary assessed at the NORCE laboratory before being applied in the present thesis (Gomiero et al., 2020; Gomiero et al., 2021). Briefly, the efficiency of the designed sampling device installed in the R/V was validated using replicates of 100 L tap water samples spiked with 900 and 50 µm sized PE particles obtained from Goodfellow Ltd. The contribution for each size class was set by particle number using a Coulter Counter-scoring technology. To determine the sampling device efficiency 200 mg (Ø= 900 µm) and 40 mg (Ø= 50 µm) PE particles, respectively, were mixed with 100 litres of tap water for each replicate and then passed through the sampling device. The filters were then removed and dried in the oven at 50° C for 3h. Samples were then analysed by µ-FTIR. The recovery efficiency spanned over 92-98% within the investigated masses.

2.5 Data Processing and Statistics

Despite using a mesh size of 10 µm during sampling, a size limit of 20 µm was set to avoid possible issues with the particle's size estimation in the nearby resolution limits of the instruments. Size was defined by the major dimension of a particle. Unfortunately, samples 1A and B had to be discarded because of too much rust to transfer it to anodisc filter. 5A, and some data from 13B are missing because of errors during the post-processing of data. Two different approaches to post-processing of spectra were used due to the use of two different microscopes.

At NORCE, the software SiMPLe (Systematic identification of Microplastic Particles in the environment), Version 1.3.2B was used to characterise the polymer types from µ-FTIR data. SiMPLe identify polymer types by comparing the IR spectra of detected particles to a reference database (Meyns et al., 2019). It also creates a raw dataset with dimensions, polymer type, and the spectra matching threshold score. Particles with a threshold score below 0.6 (60%) were removed from the dataset as this indicates a weak match between the particle and reference material (1 is a perfect match).

At IMR, a model-based machine learning/artificial intelligence (AI) approach based on random decision forests was newly developed to post-process the spectral information from the QCL-IR instrument. This method does not compare spectra to a reference database but uses a model-based classification for fast identification of MP. It uses random decision forest classifiers to obtain results for the different polymers (Hufnagl et al., 2019; Hufnagl et al., 2021; Huserbråten, In prep). The raw dataset comprises dimensions, polymer types, and p-values ranging from 0 to 1, which indicate the proportion of the particle that consists of a plastic polymer. A threshold p-value of 0.6 was applied, meaning particles were considered MP if they consisted of at least 60% polymer.

The ratio between major and minor dimensions can characterise and distinguish the particle shape as fibres (length-to-width ratio > 3) or fragments (length-to-width ratio ≤ 3) (Vianello et al., 2019). Particle information was compiled in Microsoft Excel. Visualisation and statistics were carried out with R Studio (Version 2023.03.1+446). Map was made with the package ggOceanMaps, and plots were made with ggplot2 (Vihtakari, 2022).

To assess significant difference in number of particles between stations, the lm() function was used to fit a linear regression model. Further, the glht() (Tukey) function was used to perform pairwise comparisons and assess significant differences between the stations. To assess the significant differences of size distribution in the gyre and outside the gyre, and between instruments, the Shapiro-Wilk test was used to see if the data were normally distributed. If normally distributed, a two-sided t-test was performed. If not, a Wilcoxon rank-sum test was performed. The significance of the differences was determined based on the calculated p-values with a threshold of α=0.05. Results with p-values below this threshold were considered statistically significant.

To investigate ocean surface hydrographic properties and currents, the EU Copernicus Marine Service Global Ocean Physics Analysis and Forecast model product (Le Galloudec et al., 2018) was used. The model product is based on a global application utilizing the NEMO model (Nucleus for European Modelling of the Ocean) at 0.083 x 0.083 degrees resolution. All available hydrographic profile data, as well as remote sensing sea-surface temperature and sea-surface height observations, are assimilated into the model system.

2.6 Ethics Statement

Permits to conduct this field research were provided by Stiftelsen Statsraad Lehmkuhl and the One Ocean Expedition. Unfortunately, we did not get a research permit for collecting water samples in the economic zone of Valparaiso, Cook Islands, Niue, and Tonga.

3 Results

3.1 Abundance and Distribution of Microplastic

A total of 42 subsurface seawater samples were collected at 14 stations during the 11 000 km transect from Chile to Fiji. In total, 14 700 L of water was filtered. MP particles were found in all samples analysed. Higher abundances of MP were found at stations 3 – 8 at longitudes 90° to 125°W, which is where the SPSG is located. Due to substantial variations in the results obtained from QCL-IR and μ-FTIR, the mean concentrations of MP in **Figure 5** and **Figure 6** are presented on a min-max scale ranging from 0 to 1. This scale allows for a comparative visualisation of the relative abundances of MP concentrations observed among the sampling

stations. Across the transect, MP abundances seem to have a bell-shaped distribution (**Figure 6**). For the actual particle concentrations measured, see **Figure 7** and **Table 1**.

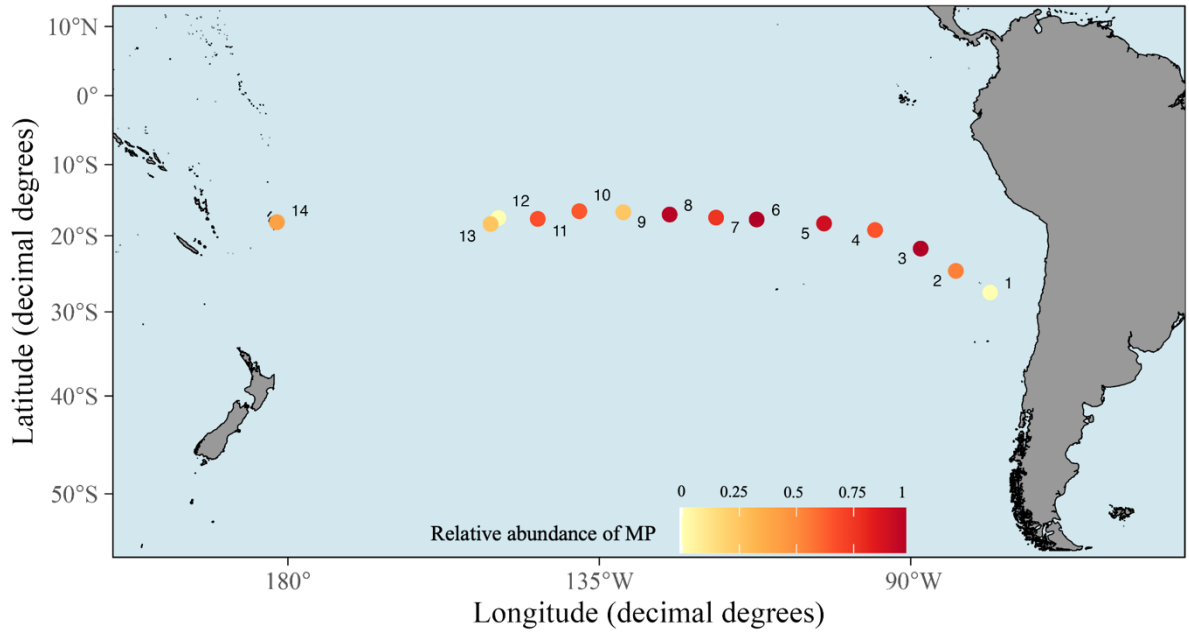

Figure 5*: Locations of 14 sampling stations in the South Pacific Ocean during the One Ocean Expedition in May – June 2022. All sampling has been conducted in open water, except stations 12 and 14, which were conducted in Papeete and Suva harbour respectively. Mean microplastic (MP) concentration (colours white to dark red) is here presented on a min-max scale from 0 to 1 to be able to visualise the differences between stations.*

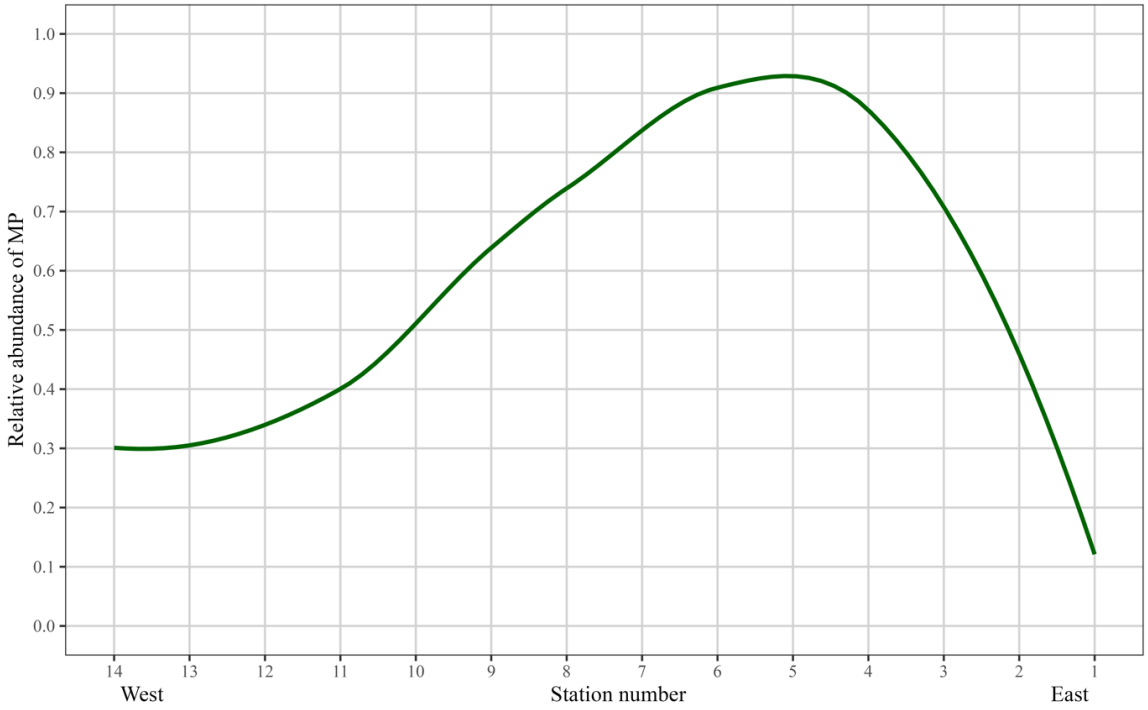

Figure 6: *Relative abundance of microplastic (MP) across 14 stations in the South Pacific Ocean. The mean concentrations have been scaled to a min-max scale from 0 to 1.*

Mean MP concentration in the South Pacific was 3564 ± 2374 MP m^{-3} ranging from 80 – 17 200 MP m^{-3} using the QCL-IR instrument, while the µ-FTIR instrument found the mean MP concentration to be 166 ± 85 MP m^{-3}, ranging from 5 – 320 MP m^{-3}. The mean MP concentration from the two instruments shows a difference of approximately 20 orders of magnitude. This demonstrates how different analysis methods can give two different pictures of MP concentrations. **Figure 7** shows the MP concentration at each station and each replicate, analysed with the two different instruments. Both methods show the same pattern, i.e., a bell-shaped distribution, with higher concentrations at stations 3 – 8, close to the SPSG. When considering results from QCL-IR, there is a significant difference in MP concentration between stations in the gyre (stations 3, 5, 7) and stations outside the gyre (stations 1, 9, 11, and 13) ($p = 0.046$). When considering results from µ-FTIR, there is not a significant difference in MP concentration between stations in the gyre (stations 4, 6, 8) and stations outside the gyre (stations 2, 10, 12, 14) ($p= 0.054$). The highest concentration found during the transect was 17600 MP m^{-3} (identified by QCL-IR) at station 3, replicate B.

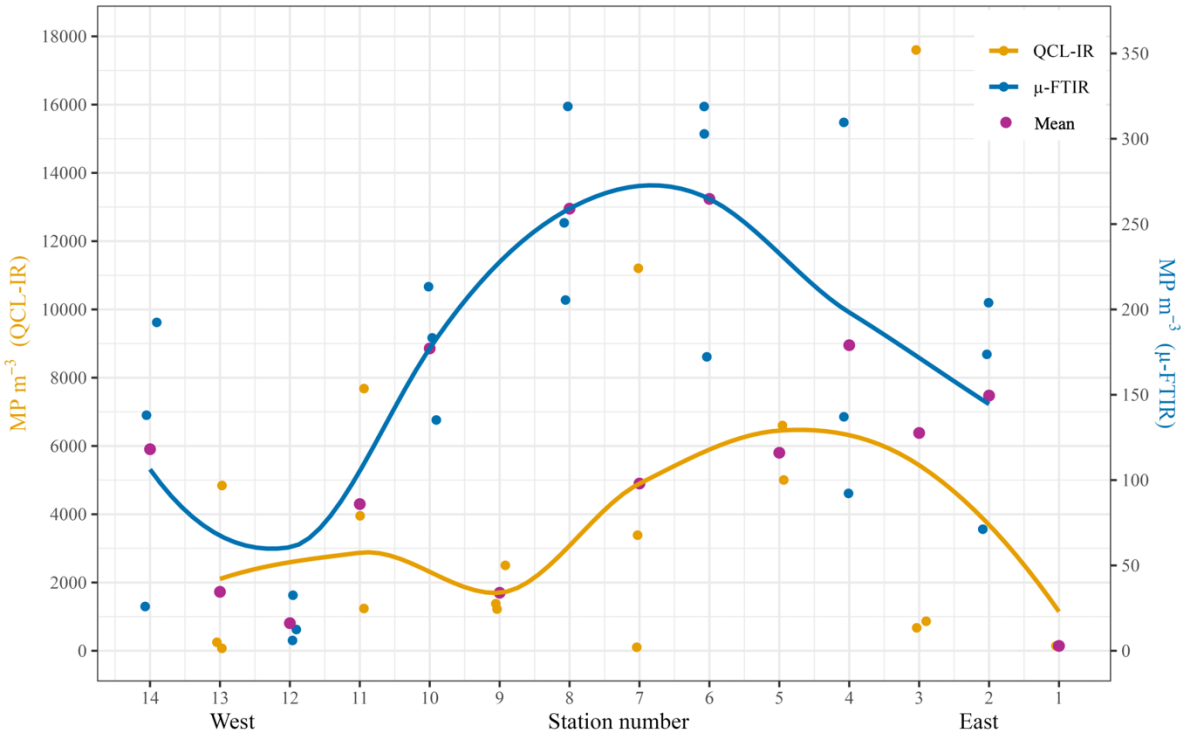

Figure 7: *Concentration of microplastic (MP m^{-3}) in subsurface water across 14 stations in the South Pacific Ocean, arranged from west to east. The two y-axes are scaled on a factor of 50 to enable a comparison of all µ-FTIR (blue) data and QCL-IR (orange) data. Purple points represent the mean concentration at each station, and the blue and orange line shows the concentration trend across stations for each instrument.*

Table 1: *Coordinates, number of particles, and mean concentration of MP at each sampling station in the South Pacific Ocean. Grey-shaded rows are analysed with QCL-IR, while the white rows are analysed with μ-FTIR. Unfortunately, station 1 only has one replicate, station 5 only has two, and some data are missing on station 13 replicate B.*

Station	Latitude	Longitude	Replicate	No. of particles	Mean Concentration (MP m^{-3})
1	27°33'2"S	78°30'35"W	A	NA	143
			B	50	
			C	NA	
2	24°43'10"S	83°27'60"W	A	61	150
			B	71	
			C	25	
3	21°43'81"S	88°32'84"W	A	303	6381
			B	6160	
			C	237	
4	19°12'31"S	95°8'60"W	A	108	179
			B	48	
			B	32	
5	18°17'72"S	102°30'72"W	A	NA	5801
			B	2312	
			C	1749	
6	17°44'56"S	112°15'38"W	A	112	265
			B	60	
			C	106	
7	17°29'17"S	118°7'12"W	A	3922	4898
			B	37	
			C	1184	
8	17°3'49"S	124°50'44"W	A	112	259
			B	72	
			C	88	
9	16°44'55"S	131°31'42"W	A	426	1699
			B	873	
			C	485	
10	16°36'3"S	137°53'58"W	A	64	177
			B	75	
			C	47	
11	17°40'12"S	143°53'36"W	A	2691	4298
			B	1385	
			C	437	
12	17°32'14"S	149°34'12"W	A	4	16
			B	11	
			C	2	
13	18°23'2"S	150°42'29"W	A	1696	>1727
			B	>28	
			C	89	
14	18°7'41"S	178°25'6"E	A	67	118
			B	48	
			C	9	

3.2 Size Distribution of Microplastics

QCL-IR measured a mean size of 56 µm, while µ-FITR measured a mean size of 111 µm, which are significantly different ($p = 0.03$). Considering both instruments, the size ranged from 20 – 5256 µm (the lower size limit was 20 µm). Each instrument identified an overwhelming majority, 98%, particles smaller than 300 µm. QCL-IR found 92% of the identified MPs to be smaller than 100 µm, while µ-FTIR found 53% smaller than 100 µm. Further, QCL-IR found 75% particles smaller than 50 µm, while µ-FTIR only found 7% smaller than 50 µm. No significant difference was found in particle size close to the centre of the gyre (stations 3 – 8) and far from the gyre (remaining stations) (QCL-IR: $p = 0.85$, µ-FTIR: $p = 1$).

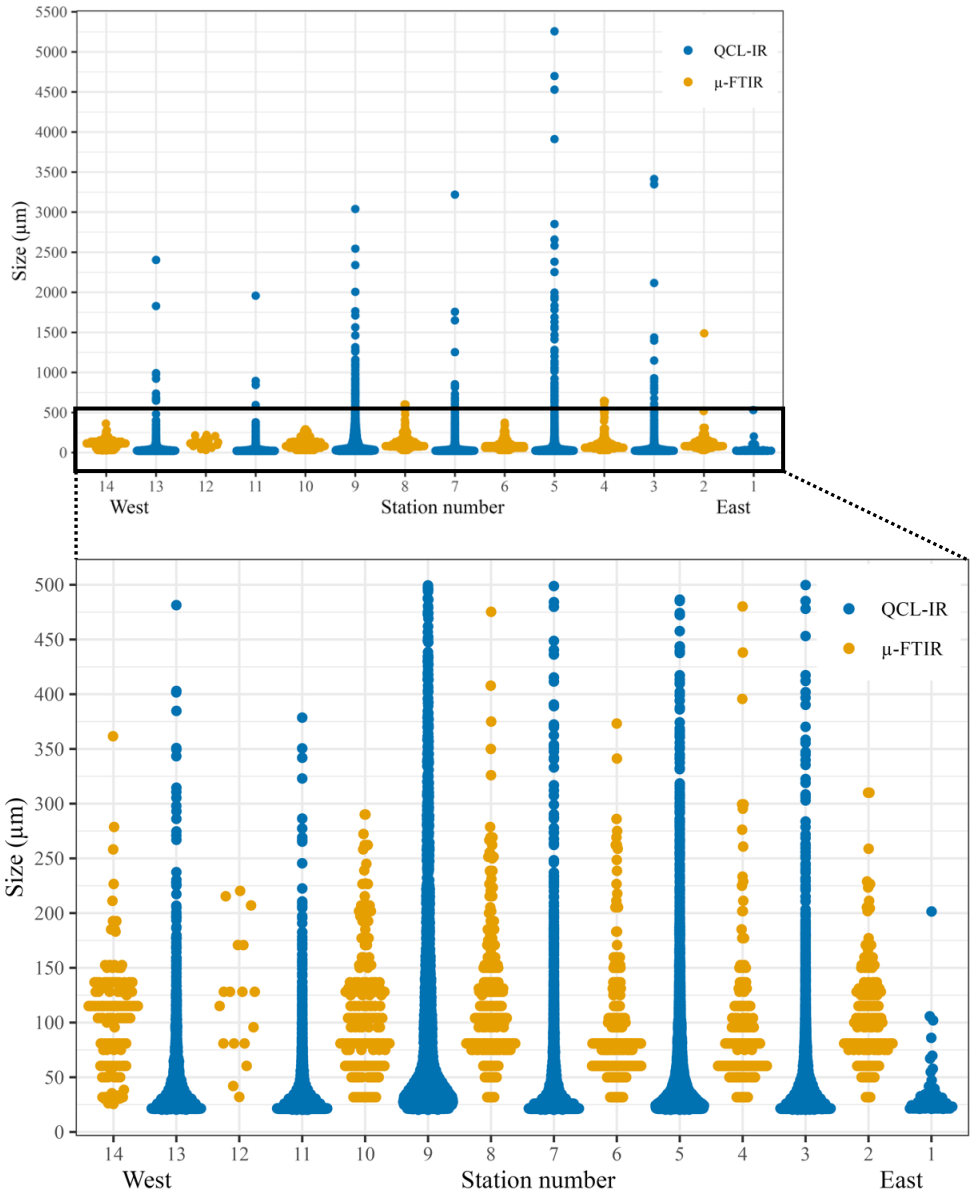

Figure 8: *Size distribution (µm) of microplastics in subsurface water at each of the 14 sampling stations in the South Pacific, arranged from west to east. Blue colour represents data from QCL-IR, while orange represents data from µ-FTIR.*

3.3 Polymer types

μ-FTIR identified PP (55%) as the dominant polymer, while QCL-IR identified PE (64%) as the dominant polymer. Further, QCL-IR identified 13% PP, 7% acrylic, 6% PET, and 5% PS. μ-FTIR identified 19% PET, 12% PE, and 3% acrylic. Acrylic included poly (methyl methacrylate), acrylic paint, polyacrylonitrile (acrylic fibre), and poly (acrylic acid). The group "Others" consists of polymers that were present in less than 2% abundance, including ABS (Acrylonitrile Butadiene Styrene), alkyd, cellulose ester, ER, poly (methyl vinyl ether-co-maleic anhydride), PVC, and PEEK (polyether ether ketone).

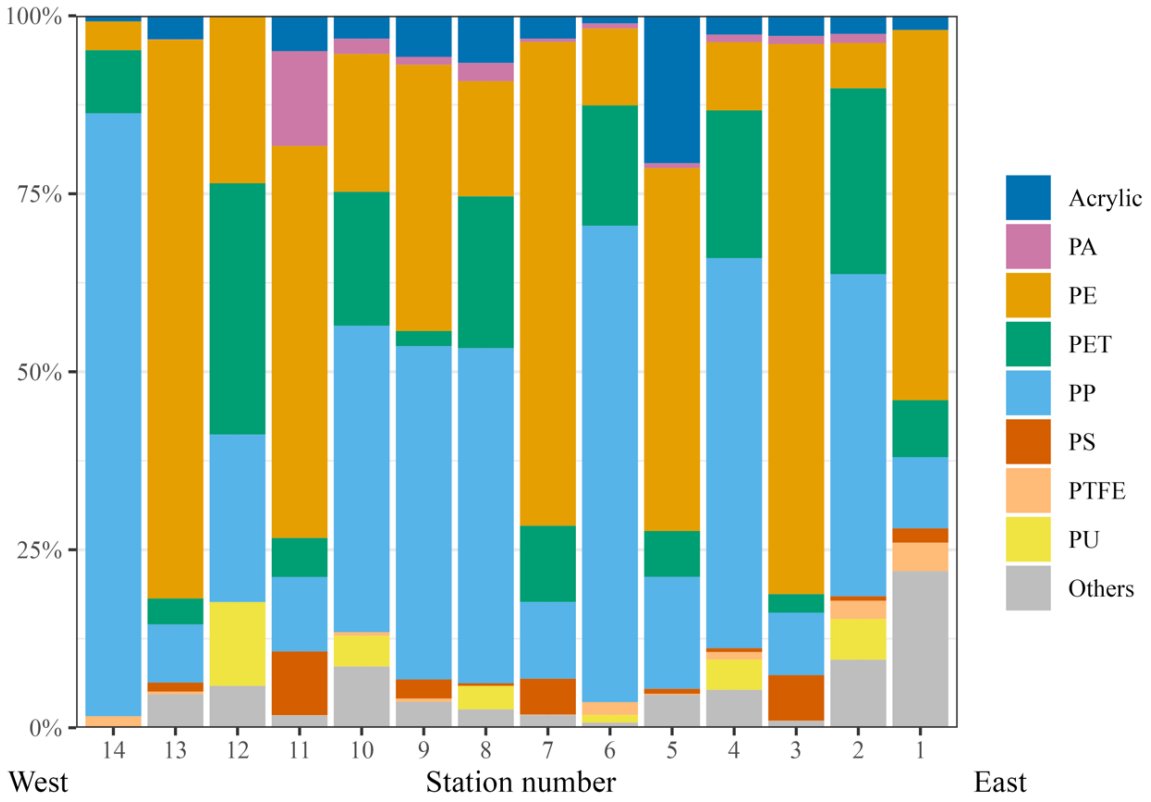

Figure 9: *Distribution of polymer types in subsurface water at each of the 14 sampling stations in the South Pacific, arranged from west to east. Samples at odd-numbered station numbers are analysed with QCL-IR, while samples from even-numbered station numbers are analysed with μ-FTIR.*

3.4 Morphology of Microplastics

In this study, MP were characterised as fibres (length-to-width ratio > 3) or fragments (length-to-width ratio ≤ 3). QCL-IR identified 92% fragments, while µ-FTIR identified 85% fragments. Hence, both instruments agree upon the dominating shape of the particles.

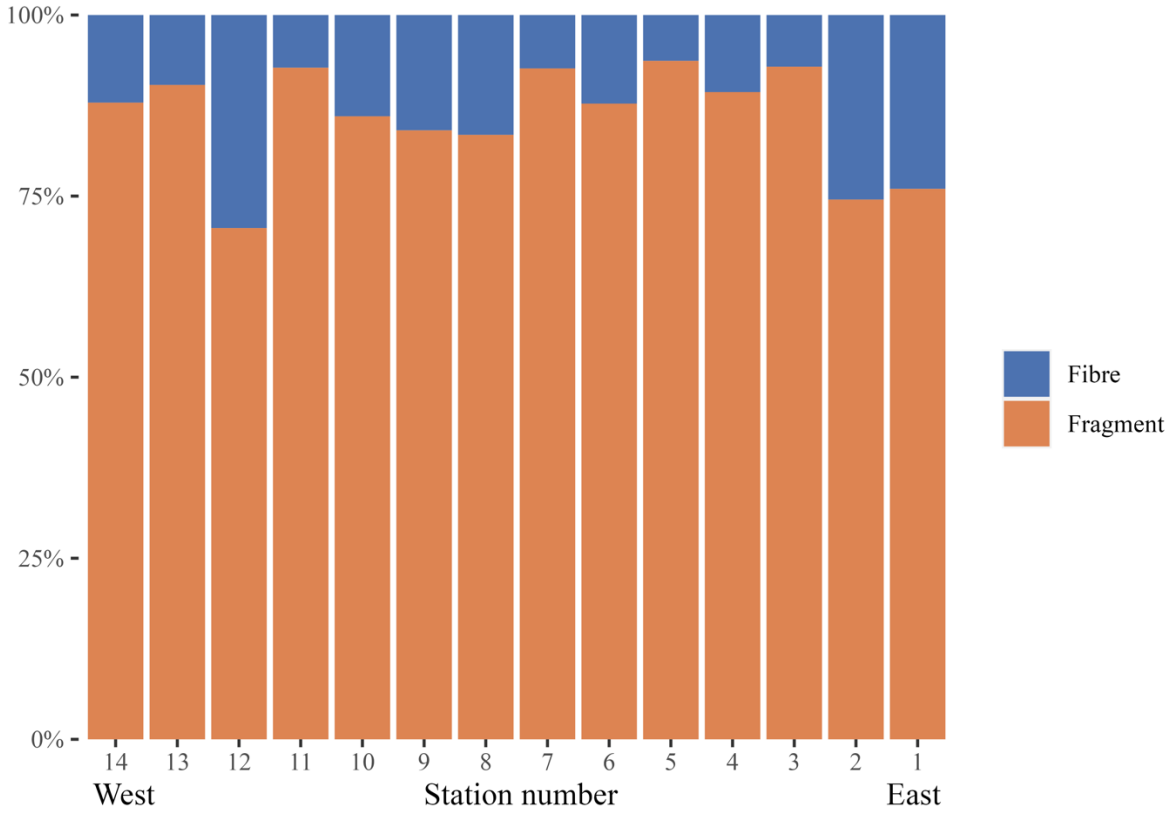

Figure 10: *Relative abundance of fragments (orange) and fibres (blue) from west to east. Samples at odd-numbered station numbers are analysed with QCL-IR, while samples from even-numbered station numbers are analysed with µ-FTIR.*

3.5 Contamination Controls

To estimate the contamination from airborne MP, passive controls were taken at the ship and the laboratory while filters were exposed to air (outside LAF-bench). To estimate the total contamination during sample preparation at the laboratory, procedural controls were handled the same way as the original samples. At the laboratory, one passive and one procedural control was taken for each batch (

Table 2). The passive control in batch 2 at IMR had the highest number of MP particles (519 particles). However, the analysis method must be considered, as the QCL-IR instrument at IMR

generally identifies more particles than μ-FTIR at NORCE. Further, PE is the most recurring polymer type, and fragments are the most recurring morphology in the contamination controls.

Table 2: *Number of particles, dominating polymer type, and dominating morphology of identified particles in contamination controls from the ship, IMR, and NORCE.*

Location (instrument)	**Batch no.**	**Station No.**	**Blank**	**No. of MPs**	**Dominating polymers**	**Dominating morphology**
Ship (μ-FTIR)	4	4	Passive	3	PE	Fragment
	6	6	Passive	11	PE	Fragment
	8	8	Passive	8	PE	Fragment
	12	12	Passive	2	PE	Fragment
IMR (QCL-IR)	1	3C, 7B, 7C, 9B, 9C, 13A	Procedure	9	PE	Fibre/ fragment
			Passive	35	PP	Fibre/ fragment
	2	5B, 5C, 7A, 11A, 11B, 13B, 13C	Procedure	18	PET	Fragment
			Passive	519	PP	Fibre/ fragment
	3	1C, 3A, 3B, 9A	Procedure	189	PE	Fragment
			Passive	7	PE	Fragment
NORCE (μ-FTIR)	1	2A, 2B, 4B, 6C, 10C, 14A, 14B	Procedure	NA	NA	NA
			Passive	1	PE	Fibre
	2	8A, 8B, 10B, 12A, 12B, 12C, 14C	Procedure	0	-	-
			Passive	0	-	-
	3	2C, 4A, 4C, 6A, 6B, 8C, 10A	Procedure	9	PP	Fragment
			Passive	1	PE	Fibre

4 Discussion

This study presents unique data on the abundance and characteristics of MPs in the open ocean of the South Pacific and the harbours of Papeete (Tahiti) and Suva (Fiji). All samples were collected using the same sampling technique, but half were analysed with μ-FTIR and half with QCL-IR. Analysation by the two instruments resulted in two different sets of data. In other words, this is not a quantitative study. In fact, very few MP studies can be categorised as quantitative since there is uncertainty regarding which method provides the most accurate results. The main goal of this study was to obtain data on the distribution of MP (including size, polymer type, and morphology) in the South Pacific. Importantly, the present study 1) identifies an accumulation zone in the SPSG, 2) emphasises the impact of different MP analysis methods on the results, and 3) points to the importance of using a mesh size smaller than 300 μm during MP sample collection.

4.1 Abundance and Distribution of Microplastics

High densities of plastic debris are typically associated with densely populated coastal areas or oceanic convergence zones (Lebreton et al., 2012). Based on that, the hypothesis put forward in this thesis was that "MP concentration is higher at stations close to the SPSG (longitudes 90° to 120°W) and in the island harbours, compared to the other stations". Suva and Papeete are the main harbours of Fiji and Tahiti. However, the highest concentration of MP was not found in the harbours, but in the middle of the open ocean at longitudes 90° to 125°W. Among the samples analysed with μ-FTIR, Papeete harbour had a significantly lower MP concentration compared to stations 6 and 8 in the open ocean ($p= 0.012$ and $p= 0.014$ respectively). This might indicate that the islands are not the main source of contamination in the SPSG. Al Nabhani et al. (2022) found no difference in the numbers of MP at populated and non-populated beaches in Fiji. This also indicates that the MP in Fiji, mainly arrive with ocean currents.

These higher concentrations found at longitudes 90° to 125°W correspond to the previous study of MP in the South Pacific (Eriksen et al., 2013) and where the SPSG is located. According to the results from QCL-IR, there was a significant difference in MP concentration between stations in the gyre and outside the gyre. Results (from both μ-FTIR and QCL-IR) demonstrated a bell-shaped distribution, which was also identified by Eriksen et al. (2013) and

modelled by Maximenko et al. (2012). The SPSG shows the most pronounced swirling convergence of the global gyres, which leads to the aggregation of particles in a very compact area. This area is approximately 90° to 120°W and 30°S (Maes et al., 2018; Maximenko et al., 2012). The transect of this study was mainly at 20°S, which means that we would probably sample even higher concentrations of MP and demonstrate an even stronger bell-shaped distribution if the transect happened 10° further south.

Model estimates by Lebreton et al. (2012) show a much lower concentration of floating debris in the southern hemisphere. The model shows that the largest contributors to plastic contamination in the SPSG are Australia/New Zealand, South America, and Southeast Asia/Indonesia (Lebreton et al., 2012). However, more recent modelling by Maes et al. (2018) identifies a surface "superconvergence" pathway connecting the South Indian Ocean to the SPSG. This shows that the South Indian Ocean might be a large contributor to plastic pollution in the SPSG and that the sources of plastics in the SPSG might have been underestimated. Actual data on MP occurrence is essential to validate oceanographic models for the transport and fate of MPs.

In the three replicates obtained from a station, some MP concentrations have values largely deviating from the two other replicates. However, since the ship was in motion while sampling, this is not unexpected. At station 3, evidence of a convergence zone is observed as indicated by the significantly high number of MPs in replicate B. Convergence zones in this context refer to patches where the concentration of MP can vary significantly over a short distance, possibly on the order of meters (Harrison et al., 2013; Lebreton et al., 2012). Considering that the ship was in motion during the sampling, it is possible that replicate A was collected outside a convergence zone, while replicate B was collected within the zone, and replicate C was collected after passing the convergence zone. The ocean is far from homogenous, and within the SPSG, there are patches within the patch and gyres within the gyre (Lebreton et al., 2012). Therefore, the high variation in MP concentration within the same station number does not necessarily mean low precision in methodology, it can rather indicate variability in concentration over relatively small space scales.

To investigate whether the variations in MP abundance among stations could be attributed to distinct waterfronts, model data (Le Galloudec et al., 2018) and data collected from the

FerryBox aboard the ship were used to visualise the distribution of water masses (**Figure 10a and b**). Unfortunately, there was some lack of data from the FerryBox on stations 2-8 and 11-14, therefore, model data had to be supplemented. The first two stations are in the coastal Humboldt current system along the South American coast and in a different water mass than the other stations. Stations 4-14 are within a warmer and higher salinity water mass, with stations 4, 5, and 6 right above the centre of the SPSG. Station 3 seems to be right in the middle of the two water masses. However, **Figure 10a** shows that all stations are within the same current system and may indicate that MP sampled at the different stations share a similar fate.

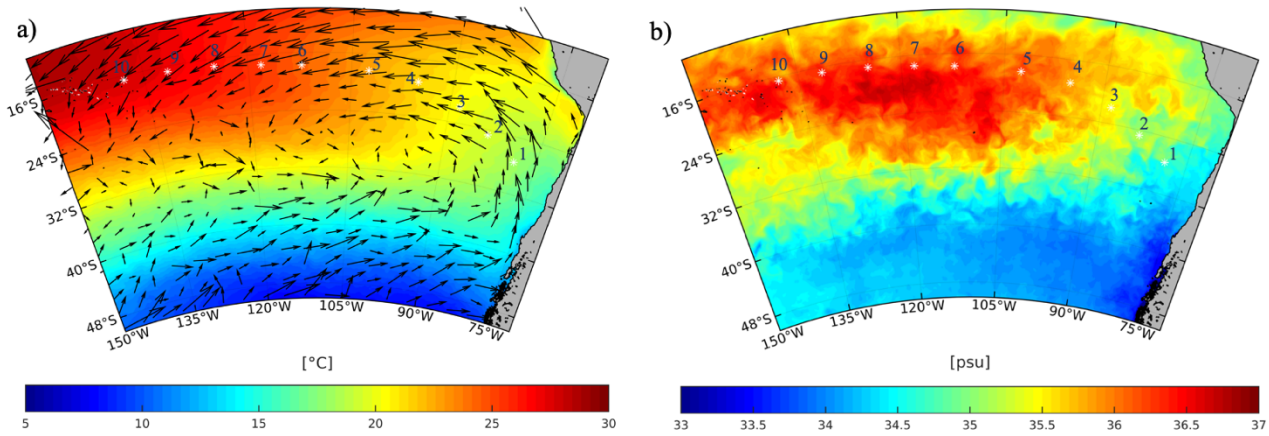

Figure 11: *Temperature gradients, directions and locations of ocean currents and the gyre (a), and salinity gradients (b) in the South Pacific Ocean.*

The differences in MP concentrations between stations (and between samples analysed with the same instrument) cannot only be related to the levels of plastic pollution in the investigated region. Methodological challenges also play a significant role in this regard. Chapter 4.7 provides an in-depth exploration of the sources of errors and an assessment of the methodology used.

4.2 Microplastic Characteristics

Investigation of particles below 300 µm in the South Pacific Ocean has never been conducted before. The results presented in this thesis supported the hypothesis: ii) All stations generally have more MP particles in the smallest size category (< 300 µm). In this study, 98% of all particles identified were smaller than 300 µm, emphasising the importance of looking at particles in that lower size range. Moreover, 92% of the particles identified by QCL-IR were

smaller than 100 µm, which means that a mesh size of 100 µm still would not be sufficient to estimate MP contamination in the ocean. However, Eriksen et al. (2013) found more particles in sizes 1000 – 2790 µm in the South Pacific, which contrasts with this study, and most other studies conducted on MP sizes globally (Conkle et al., 2018; Enders et al., 2015; Gomiero, Øysæd, et al., 2019). No significant difference was found in particle size close to the gyre's centre and far from the gyre, but this could be an interesting topic for future studies. As described by Martinez et al. (2009), the centre of the SPSG is most probably the last stop on the MP journey in the South Pacific, and it has had a lot of time to degrade on its way.

MP particles found in the South Pacific ranged from 20 – 5256 µm, with a lower size limit of 20 µm. The upper size limit, on the other hand, is uncertain. The largest particles were found in sample 5, and when looking at the largest particle (5256 µm) from the scanning on QCL-IR, it seems more like many small particles that have aggregated (**Figure 12**). Therefore, the big particles found in this study most probably consist of many small particles and are mistakenly identified as one larger particle. It also seems to be some instrumental differences in the size measurements. µ-FTIR measured significantly ($p = 0.03$) larger particles (mean: 111 µm) than QCL-IR (mean: 56 µm).

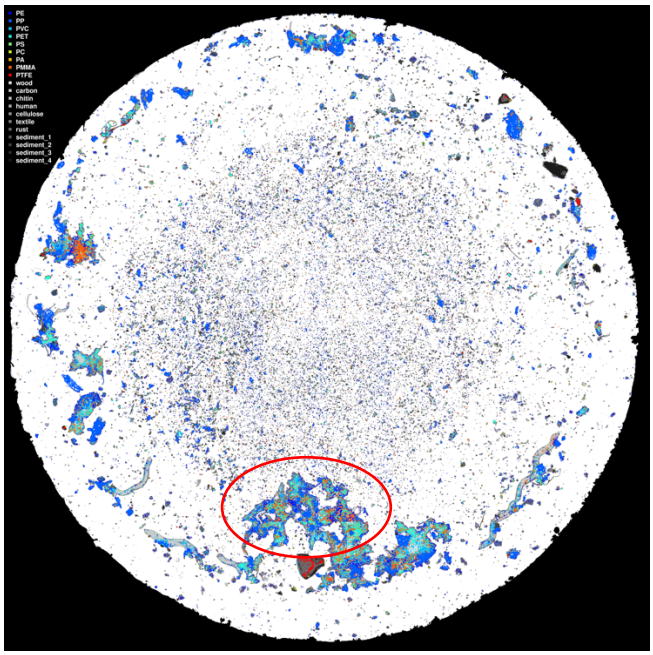

Figure 12: *Spectra map of analysis filter 1, sample 5B. Aggregation of small particles might mistakenly be identified as one larger particle.*

PE and PP were the dominating polymers in this study, corresponding to earlier studies of surface MPs (Bakir et al., 2020; Pan et al., 2022). PE and PP are commonly found in consumer products such as plastic bags, plastic bottles, and containers and could originate from the breakdown of larger plastic items. It can also be linked to fisheries, as PP and PE are used in ropes and fishing nets (Lusher et al., 2017). PE and PP have densities comparable to seawater and are, therefore, predominant in the upper water masses. However, earlier studies of subsurface MPs using pump filtration have found PET among the most frequent polymers (Hildebrandt et al., 2022; Pakhomova et al., 2022), even though PET is a high-density polymer that is expected to sink. This study found PET at all stations but only 6% – 19% of all identified particles. Acrylic (3% – 7% of MPs identified in this thesis), is a high-density polymer, like PET, and is therefore expected to be found deeper in the water column.

This study found more fragments (85% – 92%) than fibres (8% – 15%). This agrees with the study by Eriksen et al. (2018), who also found fragments as the dominant shape of MPs. MP in polar regions seems to constitute more fibres than fragments (Pakhomova et al., 2022), while MP in the tropics, subtropics, and temperate areas, fragments have been reported of higher abundance than fibres (Cui et al., 2022; Liu et al., 2021; Pakhomova et al., 2022). This might indicate that fibres can be transported over longer distances than fragments. However, it is hard to compare this characteristic between studies because some studies use the definition of a fibre to have a length-to-width ratio > 1.5 (Barrows et al., 2018), and would thereby identify a higher number of fibres, compared to this study (which use the definition of a fibre to have length-to-width ratio >3). There might also be some instrumental differences as QCL-IR seemed to identify fragments more frequently than μ-FTIR.

4.5 Impact on Marine Life

The highest number of plastic particles was found close to the centre of the SPSG. The combination of a high concentration of MP and a low concentration of food causes a significantly higher ingestion rate of MP in fish in this area compared to areas outside the centre (Markic et al., 2018). Several studies have been conducted to understand better how MP affects marine life, and the conclusion is that most species are at high risk of ecosystem disadvantage due to MP contamination (Benson et al., 2022; Kim et al., 2021; Kögel et al., 2020). The effects of MP are specifically dire for the Pacific Island countries. The economies of Pacific Island

countries rely on tourism and fisheries (Gillett & Tauati, 2018; World Health Organization, 2017), both of which heavily rely on ocean ecosystem services.

Samples were collected from five meters depth in this study and could indicate how exposed pelagic species may be. This primarily includes fish and pelagic crustaceans, but it also includes cnidarians and phytoplankton. The size of the particles is a crucial factor in determining uptake, retention, and effects in aquatic and shoreline organisms (Gomiero, Strafella, et al., 2019; Kögel et al., 2020). More plastic particle toxicity is reported for particle sizes below 10 μm compared to those above 10 μm. However, particles below 10 μm are unquantified in all environmental niches. In this study, most particles identified were <100 μm, meaning most particles are in the most dangerous size range studied. Accordingly, one study found increased mortality of shrimps exposed to particles below 100 μm, but not for those exposed to particles above 100 μm (Gray & Weinstein, 2017). Among the polymer types found in this study, PVC is the most hazardous (Lithner et al., 2011; Rochman et al., 2017) but is not among the most frequently detected polymers (less than 2%) found in this study.

The dominating shape of the MP particles in this study was fragments. When evaluating the impact of particle shape on organisms, concluding can be challenging due to the simultaneous consideration of multiple factors. This complexity makes it difficult to determine whether the observed effects stem from the particle shape or are influenced by other variables, such as polymer type or size. However, the shape of the particles significantly influences the number of particles ingested by marine animals. Fragments tend to be ingested more than fibres (Gray & Weinstein, 2017; Ory et al., 2017). In the SPSG, fish (Amberstripe scad) demonstrated a preference for ingesting blue fragments, likely due to their resemblance to their copepod prey (Ory et al., 2017).

4.6 Literature Comparison

The lack of standardised protocols for MP quantifications and identification leads to dissimilarities in methods and makes it hard to compare with previous studies. For instance, many studies that use Manta trawls have reported their results in area units making it hard to compare with other studies reporting in volume units this study. As this study has highlighted, different analysis methods greatly influence the results. QCL-IR is a quite new technology that is not so common in the MP scientific community yet. Therefore, results from μ-FTIR are more

comparable to other studies at the current time point. Different studies show different concentrations and a goal for the future is a quantitative comparison between studies. However, one pattern is clear, the lower the size limit, the more particles are found.

4.6.1 Open Ocean

There are very limited studies on MP in the open ocean of the South Pacific gyre, while there are many more studies in the northern part of the Pacific. The studies in the North Pacific using pump filtration are generally not comparable to those using Manta trawl in the same area (**Table 3**). This demonstrates how the pump filtration system manages to capture many more particles when using a smaller mesh size than Manta trawls. Results from μ-FTIR in this study in the South Pacific show almost the same concentrations as pump filtrations have revealed in the North Pacific (Cui et al., 2022; Desforges et al., 2014). Model estimates by Lebreton et al. (2012) show a much lower concentration of floating debris in the southern hemisphere, which contrasts with results from this study and the study by Eriksen et al. (2013). However, as already stated, quantitative comparisons must be made cautiously, due to the different methods and mesh sizes used.

Pump filtrations done in the Atlantic Ocean show concentrations several orders of magnitude lower than what has been found in the Pacific Ocean (La Daana et al., 2017; Lusher et al., 2014; Pakhomova et al., 2022). However, the three studies from the Atlantic in this comparison had a lower size limit of 100 and 250 μm. As observed in this study, 92% of the particles analysed with QCL-IR were smaller than 100 μm, which might explain the lower concentrations found in the Atlantic. A study by Hildebrandt et al. (2022) in the Indian Ocean used pump filtration with a lower size limit of 20 μm, just like this study, and found concentrations at approximately four orders of magnitude lower than what was found in this study (with μ-FTIR) in the South Pacific.

Table 3: *Abundance of MP in different oceans (North Pacific, South Pacific, Indian, and Atlantic Ocean) as summarized by a selection of studies. Results are given as mean ± standard deviation in MP m^{-3}, the study by Eriksen et. al. is one exception, where the result is shown as mean MP km^{-2}.*

Location	**Year**	**Sampling method**	**Lower size limit**	**Concentration (mean)**	**Most frequent polymer**	**Reference**
North-Western Pacific	2017	Manta trawl	330 µm	0.06 ± 0.03 MP m^{-3}	ER, PP	Liu et al. (2021)
North-Western Pacific	2017	Manta trawl	330 µm	0.030 ± 0.017 MP m^{-3}	PET	Mu et al. (2019)
North-Western pacific	2018	Pump filtration	44 µm	201 ± 134 MP m^{-3}	PES, nylon	Cui et al. (2022)
North-East pacific	2012	Pump filtration	62,5 µm	279 ± 178 MP m^{-3}	Not identified	Desforges et al. (2014)
Mid-North Pacific	2019	Manta trawl	330 µm	0.51 ± 0.36 MP m^{-3}	PP, PE	Pan et al. (2022)
South Pacific Ocean	2011	Manta trawl	333 µm	26 898 MP **km^{-2}**	Not identified	Eriksen et al. (2013)
South Pacific Ocean	**2022**	**Pump filtration**	**20 µm**	**3564 ± 2374 MP m^{-3} (QCL-IR) 206 ± 52 MP m^{-3} (µ-FTIR)**	**PE**	**This study**
Indian Ocean	2022	Pump filtration	20 µm	20-300 µm: 50 ± 30 MP m^{-3}	PU, PET	Hildebrandt et al. (2022)
North-East Atlantic	2013	Pump filtration	250 µm	2.46 ± 2.43 MP m^{-3}	Not identified	Lusher et al. (2014)
North and South Atlantic	2019 - 2020	Pump filtration	100 µm	0.7 ± 0.6 MP m^{-3}	PET	Pakhomova et al. (2022)
North and South Atlantic	2015	Pump filtration	250 µm	1.15 ± 1.45 MP m^{-3}	Polyester	La Daana et al. (2017)

4.6.2 South Pacific Islands

Most MP studies by the coast of South Pacific islands used a Manta trawl for sampling, and no studies using pump filtration were found (**Table 4**). Results are, therefore, hard to compare. In Suva harbour, three different methods have been used (plankton net, bottle sampling, and pump filtration (this study)), showing three completely different concentrations (0.10, 2000, and 118 MP m^{-3}, respectively). The bottle sampling showed the highest concentration, probably due to the characterisation of particles down to 0.45 µm. Studies using Manta or plankton trawl generally report much lower MP concentrations than those using pump filtration or bottle sampling. No other study of MP concentration in Papeete harbour was found, but within this study, a lower concentration was found in Papeete compared to Suva. This difference could be related to the larger population size in Suva (~90K), compared to Papeete (~27K).

***Table 4**: Abundance of MP at different South Pacific Islands as summarised by a selection of studies. Results are given as mean ± standard deviation in MP m−3.*

Location	**Year**	**Equipment**	**Lower size limit**	**Concentration (mean)**	**Most frequent polymer**	**Reference**
Vava'u, Tonga	2017	Plankton net	100 µm	1.05 ± 0.13 MP m^{-3}	PES, PE	Markic et al. (2022)
Vanuatu	2018	Manta trawl	335 µm	0,09 - 0,57 MP m^{-3}	PE, PS, PP	Bakir et al. (2020)
Papeete Harbour, Tahiti	**2022**	**Pump filtration**	**20 µm**	**16 ± 13,5 MP m^{-3} (µ-FTIR)**	**Polyester, PE**	**This study**
Atolls, French Polynesia	2017 – 2018	Manta trawl	335 µm	2.4 ± 2.3 MP m^{-3}	PE	Gardon et al. (2021)
Suva Harbour, Fiji	2016 – 2018	Plankton net	125 µm	0.10 ± 0.02 MP m^{-3}	PE, latex, PP	Ferreira et al. (2020)

Suva Harbour, Fiji	2018	Bottle sampling	0,45 μm	2,0 MP/L (2000 MP m^{-3})	PET, PE, PP	Dehm et al. (2020)
Suva Harbour, Fiji	**2022**	**Pump filtration**	**20 μm**	**118 ± 84 MP m^{-3} (μ-FTIR)**	**PP**	**This study**

4.7 Method Assessment and Future Implications

In this study, the sampling and preparation protocol for the analysis of MP in seawater samples has been standardised at two different MP laboratories in Norway (Bergen and Stavanger). However, due to two different analysis instruments and post-processing software, the analysis could not be harmonised, as the results cannot be compared directly. Despite that, this is a big first step towards harmonisation. Which laboratory you employ to analyse your data will, ideally, become irrelevant in the future. With the best sampling and analysis methods integrated and standardised, quantitative regulatory measurements and comparisons can be made, and most important, evaluation of prevention actions can be made. This study presents a protocol for identifying MPs from water samples, but this, like any other MP analysis method, has limitations.

4.7.1 Sampling Area

In Valparaiso harbour and the economic zone of Valparaiso (200 nautical miles from land), research permission was not given, and this also applies to the economic sone of Cook Islands, Niue, and Tonga. That is why there is some space between the station in French Polynesia and Fiji. Optimally there should be a higher number of stations in this study, but because of a lack of research permissions and time limitations, 14 (x3 replicates) stations were sampled during the transect. The transect is one of the least explored areas in terms of MP research and, therefore, a very interesting leg.

4.7.2 Sampling Technique

A high-volume water pump connected to the seawater intake is still recommended for future studies. Pump filtration while the ship is in motion is an effective way to sample large volumes of water. This study collected approximately 1050 L of seawater at each station number (3 x

350 L). The seawater intake of the ship in this study is old, and unfortunately, the pipes are quite rusty, which led to an accumulation of rust on the filters. On a more modern research ship, this should not be a problem. At the ship during filtration, some samplings were affected by a small leakage in the filtration unit, and particles might have escaped the filter.

Pump filtration allows us to use a smaller mesh size than 300 µm, which is extremely important in MP research as these smaller-sized particles are predominant. Filtering seawater with a mesh size of 300 µm or 100 µm gives a difference in particle number by four orders of magnitude (Covernton et al., 2019). Manta trawls are probably underestimating the abundance of MP because of the large mesh size. Using a smaller mesh size in Manta trawls could push MPs out of the way and prevent their entrance into the net (Löder & Gerdts, 2015). As reviewed by Kögel et al. (2020), more plastic particle toxicity is reported below particle size 10 µm, and future studies should aim to quantify particles even smaller than 10 µm in the environment to determine the realistic conditions.

4.7.3 Digestion and Analysis Preparation

Digestion of seawater samples is recommended as all samples contained some organic matter like zooplankton and phytoplankton. However, acids and oxidative agents could affect the polymer integrity. H_2O_2 (30%), which was used for at least five hours during the procedure, could degrade PA (nylon) (Karami et al., 2017). Only 3% PA was identified by QCL-IR, and only 1,4% PA was identified by µ-FTIR. Some of it could have degraded before analysis, but PA is also a high-density polymer and is not expected in high concentrations at surface waters.

Rust in the samples was an unexpected issue that caused us some trouble during the sample preparation and analysis. For most samples, we had to use 1 M HCl, and in some samples even concentrated 12 M HCl to remove the rust. Concentrated HCl could dissolve some plastic particles (mainly PC and PA), but temperature and time are major influencing factors (Pfeiffer & Fischer, 2020). This study used concentrated HCl for less than one minute at room temperature. Still, in this short period, the most HCl-sensitive polymers, PC and PA, might have dissolved (Dehaut et al., 2016). Since PC and PA have a higher density than water, these are not expected to be found in high quanta in surface water samples. HCl might cause clumping of PET and surface modifications of PVC during a longer exposure time (Karami et

al., 2017), but probably not in less than a minute. PE, PP, and PS show good resistance to HCl and should not be affected during this short time (Karami et al., 2017).

4.7.4 IR – Analysis

Even after HCl treatment, some samples contained a lot of rust particles. These rust particles could potentially hide some plastic particles underneath. The instruments managed to detect plastic particles even on the rustiest filters. Still, there is a chance that rust is completely covering some particles and that the instrument might underestimate the number of particles.

This study has highlighted how different analysis instruments can give two different answers to a question. Some differences between the instruments are presented in **Table 5.** It was observed that QCL-IR identified a higher number of particles (approximately 20 orders of magnitude), more particles in the smaller size range (<100 μm), and more PE than μ-FTIR. The results did not support the hypothesis: iii) The two different analysis methods with associated software will give comparable MP concentrations and characteristics. It is unknown if the higher number of particles identified by QCL-IR is because of the instrument itself (or the post-processing technology. The QCL-IR instrument, SPERO QT, was recently installed at IMR, and the post-processing method based on AI was newly developed and used for the first time in this thesis. Further research and development of the instrumentation and post-processing methods of the QCL-IR instrument are needed before harmonising the two laboratories can be achieved.

***Table 5**: Comparison of QCL-IR and μ-FTIR characteristics.*

	QCL-IR	**μ-FTIR**
Resolution (Pixel size)	4.2 μm	6.25 μm
Acquisition	Wavelength by wavelength	All wavelengths at det same time
Signal-to-noise ratio (S/N)	Higher S/N	Lower S/N
Speed	Faster	Slower
Wavelength range	Mid-infrared region	Mid-, near-, and far-infrared region
Detection size (pixels)	480 x 480	64 x 64
Field of view	~ 2 mm	~ 27 mm
Post-processing	Artificial intelligence	SiMPLe
Result	More efficient, more detailed, can detect smaller sizes due to higher resolution, new method, will benefit on validation in future studies	Reliable, identifies a wide range of chemical compounds, confirmed by extended usage within the scientific community

4.7.5 Contamination Controls and Quality Assurance

There are many different steps in the preparation procedure which also means a risk of losing particles at each step. Particles could stick to the walls of the crystalising dish and the beakers. Especially in the last step, where the samples are concentrated in an evaporation beaker, particles could dry and get stuck to the glass walls. As mentioned, a recovery test was earlier performed at the NORCE laboratory with a recovery efficiency spanning over 92-98% within the investigated masses (Gomiero et al., 2021), which is considered quite good. A recovery test should also be performed at the IMR laboratory in the future.

Of course, there was also a risk of adding particles to the samples, especially clothing fibres. The contamination controls can estimate how much contamination our samples have been

exposed to. Although, it would not be correct to subtract the number of particles in the contamination controls from the number of particles from the seawater samples. The contamination is considered low, apart from passive blank batch 2 and procedural blank batch 3 at IMR. Still, this would not greatly affect the seawater sample results. However, we should still strive for less contamination in the MP laboratories.

5 Conclusion

MP in surface water has been the subject of numerous research, but there has been limited information on MP in the South Pacific Ocean. The observed distribution pattern of MP in the South Pacific showed higher concentrations of MP in the SPSG. The high number of MP found in this study might indicate an earlier underestimation of plastic sources in the South Pacific Ocean. Generally, particles smaller than 300 μm were predominant, accounting for 98% of the identified particles. Further, PE and PP were the dominating polymers, and fragments were the dominating morphological characteristic. The sampled MPs were found in the same ocean current system, which indicates that the MP along this transect share a common fate, probably ending up in the compact accumulation area in the SPSG for an unknown timespan. Because of the high concentrations of MP and oligotrophic conditions in this area (Ras et al., 2008; Sigman & Hain, 2012), species here may suffer from an increased ingestion rate of MP (Markic et al., 2018), which is a threat to the marine ecosystems and populations at the South Pacific islands which rely on marine ecosystem services for a living.

This study presents new data to the field while keeping a critical view of MP sampling and analysis methods used today. Under-way seawater filtering at the ship's seawater intake is a promising and time-efficient way to sample MP. It also enables a lower size limit than what is usually used today. The new QCL-IR instrument gave different results than the commonly used μ-FTIR instrument. However, QCL-IR might dominate MP analysis in the future as it can provide high-quality data at a high speed (Primpke et al., 2020). Method harmonisation/standardisation must be a priority in future studies. Without methods we can trust, it is hard to see if prevention actions have an effect, and our capacity to evaluate the ecological effect critically is limited. Further, more knowledge is needed on the vertical distribution of MP, as well as their seasonal distribution.

References

Al Nabhani, K., Salzman, S., Shimeta, J., Dansie, A., & Allinson, G. (2022). A temporal assessment of microplastics distribution on the beaches of three remote islands of the Yasawa archipelago, Fiji. *Marine pollution bulletin*, *185*, 114202.

Andrady, A. L. (2011). Microplastics in the marine environment. *Marine pollution bulletin*, *62*(8), 1596-1605. https://www.sciencedirect.com/science/article/pii/S0025326X11003055?via%3Dihub

Bakir, A., Desender, M., Wilkinson, T., Van Hoytema, N., Amos, R., Airahui, S., Graham, J., & Maes, T. (2020). Occurrence and abundance of meso and microplastics in sediment, surface waters, and marine biota from the South Pacific region. *Marine pollution bulletin*, *160*, 111572.

Ballent, A., Pando, S., Purser, A., Juliano, M., & Thomsen, L. (2013). Modelled transport of benthic marine microplastic pollution in the Nazaré Canyon. *Biogeosciences*, *10*(12), 7957-7970.

Barnes, D. K. (2002). Invasions by marine life on plastic debris. *Nature*, *416*(6883), 808-809.

Barnes, D. K., Galgani, F., Thompson, R. C., & Barlaz, M. (2009). Accumulation and fragmentation of plastic debris in global environments. *Philosophical Transactions of the Royal Society B: Biological Sciences*, *364*(1526), 1985-1998. https://www.ncbi.nlm.nih.gov/pmc/articles/PMC2873009/pdf/rstb20080205.pdf

Barnett, J., & Adger, W. N. (2003). Climate dangers and atoll countries. *Climatic change*, *61*(3), 321-337.

Barrows, A., Cathey, S. E., & Petersen, C. W. (2018). Marine environment microfiber contamination: Global patterns and the diversity of microparticle origins. *Environmental Pollution*, *237*, 275-284.

Behrenfeld, M. J., & Falkowski, P. G. (1997). Photosynthetic rates derived from satellite-based chlorophyll concentration. *Limnology and oceanography*, *42*(1), 1-20.

Benson, N. U., Agboola, O. D., Fred-Ahmadu, O. H., De-la-Torre, G. E., Oluwalana, A., & Williams, A. B. (2022). Micro (nano) plastics prevalence, food web interactions, and toxicity assessment in aquatic organisms: a review. *Frontiers in Marine Science*, *9*, 291.

Bergmann, M., Collard, F., Fabres, J., Gabrielsen, G. W., Provencher, J. F., Rochman, C. M., van Sebille, E., & Tekman, M. B. (2022). Plastic pollution in the Arctic. *Nature Reviews Earth & Environment*, *3*(5), 323-337.

Bhattacharya, P., Lin, S., Turner, J. P., & Ke, P. C. (2010). Physical adsorption of charged plastic nanoparticles affects algal photosynthesis. *The journal of physical chemistry C*, *114*(39), 16556-16561.

Borrelle, S. B., Ringma, J., Law, K. L., Monnahan, C. C., Lebreton, L., McGivern, A., Murphy, E., Jambeck, J., Leonard, G. H., & Hilleary, M. A. (2020). Predicted growth in plastic waste exceeds efforts to mitigate plastic pollution. *Science*, *369*(6510), 1515-1518.

Bourdages, M. P., Provencher, J. F., Baak, J. E., Mallory, M. L., & Vermaire, J. C. (2021). Breeding seabirds as vectors of microplastics from sea to land: Evidence from colonies in Arctic Canada. *Science of the Total Environment*, *764*, 142808.

Bråte, I., Halsband, C., Allan, I., & Thomas, K. (2014). Report made for the Norwegian Environment Agency: Microplastics in marine environments: Occurrence, distribution and effects. In.

Browne, M. A., Niven, S. J., Galloway, T. S., Rowland, S. J., & Thompson, R. C. (2013). Microplastic moves pollutants and additives to worms, reducing functions linked to health and biodiversity. *Current biology*, *23*(23), 2388-2392.

Carpenter, E. J., & Smith Jr, K. (1972). Plastics on the Sargasso Sea surface. *Science*, *175*(4027), 1240-1241.

Cassone, B. J., Grove, H. C., Elebute, O., Villanueva, S. M., & LeMoine, C. M. (2020). Role of the intestinal microbiome in low-density polyethylene degradation by caterpillar larvae of the greater wax moth, Galleria mellonella. *Proceedings of the Royal Society B*, *287*(1922), 20200112.

Chastel, O., Lacroix, A., Weimerskirch, H., & Gabrielsen, G. W. (2005). Modulation of prolactin but not corticosterone responses to stress in relation to parental effort in a long-lived bird. *Hormones and behavior*, *47*(4), 459-466.

Chubarenko, I., Bagaev, A., Zobkov, M., & Esiukova, E. (2016). On some physical and dynamical properties of microplastic particles in marine environment. *Marine pollution bulletin*, *108*(1-2), 105-112.

Cincinelli, A., Scopetani, C., Chelazzi, D., Lombardini, E., Martellini, T., Katsoyiannis, A., Fossi, M. C., & Corsolini, S. (2017). Microplastic in the surface waters of the Ross Sea (Antarctica): occurrence, distribution and characterization by FTIR. *Chemosphere*, *175*, 391-400. https://www.sciencedirect.com/science/article/pii/S0045653517302023?via%3Dihub

Cole, M., Lindeque, P., Fileman, E., Halsband, C., Goodhead, R., Moger, J., & Galloway, T. S. (2013). Microplastic ingestion by zooplankton. *Environmental science & technology*, *47*(12), 6646-6655.

Conkle, J. L., Báez Del Valle, C. D., & Turner, J. W. (2018). Are we underestimating microplastic contamination in aquatic environments? *Environmental management*, *61*(1), 1-8.

Covernton, G. A., Pearce, C. M., Gurney-Smith, H. J., Chastain, S. G., Ross, P. S., Dower, J. F., & Dudas, S. E. (2019). Size and shape matter: a preliminary analysis of microplastic sampling technique in seawater studies with implications for ecological risk assessment. *Science of the Total Environment*, *667*, 124-132.

Cózar, A., Echevarría, F., González-Gordillo, J. I., Irigoien, X., Úbeda, B., Hernández-León, S., Palma, Á. T., Navarro, S., García-de-Lomas, J., & Ruiz, A. (2014). Plastic debris in the open ocean. *Proceedings of the National Academy of Sciences*, *111*(28), 10239-10244. https://www.pnas.org/doi/pdf/10.1073/pnas.1314705111

Cui, Y., Liu, M., Selvam, S., Ding, Y., Wu, Q., Pitchaimani, V. S., Huang, P., Ke, H., Zheng, H., & Liu, F. (2022). Microplastics in the surface waters of the South China sea and the western Pacific Ocean: Different size classes reflecting various sources and transport. *Chemosphere*, *299*, 134456.

Dassow, P. v. (2014). Biological oceanography, biogeochemical cycles, and pelagic ecosystem functioning of the east-central South Pacific Gyre: focus on Easter Island and Salas y Gómez Island.

Dawson, A. L., Kawaguchi, S., King, C. K., Townsend, K. A., King, R., Huston, W. M., & Bengtson Nash, S. M. (2018). Turning microplastics into nanoplastics through digestive fragmentation by Antarctic krill. *Nature communications*, *9*(1), 1-8.

Dehaut, A., Cassone, A.-L., Frère, L., Hermabessiere, L., Himber, C., Rinnert, E., Rivière, G., Lambert, C., Soudant, P., & Huvet, A. (2016). Microplastics in seafood: Benchmark protocol for their extraction and characterization. *Environmental Pollution*, *215*, 223-233.

Dehm, J., Singh, S., Ferreira, M., & Piovano, S. (2020). Microplastics in subsurface coastal waters along the southern coast of Viti Levu in Fiji, South Pacific. *Marine pollution bulletin*, *156*, 111239.

Desforges, J.-P. W., Galbraith, M., Dangerfield, N., & Ross, P. S. (2014). Widespread distribution of microplastics in subsurface seawater in the NE Pacific Ocean. *Marine pollution bulletin*, *79*(1-2), 94-99.

Duncan, E. M., Broderick, A. C., Fuller, W. J., Galloway, T. S., Godfrey, M. H., Hamann, M., Limpus, C. J., Lindeque, P. K., Mayes, A. G., & Omeyer, L. C. (2019). Microplastic ingestion ubiquitous in marine turtles. *Global change biology*, *25*(2), 744-752.

Enders, K., Lenz, R., Stedmon, C. A., & Nielsen, T. G. (2015). Abundance, size and polymer composition of marine microplastics≥ 10 μm in the Atlantic Ocean and their modelled vertical distribution. *Marine pollution bulletin*, *100*(1), 70-81.

Eriksen, M., Liboiron, M., Kiessling, T., Charron, L., Alling, A., Lebreton, L., Richards, H., Roth, B., Ory, N. C., & Hidalgo-Ruz, V. (2018). Microplastic sampling with the AVANI trawl compared to two neuston trawls in the Bay of Bengal and South Pacific. *Environmental Pollution*, *232*, 430-439.

Eriksen, M., Maximenko, N., Thiel, M., Cummins, A., Lattin, G., Wilson, S., Hafner, J., Zellers, A., & Rifman, S. (2013). Plastic pollution in the South Pacific subtropical gyre. *Marine pollution bulletin*, *68*(1-2), 71-76.

Evenset, A., Leknes, H., Christensen, G. N., Warner, N., Remberger, M., & Gabrielsen, G. W. (2009). Screening of new contaminants in samples from the Norwegian Arctic: silver, platinum, sucralose, bisphenol A, tetrabrombisphenol A, siloxanes, phtalates (DEHP), phosphororganic flame retardants.

Farrell, P., & Nelson, K. (2013). Trophic level transfer of microplastic: Mytilus edulis (L.) to Carcinus maenas (L.). *Environmental Pollution*, *177*, 1-3.

Ferreira, M., Thompson, J., Paris, A., Rohindra, D., & Rico, C. (2020). Presence of microplastics in water, sediments and fish species in an urban coastal environment of Fiji, a Pacific small island developing state. *Marine pollution bulletin*, *153*, 110991.

Gardon, T., El Rakwe, M., Paul-Pont, I., Le Luyer, J., Thomas, L., Prado, E., Boukerma, K., Cassone, A.-L., Quillien, V., & Soyez, C. (2021). Microplastics contamination in pearl-farming lagoons of French Polynesia. *Journal of Hazardous Materials*, *419*, 126396.

Gillett, R., & Tauati, M. I. (2018). Fisheries of the Pacific Islands: regional and national information. *FAO fisheries and aquaculture technical paper*(625), I-400.

Gomiero, A., Haave, M., Kögel, T., Bjorøy, Ø., Gjessing, M., Lea, T. B., Horve, E., Martins, C., & Olafsen, T. (2020). TRACKing of PLASTtic emissions from aquaculture industry (TrackPlast).

Gomiero, A., Øysæd, K. B., Agustsson, T., van Hoytema, N., van Thiel, T., & Grati, F. (2019). First record of characterization, concentration and distribution of microplastics in coastal sediments of an urban fjord in south west Norway using a thermal degradation method. *Chemosphere*, *227*, 705-714.

Gomiero, A., Øysæd, K. B., Palmas, L., & Skogerbø, G. (2021). Application of GCMS-pyrolysis to estimate the levels of microplastics in a drinking water supply system. *Journal of Hazardous Materials*, *416*, 125708.

Gomiero, A., Strafella, P., Øysæd, K. B., & Fabi, G. (2019). First occurrence and composition assessment of microplastics in native mussels collected from coastal and offshore areas of the northern and central Adriatic Sea. *Environmental Science and Pollution Research*, *26*(24), 24407-24416.

Graham, E. R., & Thompson, J. T. (2009). Deposit-and suspension-feeding sea cucumbers (Echinodermata) ingest plastic fragments. *Journal of experimental marine biology and ecology*, *368*(1), 22-29.

Gray, A. D., & Weinstein, J. E. (2017). Size-and shape-dependent effects of microplastic particles on adult daggerblade grass shrimp (Palaemonetes pugio). *Environmental*

toxicology and chemistry, *36*(11), 3074-3080. https://setac.onlinelibrary.wiley.com/doi/pdfdirect/10.1002/etc.3881?download=true

Grøsvik, B. E., Granberg, M. E., Kögel, T., Lusher, A. L., Gomiero, A., Halldorsson, H. P., Madsen, A. K., Baak, J. E., Guls, H. D., & Magnusson, K. (2022). Microplastics in Arctic invertebrates: status on occurrence and recommendations for future monitoring. *Arctic Science*.

Haave, M., Lorenz, C., Primpke, S., & Gerdts, G. (2019). Different stories told by small and large microplastics in sediment-first report of microplastic concentrations in an urban recipient in Norway. *Marine pollution bulletin*, *141*, 501-513.

Hale, R. C., Seeley, M. E., La Guardia, M. J., Mai, L., & Zeng, E. Y. (2020). A global perspective on microplastics. *Journal of Geophysical Research: Oceans*, *125*(1), e2018JC014719.

Harrison, C. S., Siegel, D. A., & Mitarai, S. (2013). Filamentation and eddy− eddy interactions in marine larval accumulation and transport. *Marine Ecology Progress Series*, *472*, 27-44.

Hidalgo-Ruz, V., Gutow, L., Thompson, R. C., & Thiel, M. (2012). Microplastics in the marine environment: a review of the methods used for identification and quantification. *Environmental science & technology*, *46*(6), 3060-3075.

Hildebrandt, L., El Gareb, F., Zimmermann, T., Klein, O., Kerstan, A., Emeis, K.-C., & Pröfrock, D. (2022). Spatial distribution of microplastics in the tropical Indian Ocean based on laser direct infrared imaging and microwave-assisted matrix digestion. *Environmental Pollution*, *307*, 119547.

Hufnagl, B., Steiner, D., Renner, E., Löder, M. G., Laforsch, C., & Lohninger, H. (2019). A methodology for the fast identification and monitoring of microplastics in environmental samples using random decision forest classifiers. *Analytical Methods*, *11*(17), 2277-2285.

Hufnagl, B., Stibi, M., Martirosyan, H., Wilczek, U., Möller, J. N., Löder, M. G., Laforsch, C., & Lohninger, H. (2021). Computer-assisted analysis of microplastics in environmental samples based on μFTIR imaging in combination with machine learning. *Environmental science & technology letters*, *9*(1), 90-95.

Huserbråten, M. (In prep).

Jian, Q., Wang, S., Zhang, P., Zhang, J., Zhao, L., & Liu, D. (2022). Microplastic Variations in Land-Based Sources of Coastal Water Affected by Tropical Typhoon Events in Zhanjiang Bay, China. *Water*, *14*(9), 1455.

Karami, A., Golieskardi, A., Choo, C. K., Romano, N., Ho, Y. B., & Salamatinia, B. (2017). A high-performance protocol for extraction of microplastics in fish. *Science of the Total Environment*, *578*, 485-494.

Kershaw, P. (2015). *Sources, fate and effects of microplastics in the marine environment: a global assessment* (1020-4873).

Khoironi, A., Hadiyanto, H., Anggoro, S., & Sudarno, S. (2020). Evaluation of polypropylene plastic degradation and microplastic identification in sediments at Tambak Lorok coastal area, Semarang, Indonesia. *Marine pollution bulletin*, *151*, 110868. https://www.sciencedirect.com/science/article/pii/S0025326X19310240?via%3Dihub

Kiessling, T., Gutow, L., & Thiel, M. (2015). Marine litter as habitat and dispersal vector. In *Marine anthropogenic litter* (pp. 141-181). Springer, Cham.

Kim, J.-H., Yu, Y.-B., & Choi, J.-H. (2021). Toxic effects on bioaccumulation, hematological parameters, oxidative stress, immune responses and neurotoxicity in fish exposed to microplastics: A review. *Journal of Hazardous Materials*, *413*, 125423.

Koelmans, A. A., Redondo-Hasselerharm, P. E., Nor, N. H. M., de Ruijter, V. N., Mintenig, S. M., & Kooi, M. (2022). Risk assessment of microplastic particles. *Nature Reviews Materials*, *7*(2), 138-152.

Kögel, T., Bjorøy, Ø., Toto, B., Bienfait, A. M., & Sanden, M. (2020). Micro-and nanoplastic toxicity on aquatic life: Determining factors. *Science of the Total Environment*, *709*, 136050.

Kowalski, N., Reichardt, A. M., & Waniek, J. J. (2016). Sinking rates of microplastics and potential implications of their alteration by physical, biological, and chemical factors. *Marine pollution bulletin*, *109*(1), 310-319. https://www.sciencedirect.com/science/article/pii/S0025326X16303848?via%3Dihub

La Daana, K. K., Officer, R., Lyashevska, O., Thompson, R. C., & O'Connor, I. (2017). Microplastic abundance, distribution and composition along a latitudinal gradient in the Atlantic Ocean. *Marine pollution bulletin*, *115*(1-2), 307-314.

Law, K. L., & Thompson, R. C. (2014). Microplastics in the seas. *Science*, *345*(6193), 144-145.

Le Galloudec, O., Law Chune, S., Nouel, L., Fernandez, E., Derval, C., Tressol, M., Dussurget, R., Biardeau, A., & Tonani, M. (2018). Product user manual for the global ocean physical reanalysis product GLOBAL_REANALYSIS_PHY_001_030. *COPERNICUS Marine Environment Monitoring Service*. https://catalogue.marine.copernicus.eu/documents/PUM/CMEMS-GLO-PUM-001-024.pdf

Lebreton, L.-M., Greer, S., & Borrero, J. C. (2012). Numerical modelling of floating debris in the world's oceans. *Marine pollution bulletin*, *64*(3), 653-661.

Lehtiniemi, M., Hartikainen, S., Näkki, P., Engström-Öst, J., Koistinen, A., & Setälä, O. (2018). Size matters more than shape: Ingestion of primary and secondary microplastics by small predators. *Food webs*, *17*, e00097.

Lithner, D., Larsson, Å., & Dave, G. (2011). Environmental and health hazard ranking and assessment of plastic polymers based on chemical composition. *Science of the Total Environment*, *409*(18), 3309-3324.

Liu, G., Jiang, R., You, J., Muir, D. C., & Zeng, E. Y. (2019). Microplastic impacts on microalgae growth: effects of size and humic acid. *Environmental science & technology*, *54*(3), 1782-1789.

Liu, K., Wang, X., Wei, N., Song, Z., & Li, D. (2019). Accurate quantification and transport estimation of suspended atmospheric microplastics in megacities: Implications for human health. *Environment international*, *132*, 105127. https://www.sciencedirect.com/science/article/pii/S0160412019325206?via%3Dihub

Liu, M., Ding, Y., Huang, P., Zheng, H., Wang, W., Ke, H., Chen, F., Liu, L., & Cai, M. (2021). Microplastics in the western Pacific and South China Sea: Spatial variations reveal the impact of Kuroshio intrusion. *Environmental Pollution*, *288*, 117745.

Löder, M. G., & Gerdts, G. (2015). Methodology used for the detection and identification of microplastics—a critical appraisal. *Marine anthropogenic litter*, 201-227.

Lusher, A. (2015). Microplastics in the marine environment: distribution, interactions and effects. In *Marine anthropogenic litter* (pp. 245-307). Springer, Cham.

Lusher, A., Hollman, P., & Mendoza-Hill, J. (2017). *Microplastics in fisheries and aquaculture: status of knowledge on their occurrence and implications for aquatic organisms and food safety*. FAO.

Lusher, A. L., Burke, A., O'Connor, I., & Officer, R. (2014). Microplastic pollution in the Northeast Atlantic Ocean: validated and opportunistic sampling. *Marine pollution bulletin*, *88*(1-2), 325-333.

Lusher, A. L., Hurley, R., Arp, H. P. H., Booth, A. M., Bråte, I. L. N., Gabrielsen, G. W., Gomiero, A., Gomes, T., Grøsvik, B. E., & Green, N. (2021). Moving forward in microplastic research: A Norwegian perspective. *Environment International*, *157*, 106794.

Lusher, A. L., Tirelli, V., O'Connor, I., & Officer, R. (2015). Microplastics in Arctic polar waters: the first reported values of particles in surface and sub-surface samples. *Scientific reports*, *5*(1), 1-9.

Ma, J., Zhao, J., Zhu, Z., Li, L., & Yu, F. (2019). Effect of microplastic size on the adsorption behavior and mechanism of triclosan on polyvinyl chloride. *Environmental Pollution*, *254*, 113104. https://www.sciencedirect.com/science/article/pii/S0269749119336310?via%3Dihub

Maes, C., Grima, N., Blanke, B., Martinez, E., Paviet-Salomon, T., & Huck, T. (2018). A surface "superconvergence" pathway connecting the South Indian Ocean to the subtropical South Pacific gyre. *Geophysical Research Letters*, *45*(4), 1915-1922.

Manzoor, S., Naqash, N., Rashid, G., & Singh, R. (2021). Plastic material degradation and formation of microplastic in the environment: A review. *Materials Today: Proceedings*.

Markic, A., Bridson, J. H., Morton, P., Hersey, L., Maes, T., & Bowen, M. (2022). Microplastic pollution in the surface waters of Vava'u, Tonga. *Marine pollution bulletin*, *185*, 114243.

Markic, A., Niemand, C., Bridson, J. H., Mazouni-Gaertner, N., Gaertner, J.-C., Eriksen, M., & Bowen, M. (2018). Double trouble in the South Pacific subtropical gyre: Increased plastic ingestion by fish in the oceanic accumulation zone. *Marine pollution bulletin*, *136*, 547-564.

Martinez, E., Maamaatuaiahutapu, K., & Taillandier, V. (2009). Floating marine debris surface drift: convergence and accumulation toward the South Pacific subtropical gyre. *Marine pollution bulletin*, *58*(9), 1347-1355.

Mato, Y., Isobe, T., Takada, H., Kanehiro, H., Ohtake, C., & Kaminuma, T. (2001). Plastic resin pellets as a transport medium for toxic chemicals in the marine environment. *Environmental science & technology*, *35*(2), 318-324.

Maximenko, N., Hafner, J., & Niiler, P. (2012). Pathways of marine debris derived from trajectories of Lagrangian drifters. *Marine pollution bulletin*, *65*(1-3), 51-62. https://www.sciencedirect.com/science/article/pii/S0025326X11002189?via%3Dihub

Meyns, M., Primpke, S., & Gerdts, G. (2019). Library based identification and characterisation of polymers with nano-FTIR and IR-sSNOM imaging. *Analytical Methods*, *11*(40), 5195-5202.

Morel, A., Claustre, H., & Gentili, B. (2010). The most oligotrophic subtropical zones of the global ocean: similarities and differences in terms of chlorophyll and yellow substance. *Biogeosciences*, *7*(10), 3139-3151.

Mu, J., Zhang, S., Qu, L., Jin, F., Fang, C., Ma, X., Zhang, W., & Wang, J. (2019). Microplastics abundance and characteristics in surface waters from the Northwest Pacific, the Bering Sea, and the Chukchi Sea. *Marine pollution bulletin*, *143*, 58-65.

Neumann, S., Harju, M., Herzke, D., Anker-Nilssen, T., Christensen-Dalsgaard, S., Langset, M., & Gabrielsen, G. W. (2021). Ingested plastics in northern fulmars (Fulmarus glacialis): A pathway for polybrominated diphenyl ether (PBDE) exposure? *Science of the Total Environment*, *778*, 146313.

Ory, N. C., Sobral, P., Ferreira, J. L., & Thiel, M. (2017). Amberstripe scad Decapterus muroadsi (Carangidae) fish ingest blue microplastics resembling their copepod prey along the coast of Rapa Nui (Easter Island) in the South Pacific subtropical gyre. *Science of the Total Environment*, *586*, 430-437.

Pakhomova, S., Berezina, A., Lusher, A. L., Zhdanov, I., Silvestrova, K., Zavialov, P., van Bavel, B., & Yakushev, E. (2022). Microplastic variability in subsurface water from the Arctic to Antarctica. *Environmental Pollution*, *298*, 118808.

Pan, Z., Liu, Q., Sun, X., Li, W., Zou, Q., Cai, S., & Lin, H. (2022). Widespread occurrence of microplastic pollution in open sea surface waters: Evidence from the mid-North Pacific Ocean. *Gondwana Research*, *108*, 31-40.

Pfeiffer, F., & Fischer, E. K. (2020). Various digestion protocols within microplastic sample processing—evaluating the resistance of different synthetic polymers and the efficiency of biogenic organic matter destruction. *Frontiers in Environmental Science*, *8*, 572424.

Plastics-Europe. (2022). An analysis of European plastics production, demand and waste data. *Plastic-The Facts*.

Prata, J. C., da Costa, J. P., Duarte, A. C., & Rocha-Santos, T. (2019). Methods for sampling and detection of microplastics in water and sediment: a critical review. *TrAC Trends in Analytical Chemistry*, *110*, 150-159.

Primpke, S., Godejohann, M., & Gerdts, G. (2020). Rapid identification and quantification of microplastics in the environment by quantum cascade laser-based hyperspectral infrared chemical imaging. *Environmental science & technology*, *54*(24), 15893-15903.

Ras, J., Claustre, H., & Uitz, J. (2008). Spatial variability of phytoplankton pigment distributions in the Subtropical South Pacific Ocean: comparison between in situ and predicted data. *Biogeosciences*, *5*(2), 353-369.

Rebolledo, E. L. B., Van Franeker, J. A., Jansen, O. E., & Brasseur, S. M. (2013). Plastic ingestion by harbour seals (Phoca vitulina) in The Netherlands. *Marine pollution bulletin*, *67*(1-2), 200-202.

Rochman, C. M., Hoh, E., Kurobe, T., & Teh, S. J. (2013). Ingested plastic transfers hazardous chemicals to fish and induces hepatic stress. *Scientific reports*, *3*(1), 1-7.

Rochman, C. M., Parnis, J. M., Browne, M. A., Serrato, S., Reiner, E. J., Robson, M., Young, T., Diamond, M. L., & Teh, S. J. (2017). Direct and indirect effects of different types of microplastics on freshwater prey (Corbicula fluminea) and their predator (Acipenser transmontanus). *PloS one*, *12*(11), e0187664.

Rudel, R. A., Camann, D. E., Spengler, J. D., Korn, L. R., & Brody, J. G. (2003). Phthalates, alkylphenols, pesticides, polybrominated diphenyl ethers, and other endocrine-disrupting compounds in indoor air and dust. *Environmental science & technology*, *37*(20), 4543-4553.

Schönlau, C., Karlsson, T. M., Rotander, A., Nilsson, H., Engwall, M., van Bavel, B., & Kärrman, A. (2020). Microplastics in sea-surface waters surrounding Sweden sampled by manta trawl and in-situ pump. *Marine pollution bulletin*, *153*, 111019.

Semcesen, P. O., & Wells, M. G. (2021). Biofilm growth on buoyant microplastics leads to changes in settling rates: Implications for microplastic retention in the Great Lakes. *Marine pollution bulletin*, *170*, 112573.

Setälä, O., Norkko, J., & Lehtiniemi, M. (2016). Feeding type affects microplastic ingestion in a coastal invertebrate community. *Marine pollution bulletin*, *102*(1), 95-101.

Sheavly, S., & Register, K. (2007). Marine debris & plastics: environmental concerns, sources, impacts and solutions. *Journal of Polymers and the Environment*, *15*(4), 301-305.

Sigman, D. M., & Hain, M. P. (2012). The biological productivity of the ocean. *Nature Education Knowledge*, *3*(10), 21.

Tamminga, M., Stoewer, S.-C., & Fischer, E. K. (2019). On the representativeness of pump water samples versus manta sampling in microplastic analysis. *Environmental Pollution*, *254*, 112970.

Van Sebille, E., Aliani, S., Law, K. L., Maximenko, N., Alsina, J. M., Bagaev, A., Bergmann, M., Chapron, B., Chubarenko, I., & Cózar, A. (2020). The physical oceanography of the transport of floating marine debris. *Environmental Research Letters*, *15*(2), 023003.

Varea, R., Piovano, S., & Ferreira, M. (2020). Knowledge gaps in ecotoxicology studies of marine environments in Pacific Island Countries and Territories–A systematic review. *Marine pollution bulletin*, *156*, 111264.

Vianello, A., Jensen, R. L., Liu, L., & Vollertsen, J. (2019). Simulating human exposure to indoor airborne microplastics using a Breathing Thermal Manikin. *Scientific reports*, *9*(1), 1-11.

Vihtakari, M. (2022). ggOceanMaps: Plot data on oceanographic maps using "ggplot2". *R package version*, *1*(7).

World Health Organization. (2017). *WHO Country Cooperation Strategy 2018-2022 : Pacific Island Countries and Areas.* . https://apps.who.int/iris/handle/10665/272806

Wright, S. L., Thompson, R. C., & Galloway, T. S. (2013). The physical impacts of microplastics on marine organisms: a review. *Environmental Pollution*, *178*, 483-492.

Zettler, E. R., Mincer, T. J., & Amaral-Zettler, L. A. (2013). Life in the "plastisphere": microbial communities on plastic marine debris. *Environmental science & technology*, *47*(13), 7137-7146.

Appendices

Appendix A – Materials

Table 6A - Equipment used during sample preparation.

Equipment	**Application**	**Supplier**
Stainless steel filter, 10 µm	Filtration of samples	Rolf Kørner GmbH
Glass wear (crystallising dishes, beakers, and pipettes)	Preparation of samples	VWR
Anodisc filter	Filter for analysation	Whatman
Filtration glass wear	Filtration of solutions	Millipore
Tweezers	To remove/flush filters	-

Table 7A - Instruments used during the procedure.

Application	**Laboratory**	**Instrument**	**Supplier**
Laminar flow bench	NORCE	UTV-S-AR Safety cabinet	GRANT Bio
	HI	UCS 2-4 Safety cabinet	Faster
Ultrasonic cleaner	NORCE	Branson 200	Branson
	HI	Elmasonic P 60 H	Elma Schmidbauer GmbH
Cleaning of equipment	NORCE	Muffle oven	L3/12 Nabertherm GmbH
	HI	LHT oven	Carbolite Gero
Vacuum pump	NORCE	Chemical duty pump, 220 V750 Hz	Millipore
	HI	Diaphragm Pump, MPC 090 E	Welch
Analysis	NORCE	µFTIR - Nicolet iN10 MX Infrared Imaging Microscope	Thermo Fisher

	HI	IR- microscope – SPERO QT	Daylight solutions
Heating cabinet/ stirrer	NORCE	Termaks TS4151	Termaks
	HI	Innova 42	New Brunswick
Sample evaporation	NORCE	Zymark Turbo Vap 500	Zymark
	HI	TurboVap II	Biotage

Table 8A - Chemicals used during sample preparation.

Chemicals	**Formula**	**Supplier**
Hydrogen chloride acid 37%	HCl	Sigma Aldrich
Hydrogen peroxide 30%	H_2O_2	Sigma Aldrich
Ethanol	C_2H_6O	Antibac

Table 9A - Enzymes used during digestion.

Enzymes	**Lot**	**Supplier**
Cellulase, enzyme blend	SLCC1677	Sigma Aldrich
Viscozyme L, cellulolytic enzyme mixture	SLBZ5039	Sigma Aldrich

Table 10A - Composition of Acetate Buffer used in sample preparation.

Buffer	**Chemical**	**Mass**	**Molarity**
Acetate Buffer (0,1M, pH 4,8)	Sodium Acetate (mw: 82 g/mol)	11,544 g	0,07 M
	Acetic Acid (mw: 60,05 g/mol)	3,556 g	0,03 M
	HCl	Adjusting pH to 0,1M	1M

Table 11A - Softwares used for post-processing of data.

Software	**Application**	**Supplier**
Excel, version16.73	Datasheets	Microsoft
R – studio, version 2023.03.1+446	Statistical analysis and graphics	Posit, PBC
SiMPLe, version 1.3.2B	Reference database	SiMPLe
ChemVision, version 3.3.8	SPERO software and reference database	DRS Daylight Solutions
Machin learning (Hufnagl et al., 2021; Huserbråten, In prep)	Model based identification	-

Appendix B – Pictures and spectra maps

µ-FTIR - samples

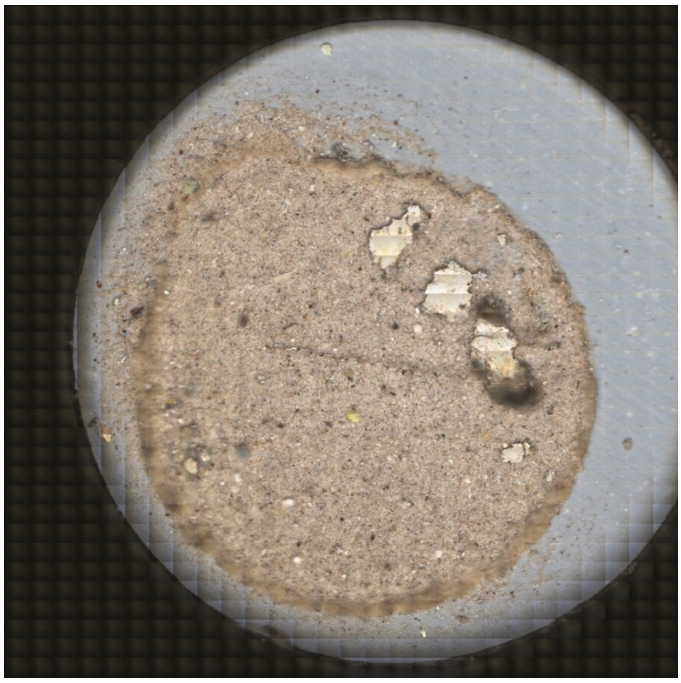

Figure 13B - Picture of analysis filter for sample 2A

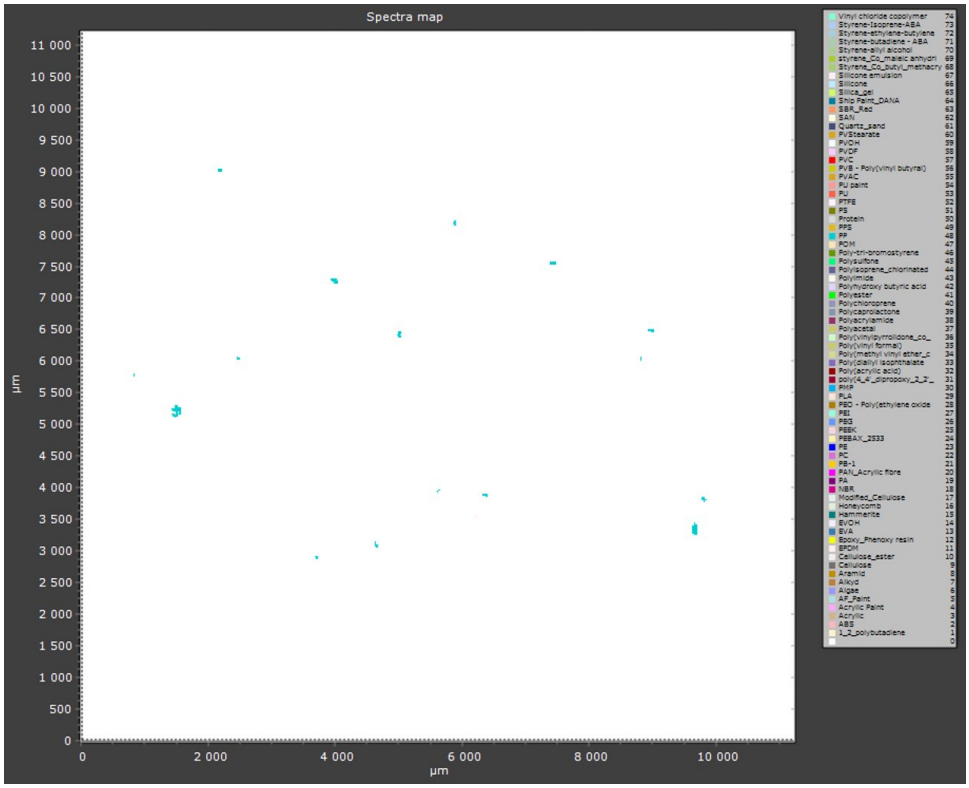

Figure 14B - Spectra map of sample 2A

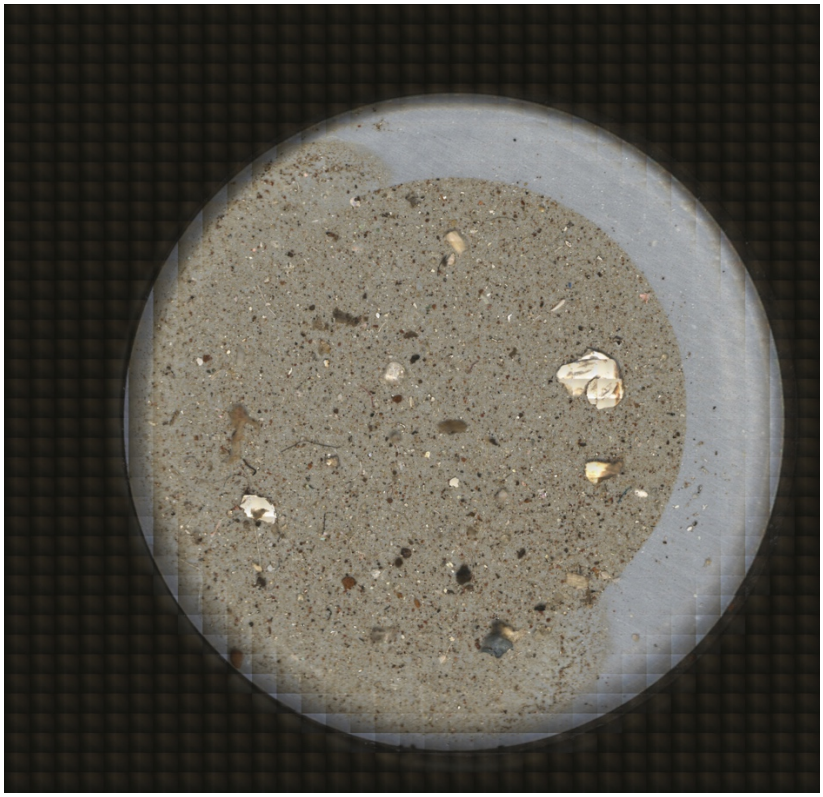

Figure 15B – Picture of analysis filter for sample 2B

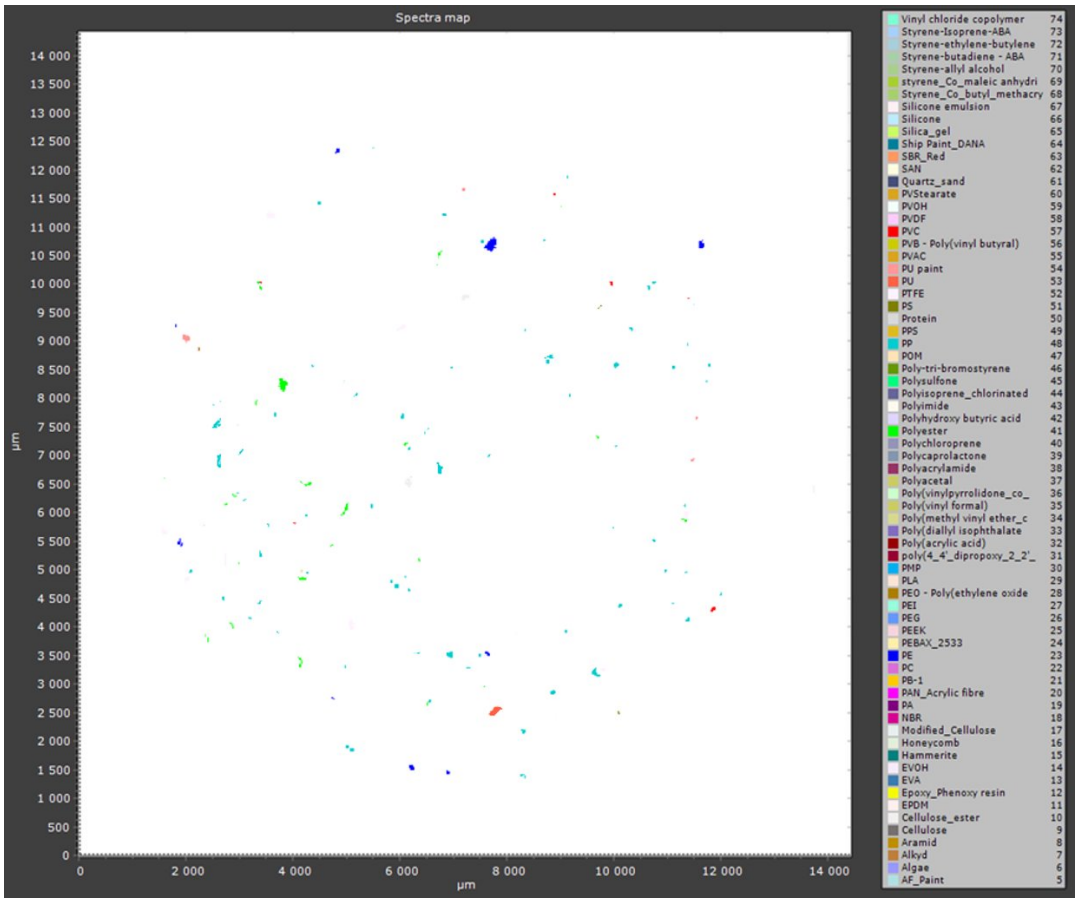

Figure 16B - Spectra map of sample 2B

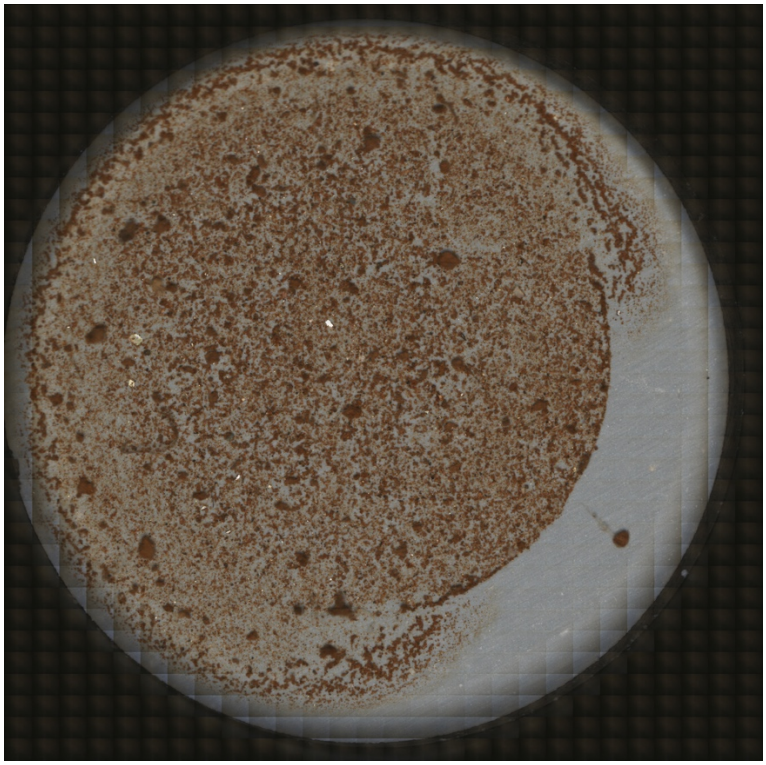

Figure 17B – Picture of analysis filter for sample 2C

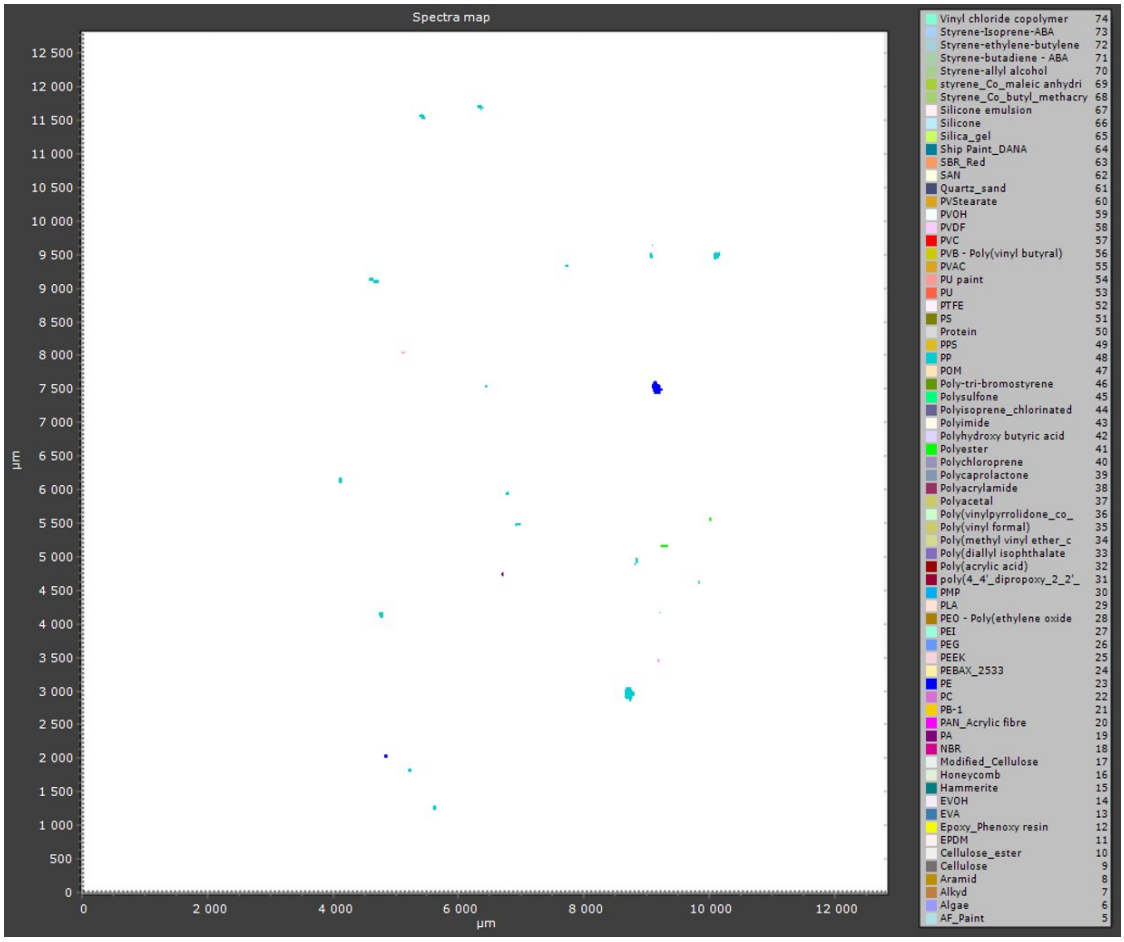

Figure 18B - Spectra map of sample 2C

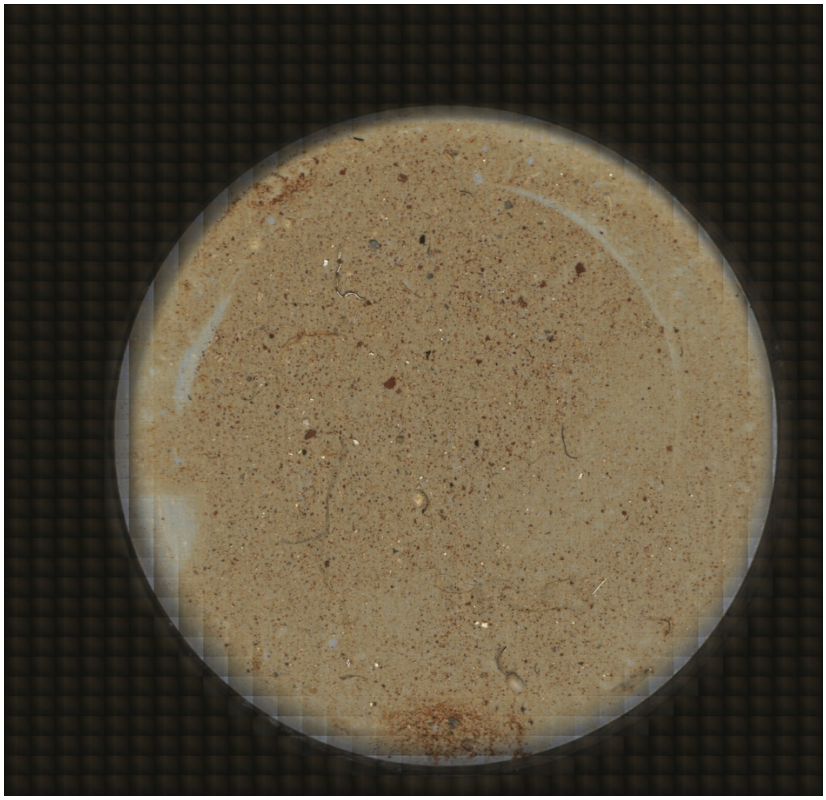

Figure 19B - Picture of analysis filter for sample 4A.

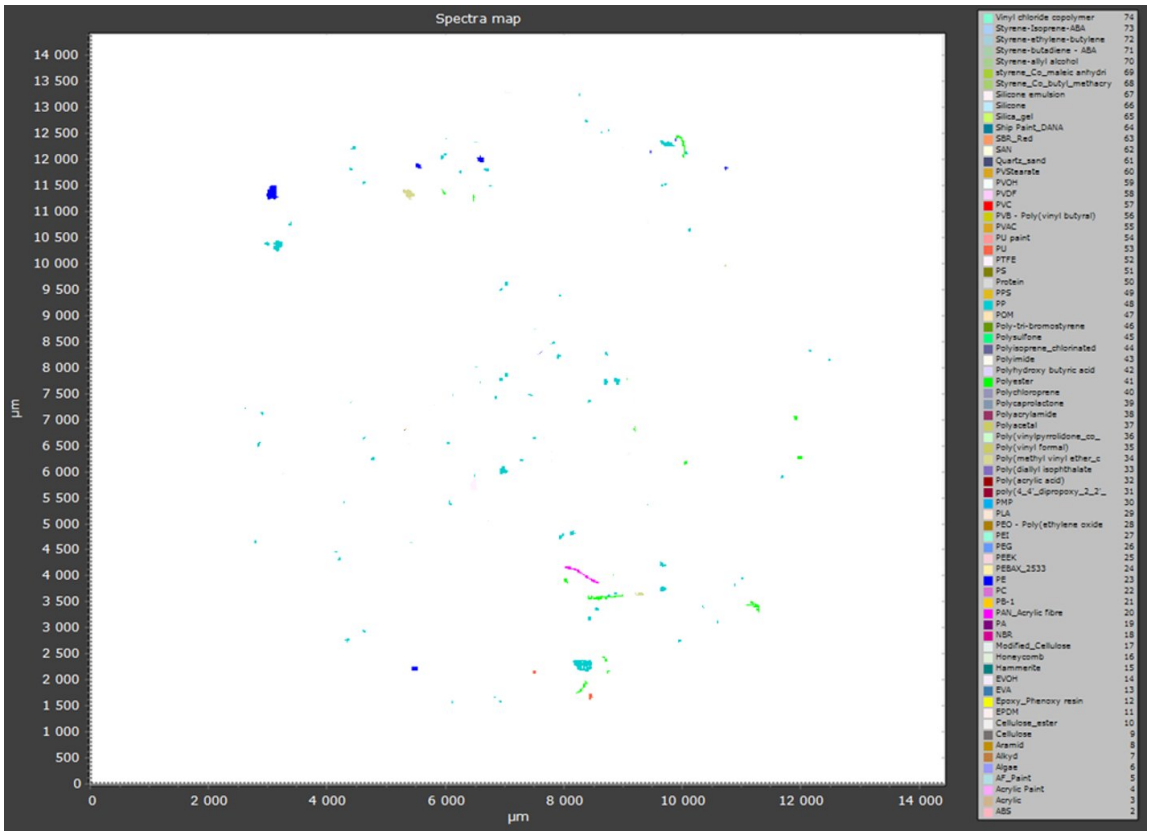

Figure 20B - Spectra map of sample 4A

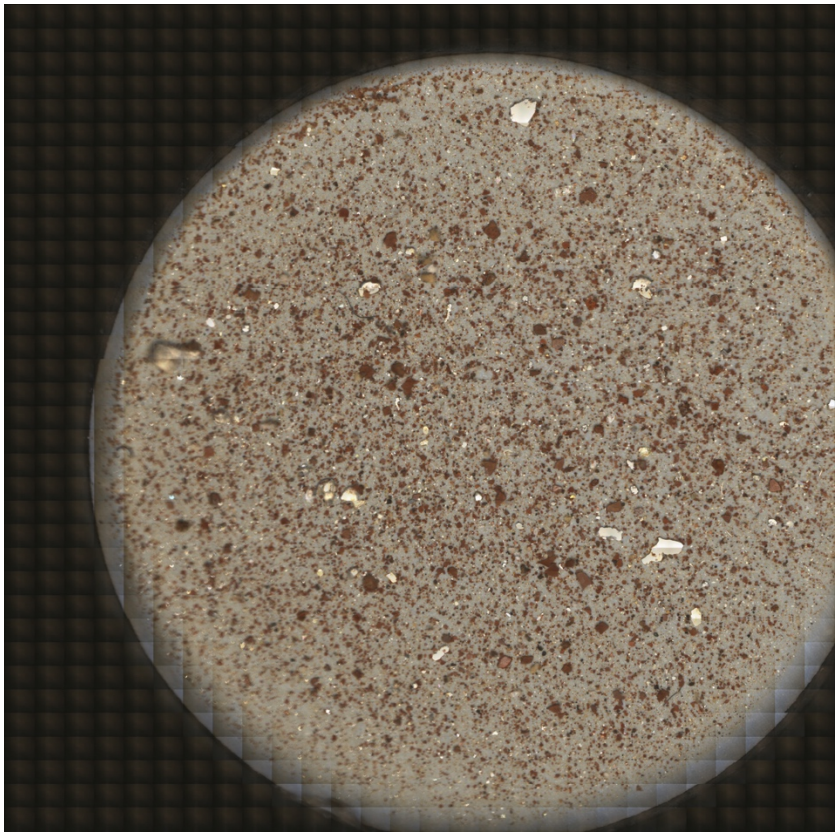

Figure 21B - Picture of analysis filter for sample 4B

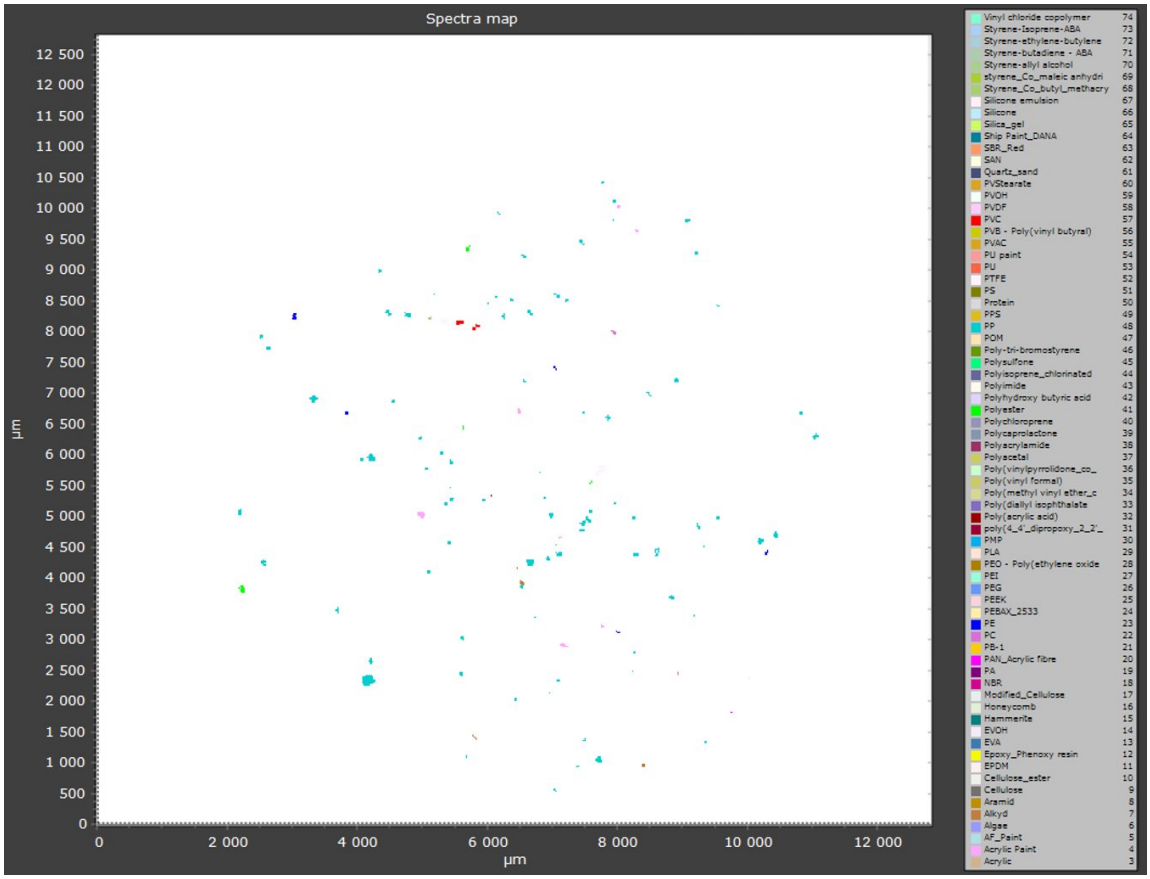

Figure 22B - Spectra map of sample 4B

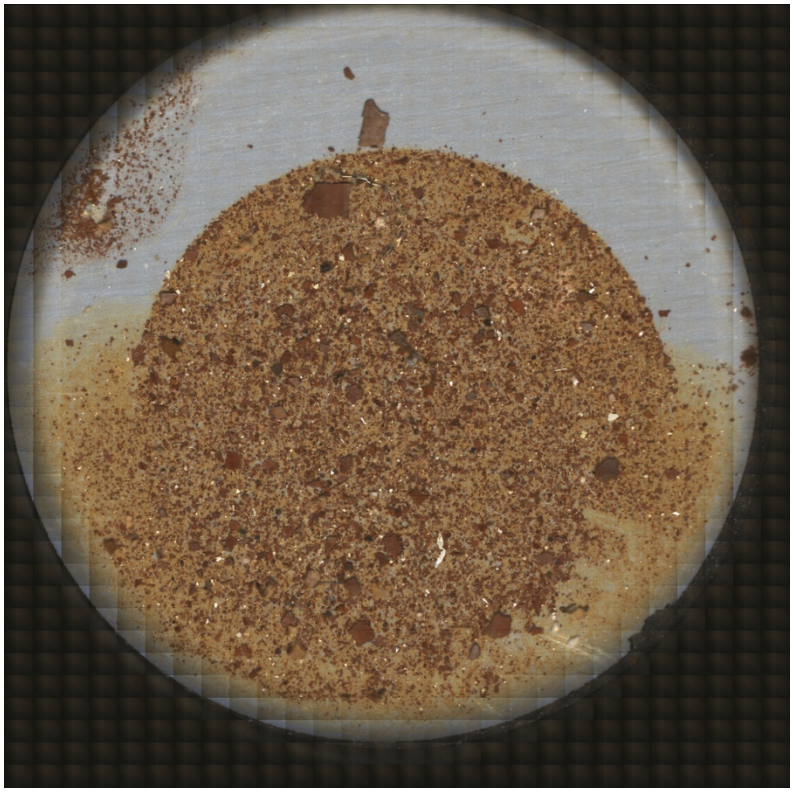

Figure 23B - Picture of analysis filter for sample 4C

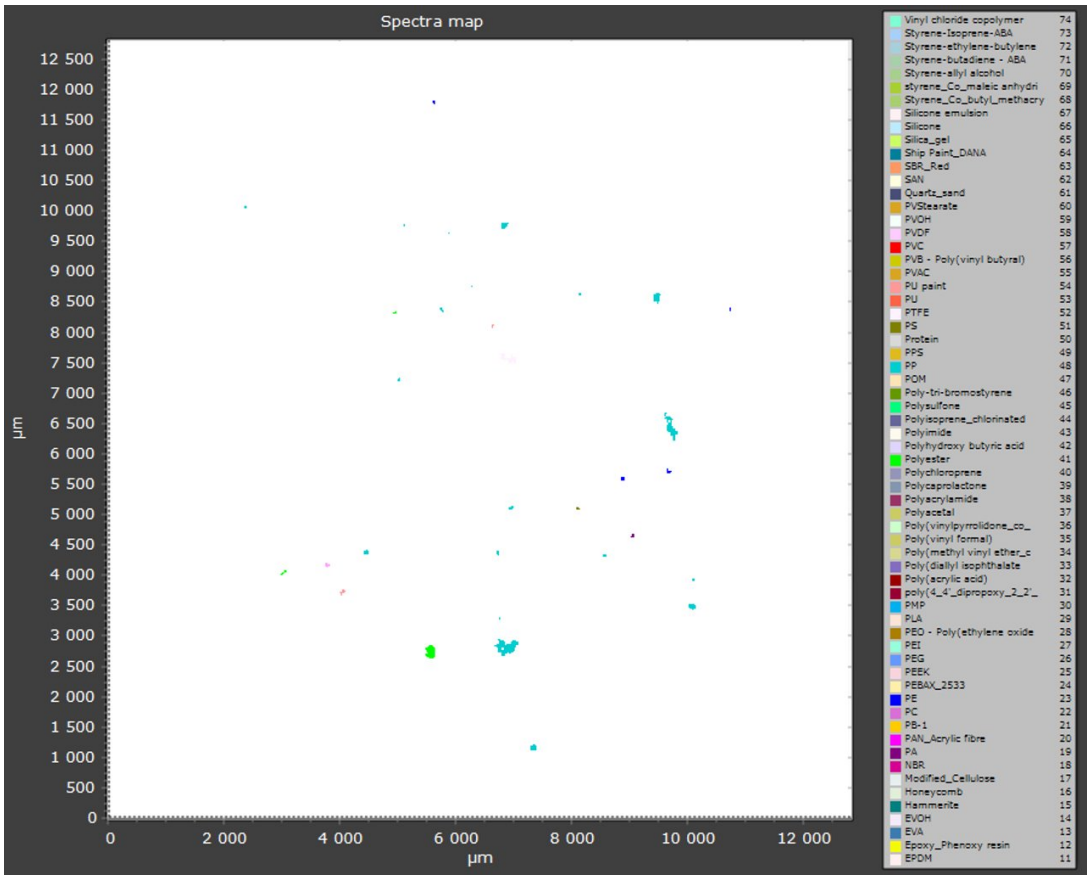

Figure 24B - Spectra map of sample 4C

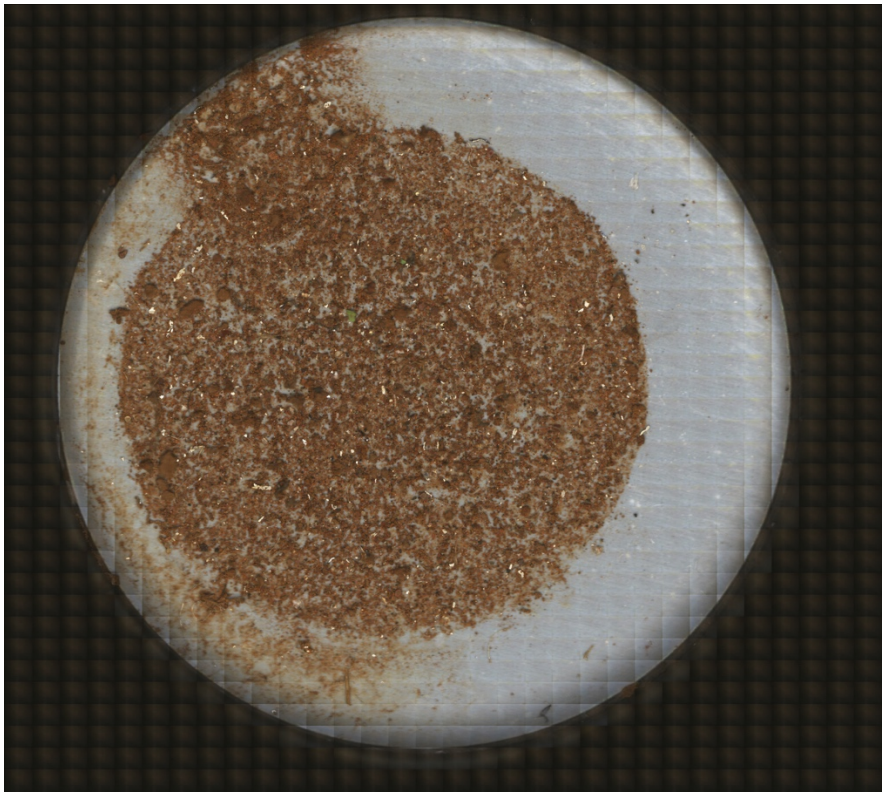

Figure 25B - Picture of analysis filter for sample 6A

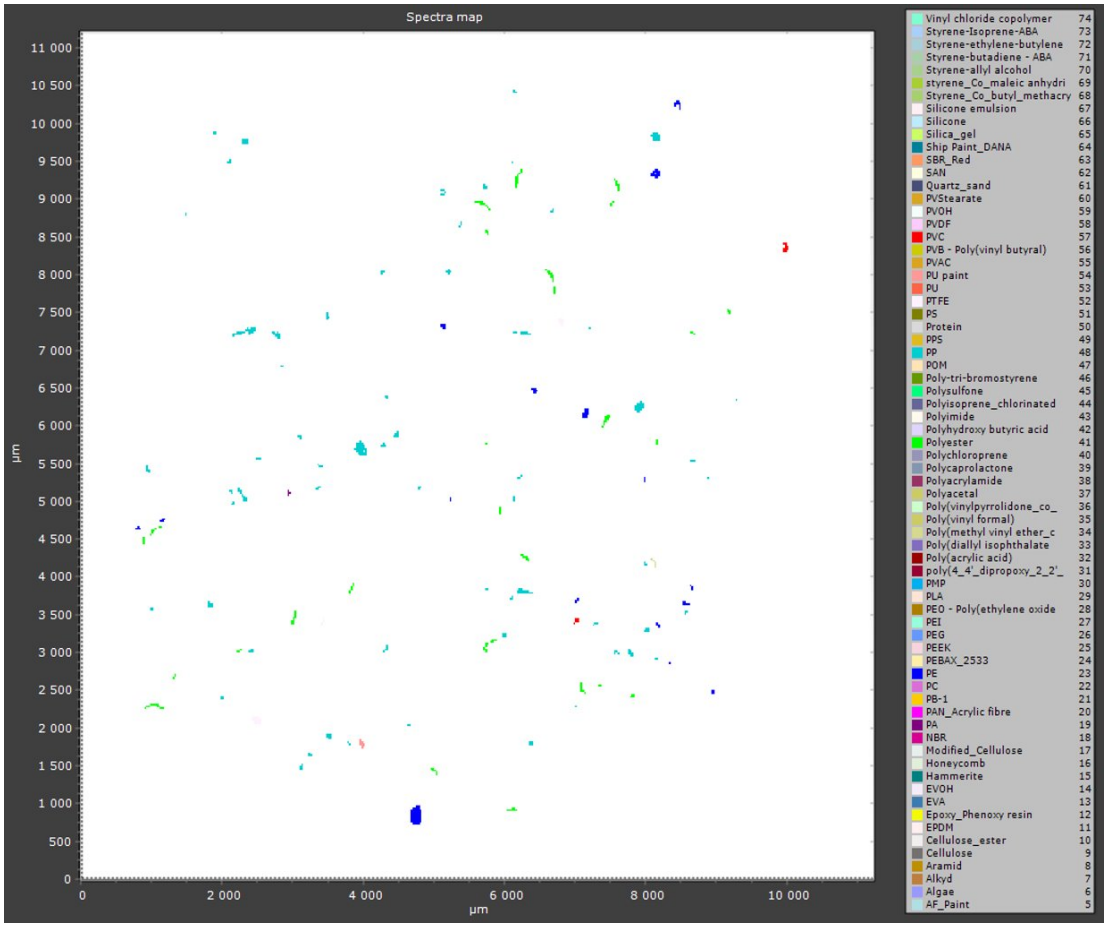

Figure 26B - Spectra map of sample 6A

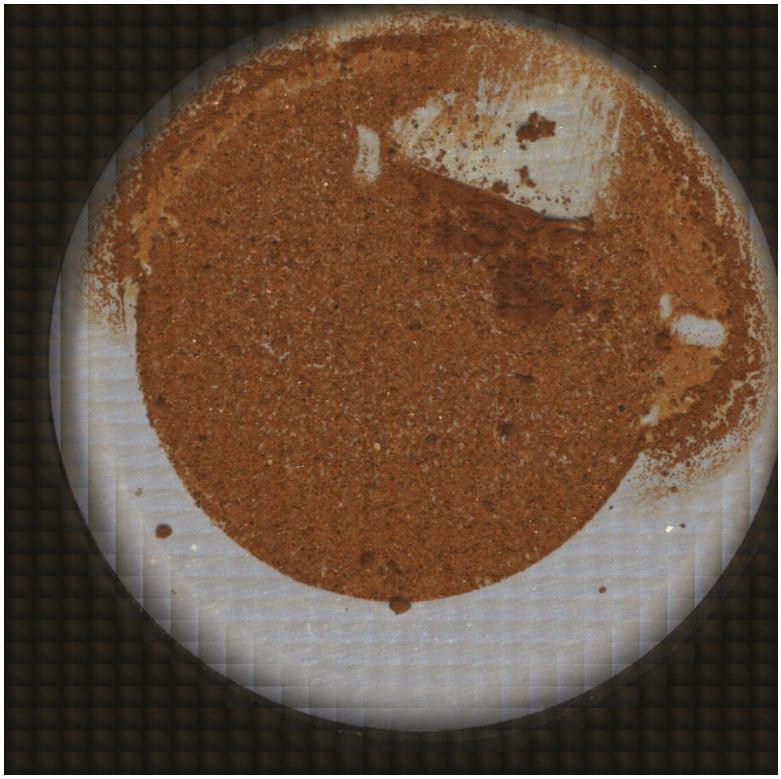

Figure 27B - Picture of analysis filter for sample 6B

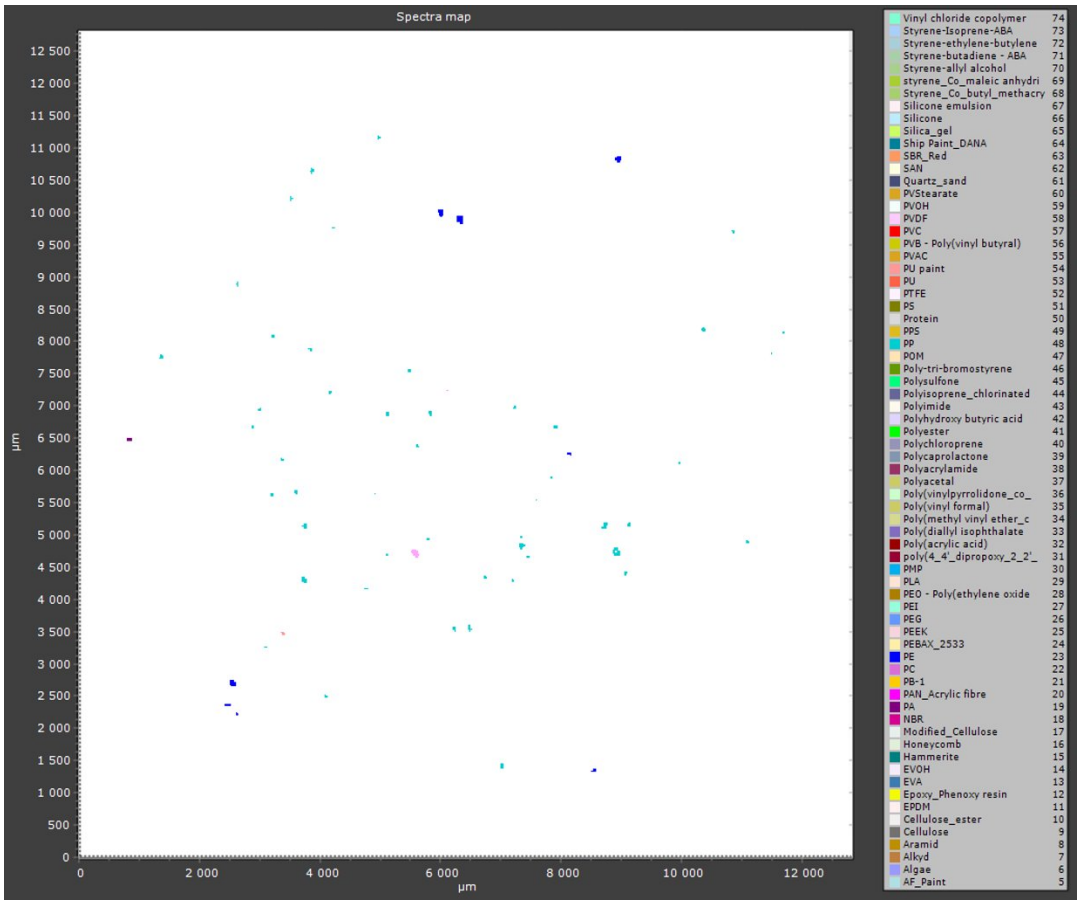

Figure 28B - Spectra map of sample 6B

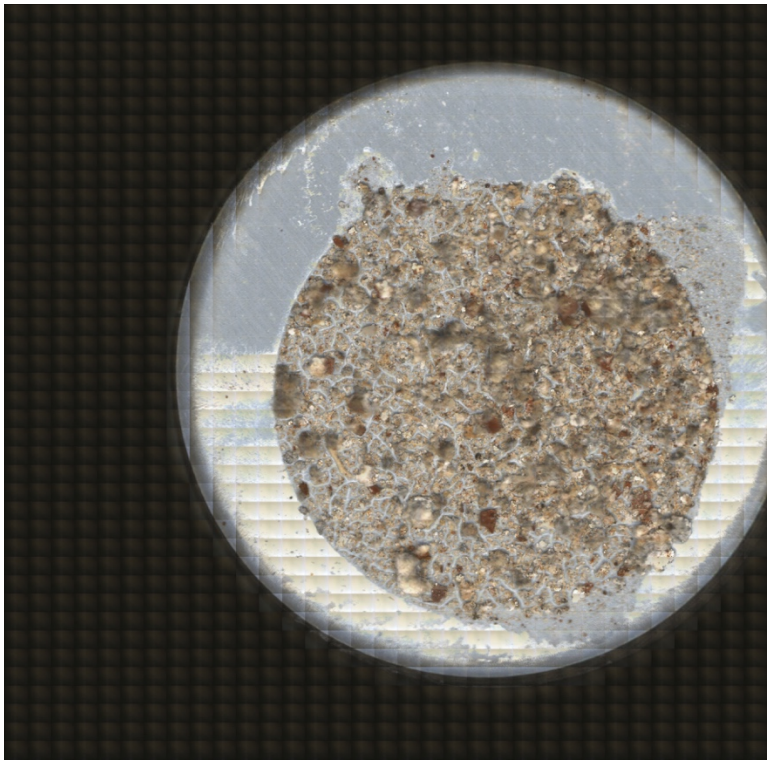

Figure 29B - Picture of analysis filter for sample 6C

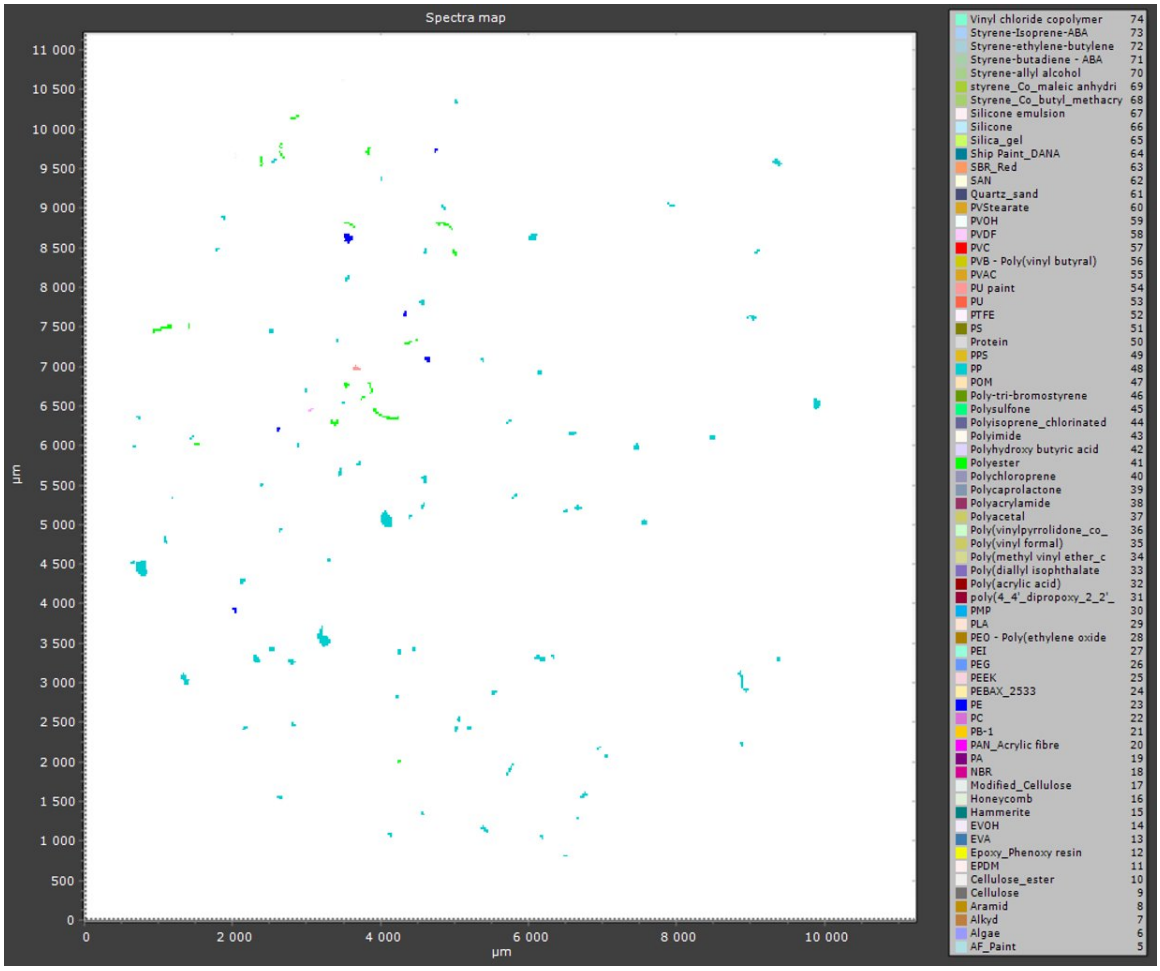

Figure 30B - Spectra map of sample 6C

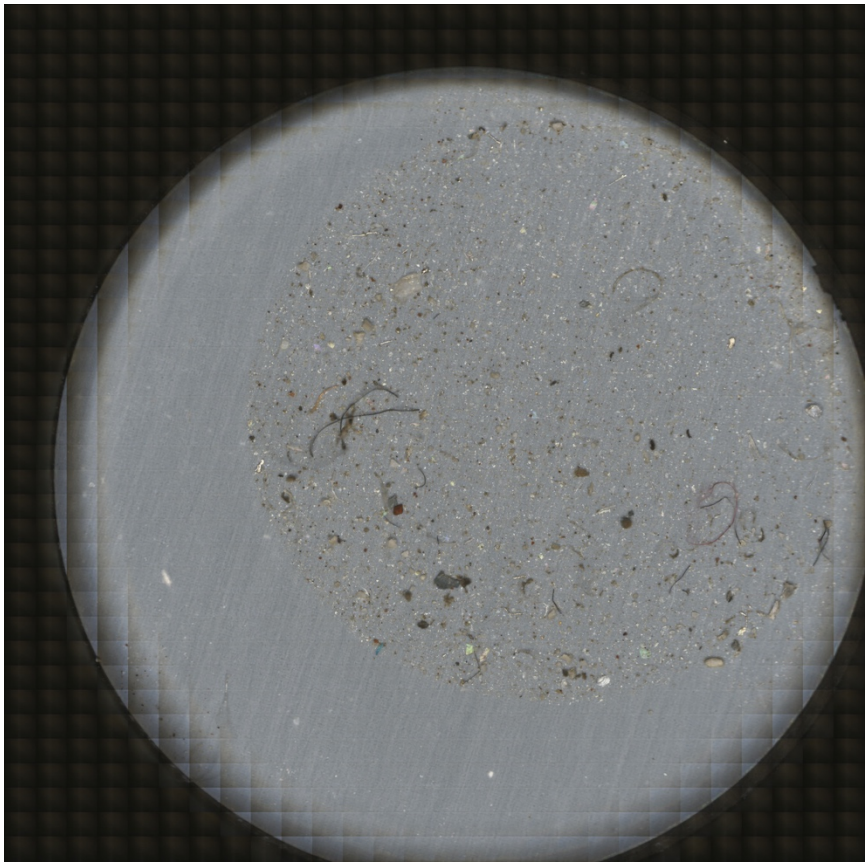

Figure 31B - Picture of analysis filter for sample 8A

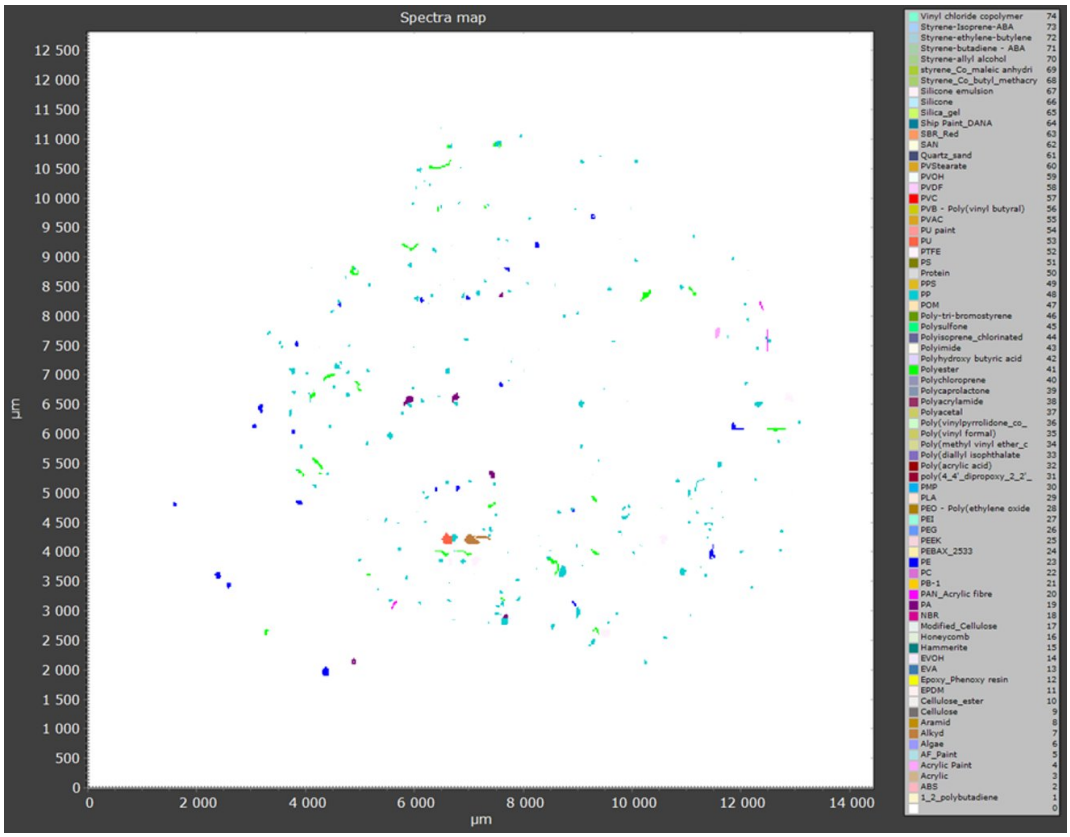

Figure 32B - Spectra map of sample 8A

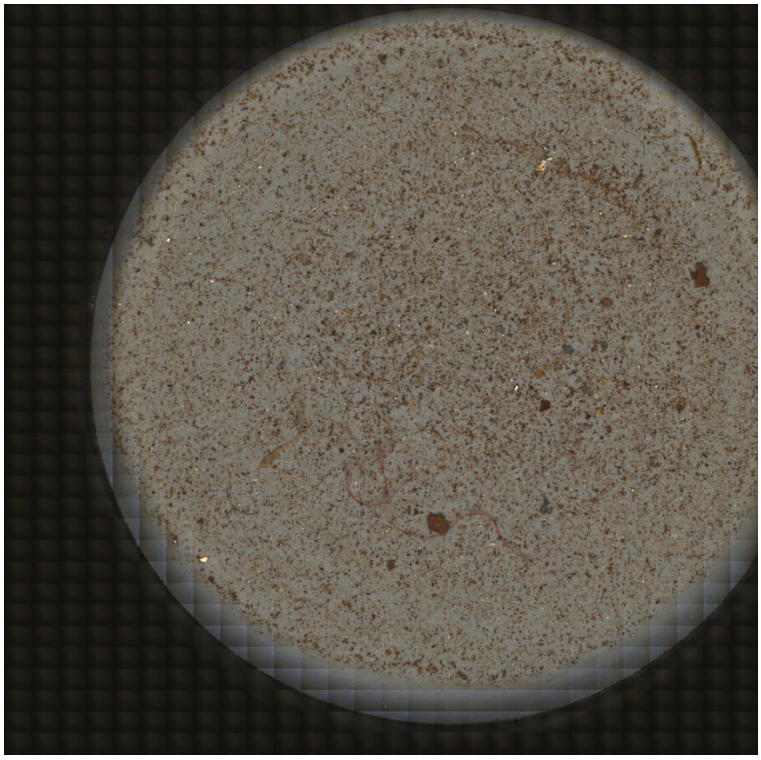

Figure 33B - Picture of analysis filter for sample 8B

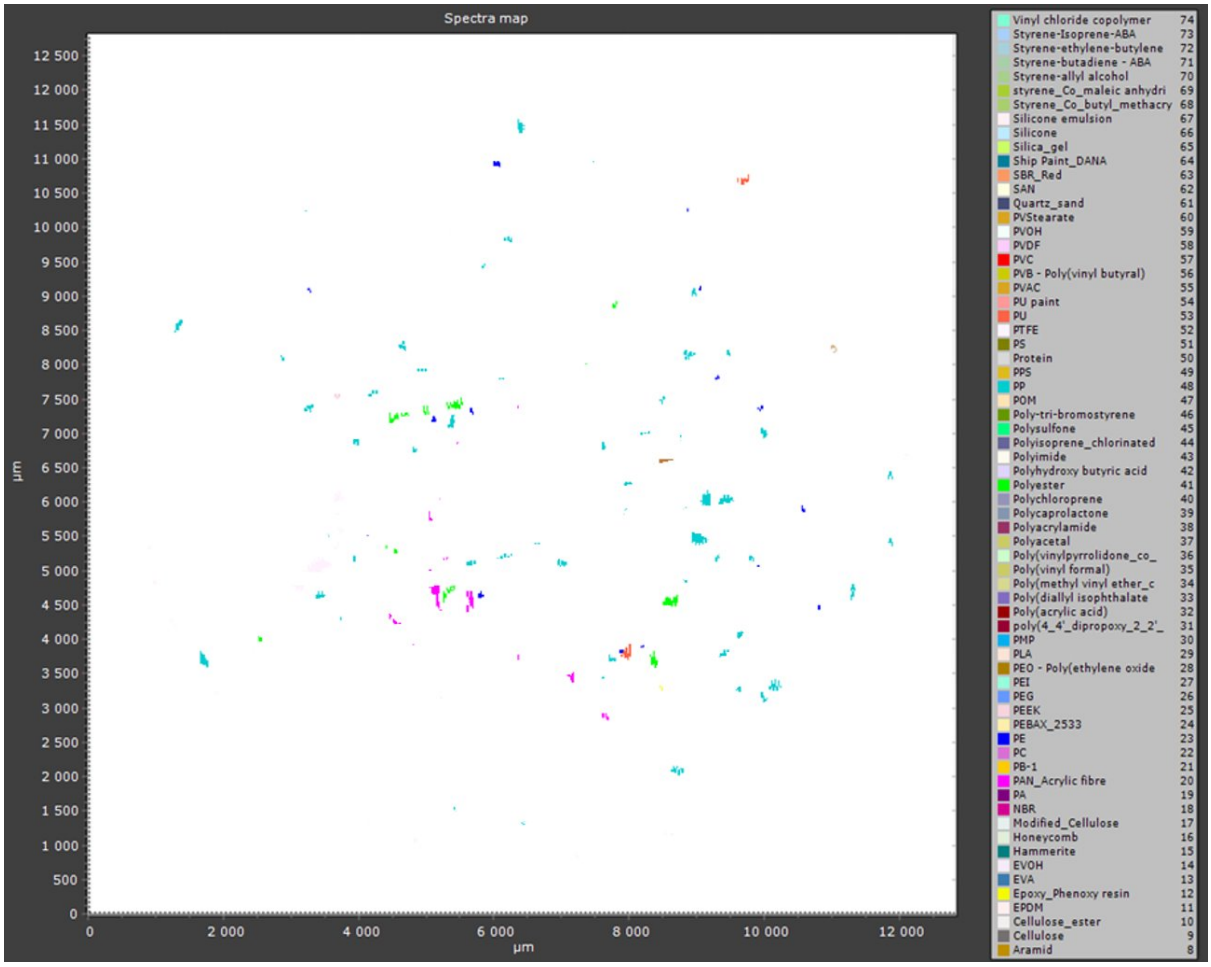

Figure 34B - Spectra map of sample 8B

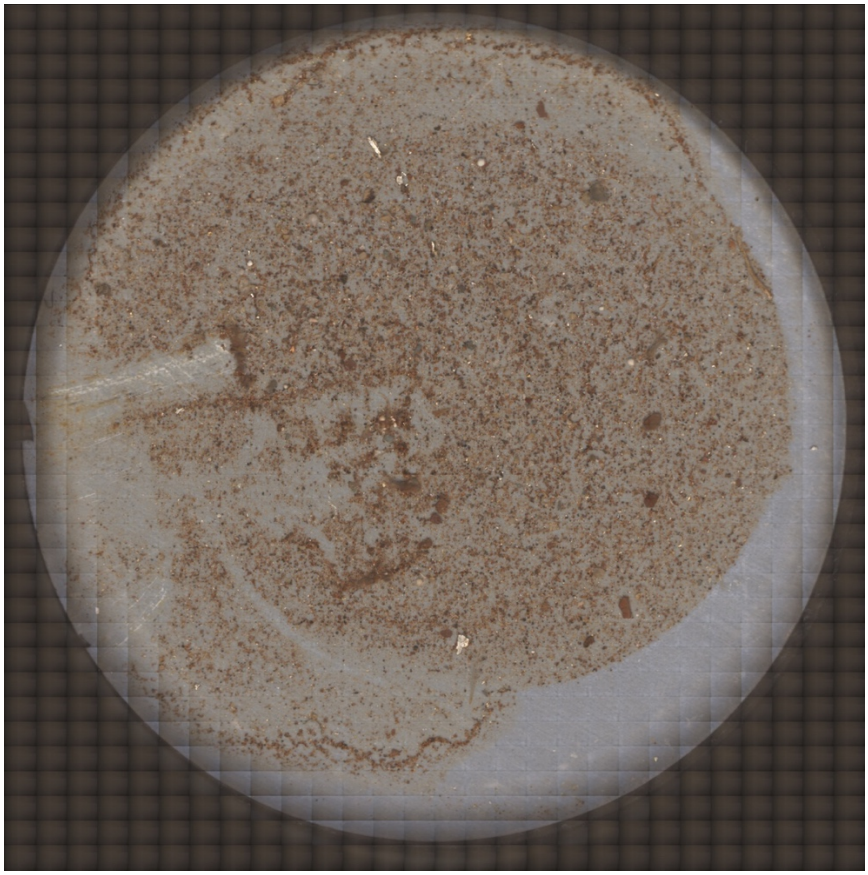

Figure 35B - Picture of analysis filter for sample 8C

Spectra map of sample 8C – NA

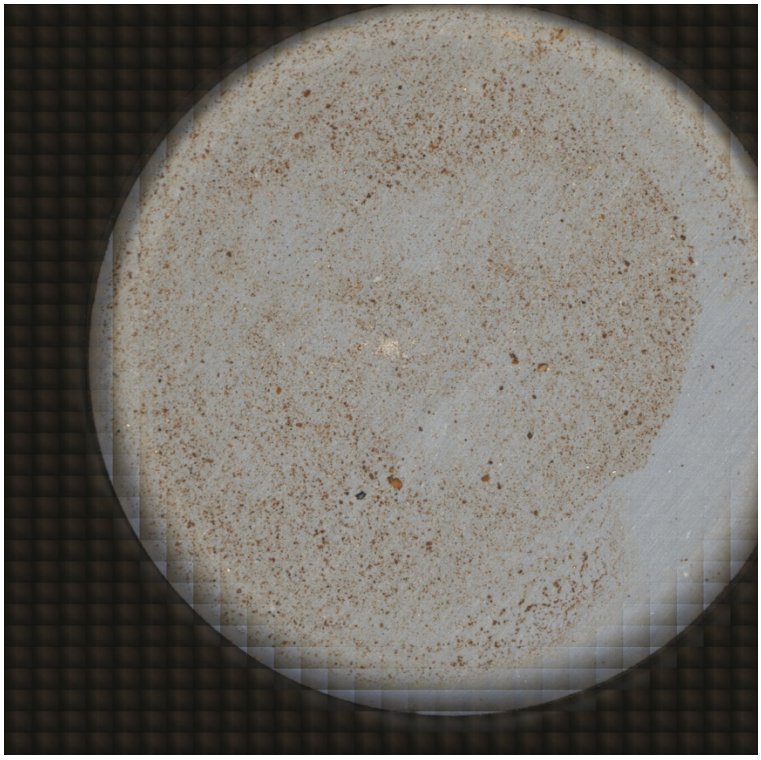

Figure 36B - Picture of analysis filter for sample 10A

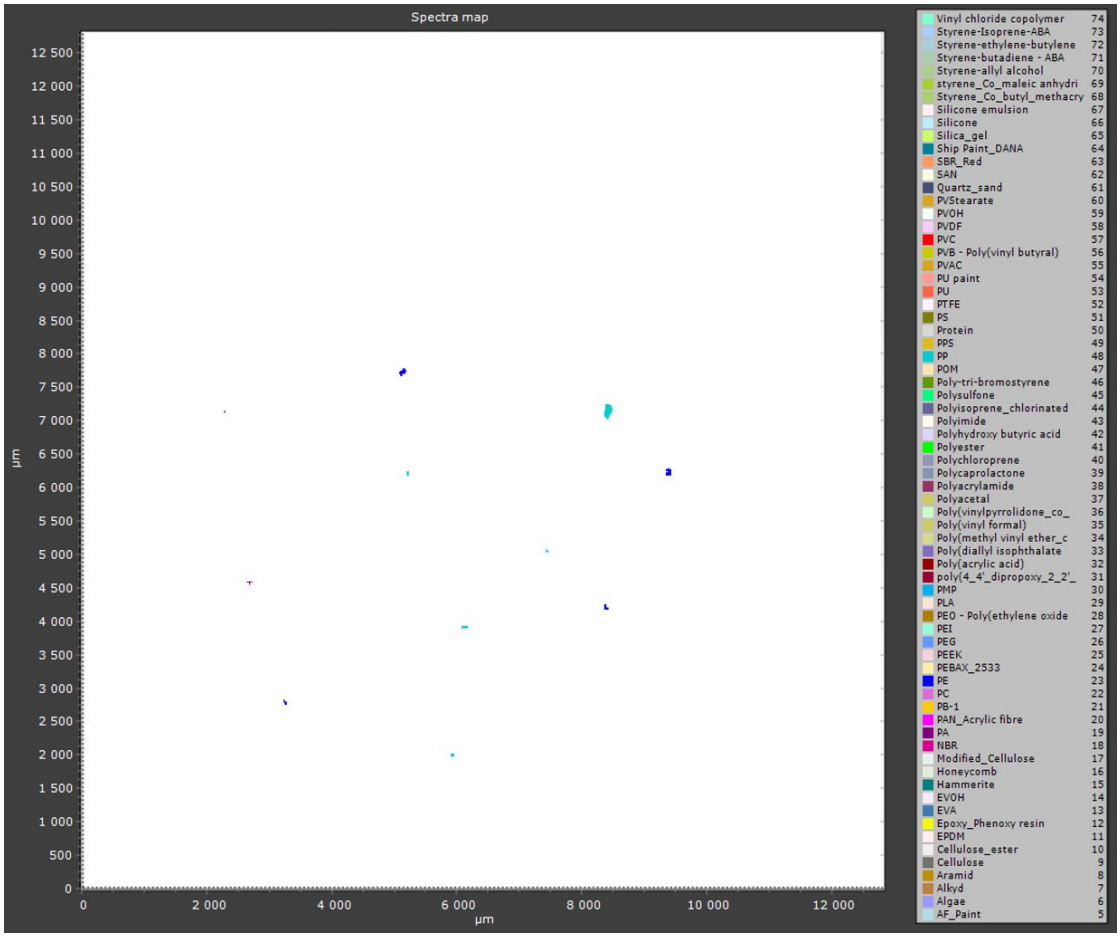

Figure 37B - Spectra map of sample 10A

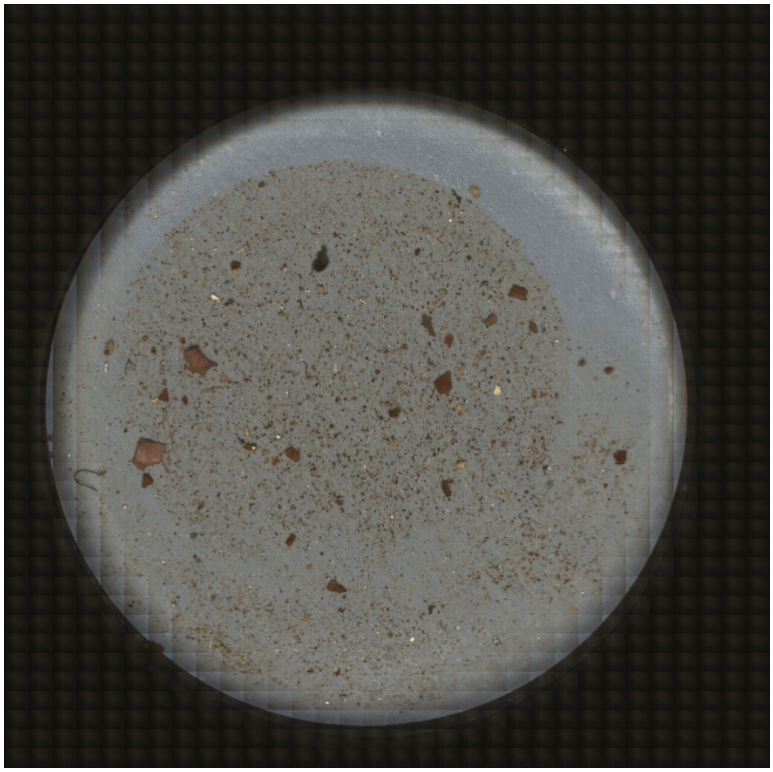

Figure 38B - Picture of analysis filter for sample 10B

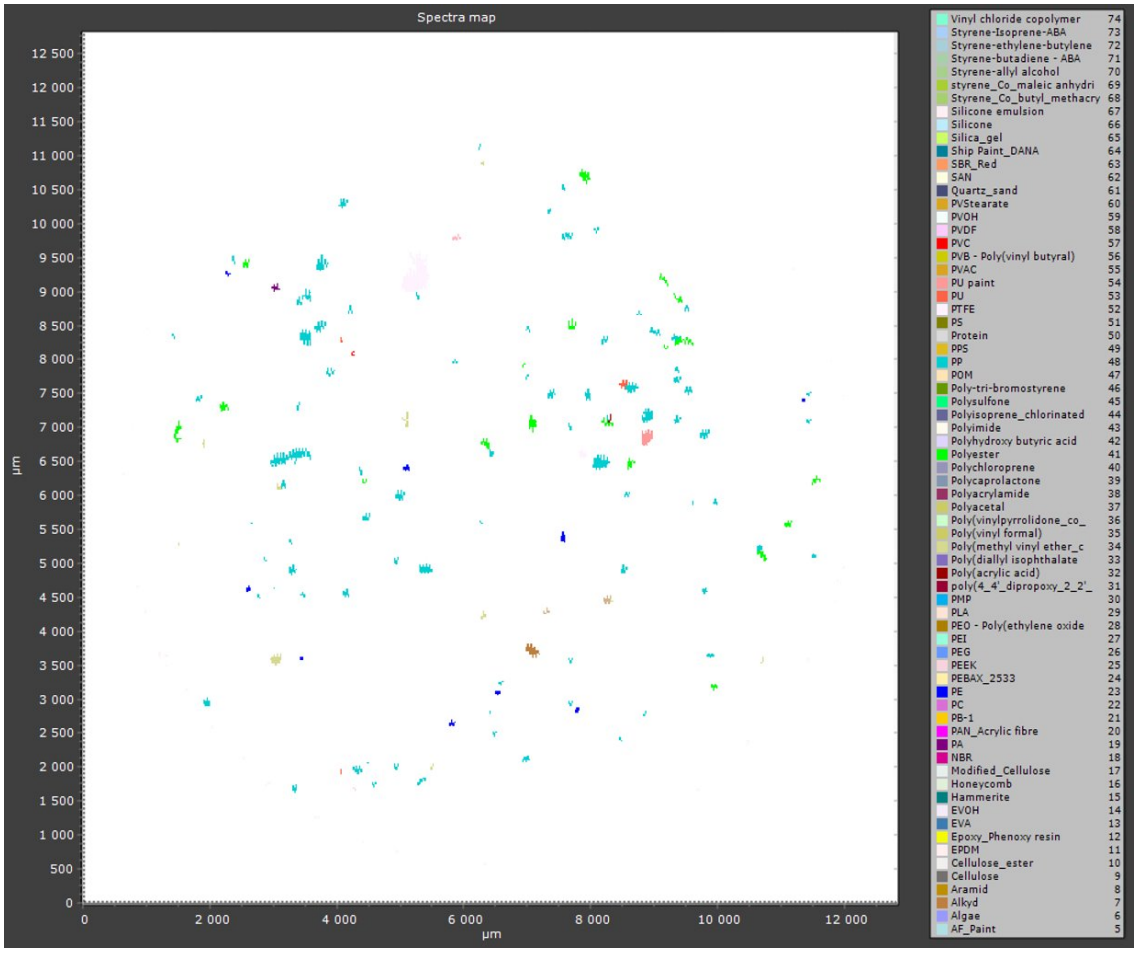

Figure 39B - Spectra map of sample 10B

Figure 40B - Picture of analysis filter for sample 10C

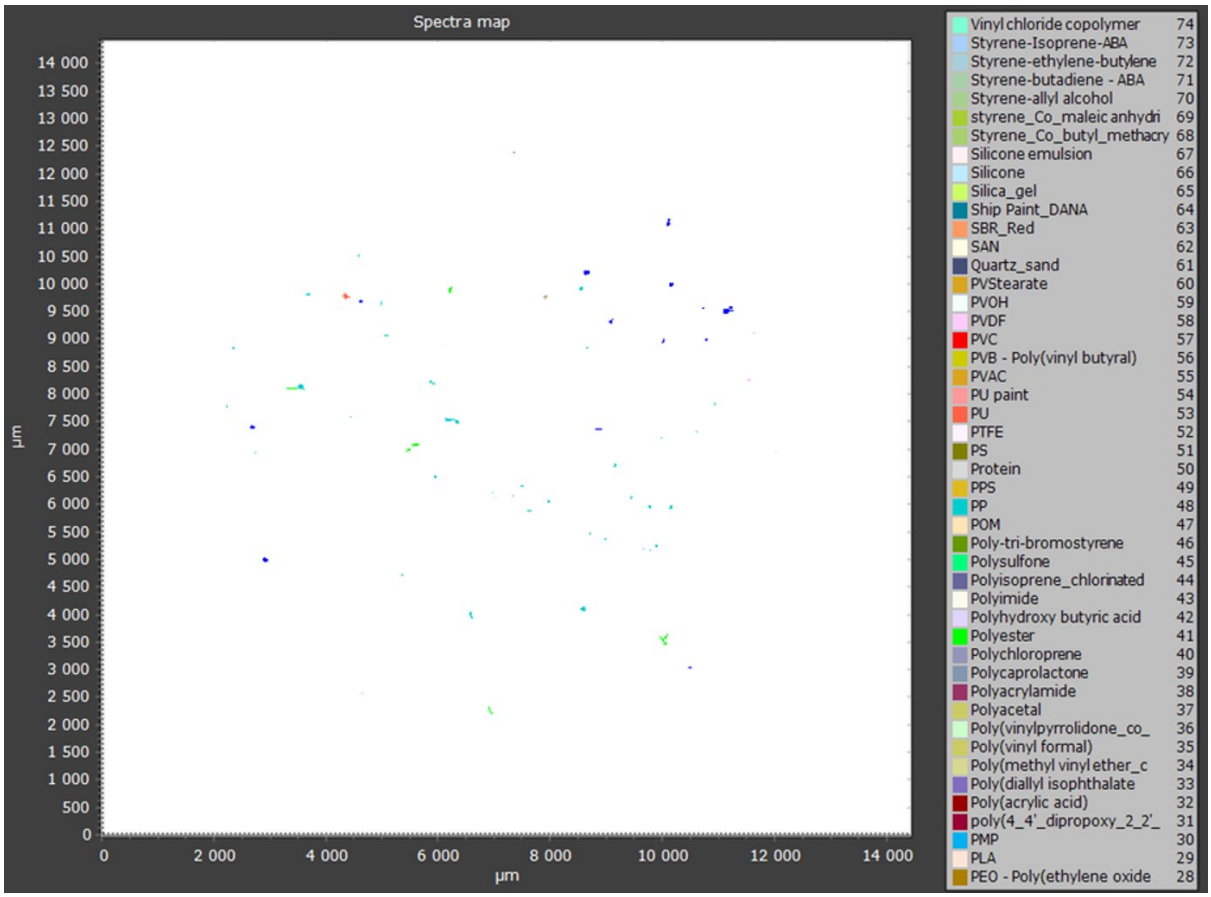

Figure 41B - Spectra map of sample 10C

Picture of analysis filter for sample 12A - NA

Spectra map of sample 12A – NA

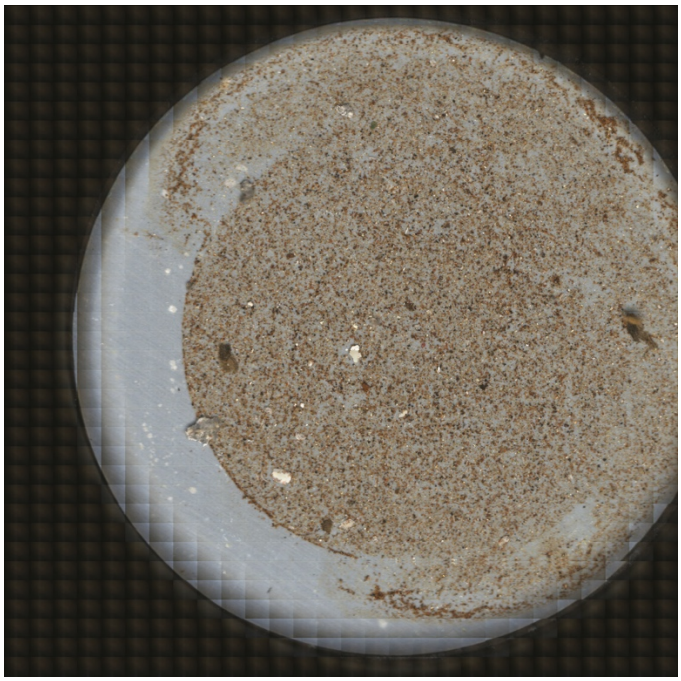

Figure 42B - Picture of analysis filter for sample 12B

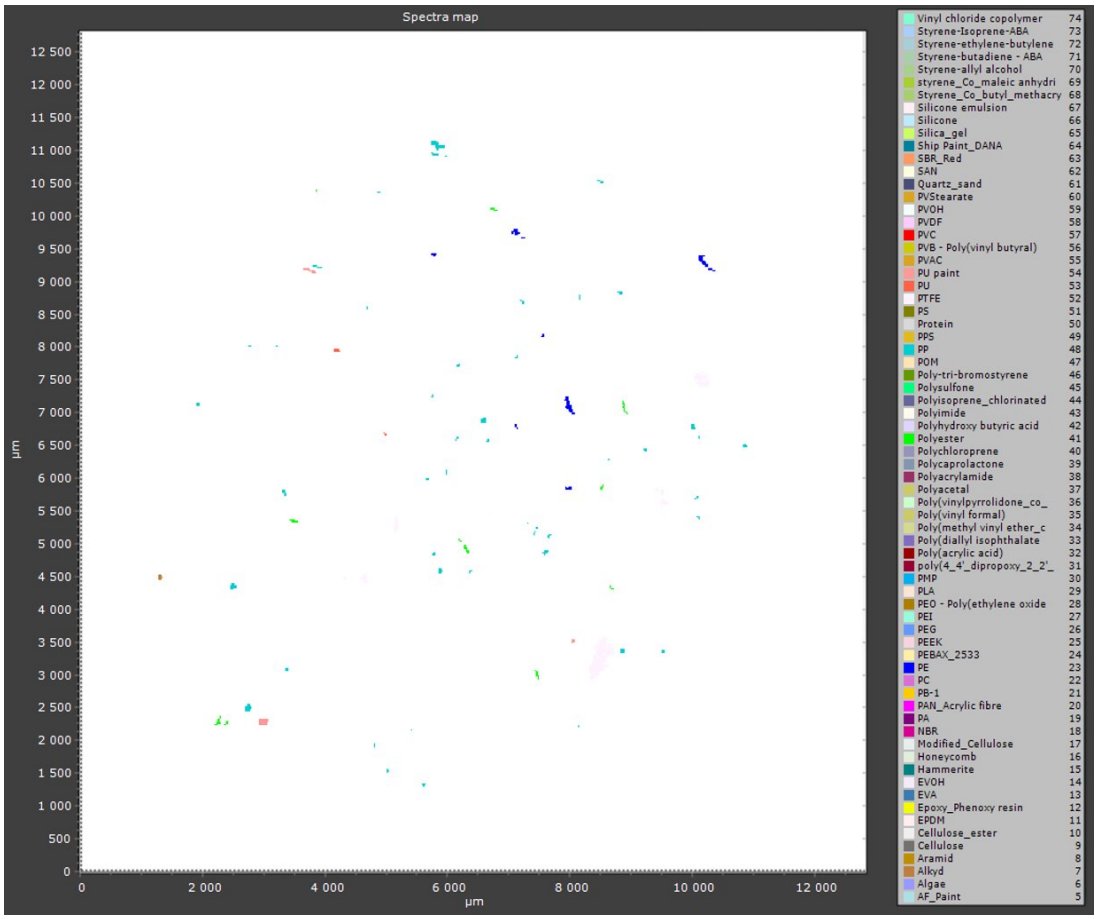

Figure 43B - Spectra map of sample 12B

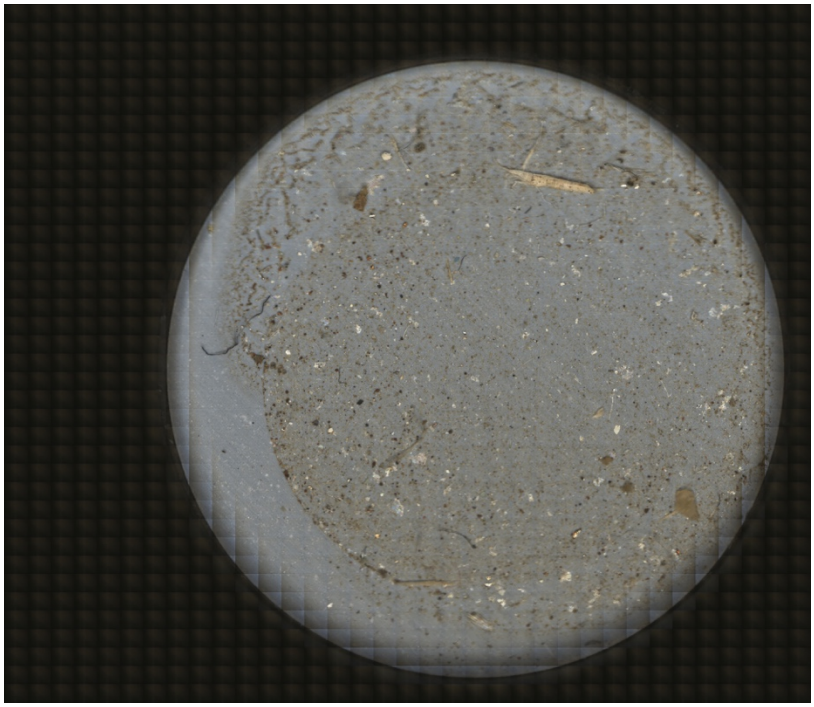

Figure 44B - Picture of analysis filter for sample 12C

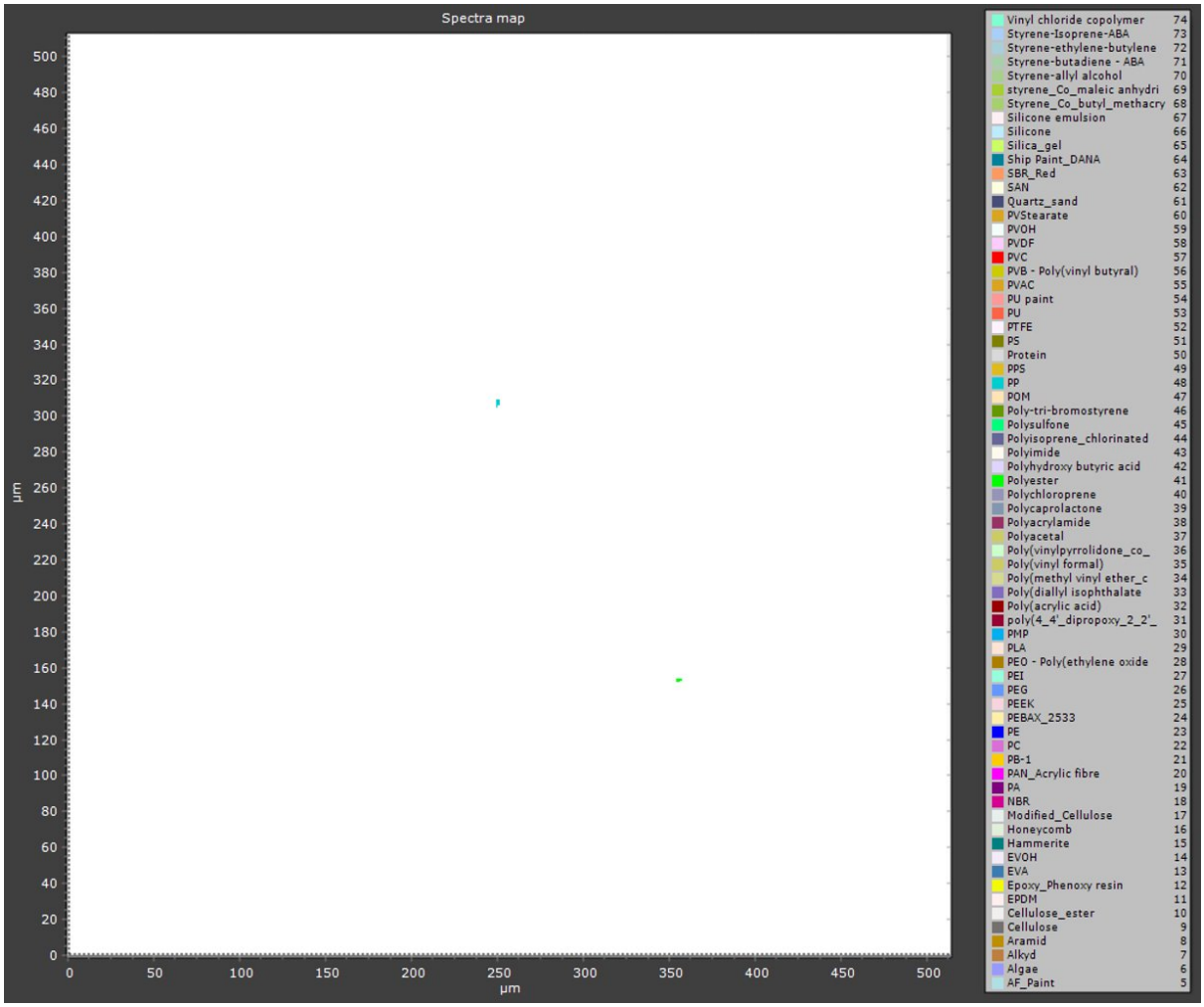

Figure 45B - Spectra map of sample 12C

Figure 46B - Picture of analysis filter for sample 14A

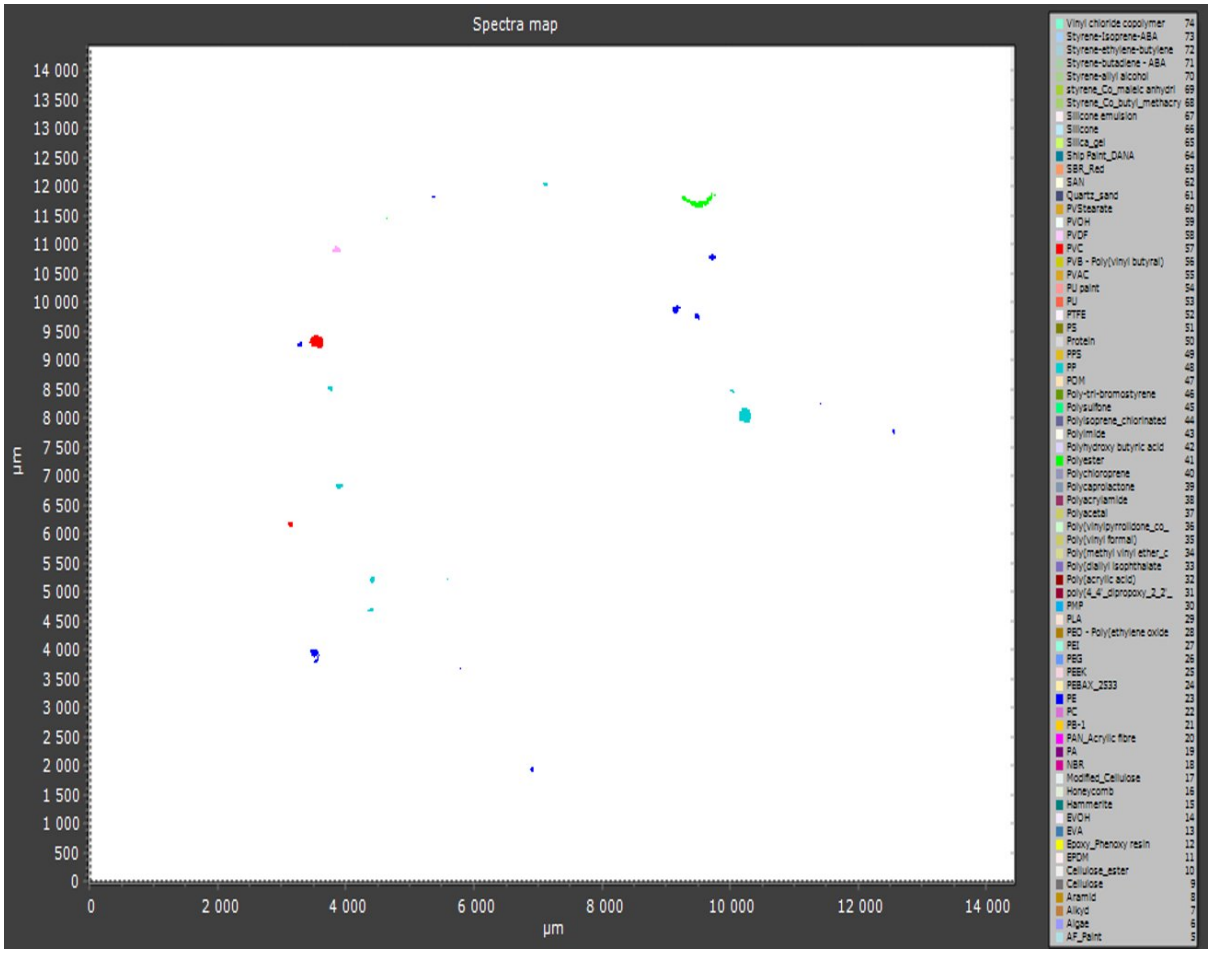

Figure 47B - Spectra map of sample 14A

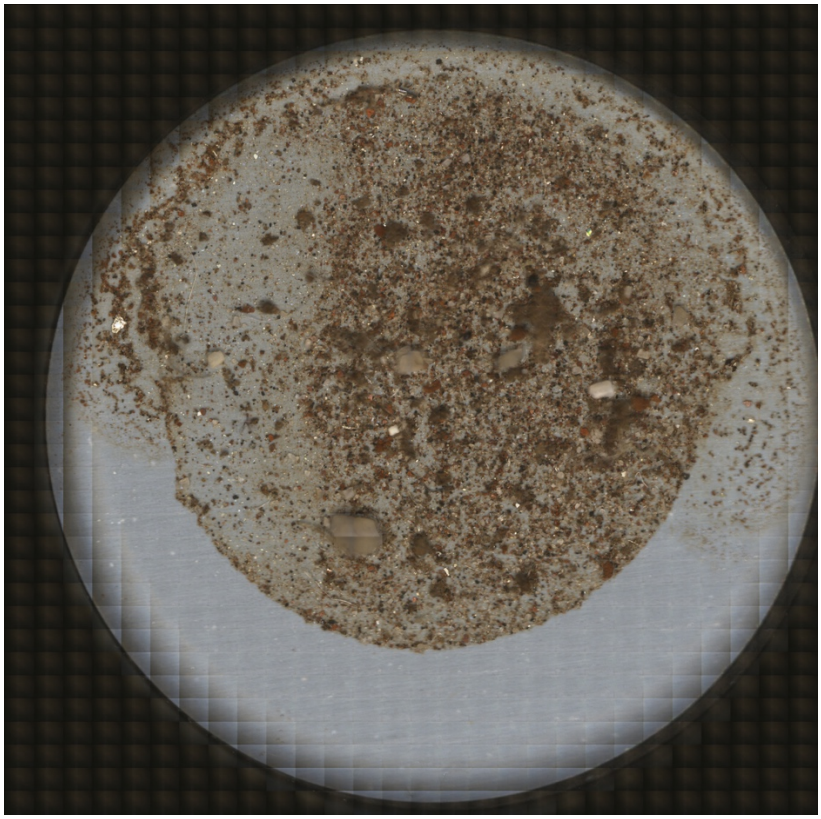

Figure 48B - Picture of analysis filter for sample 14B

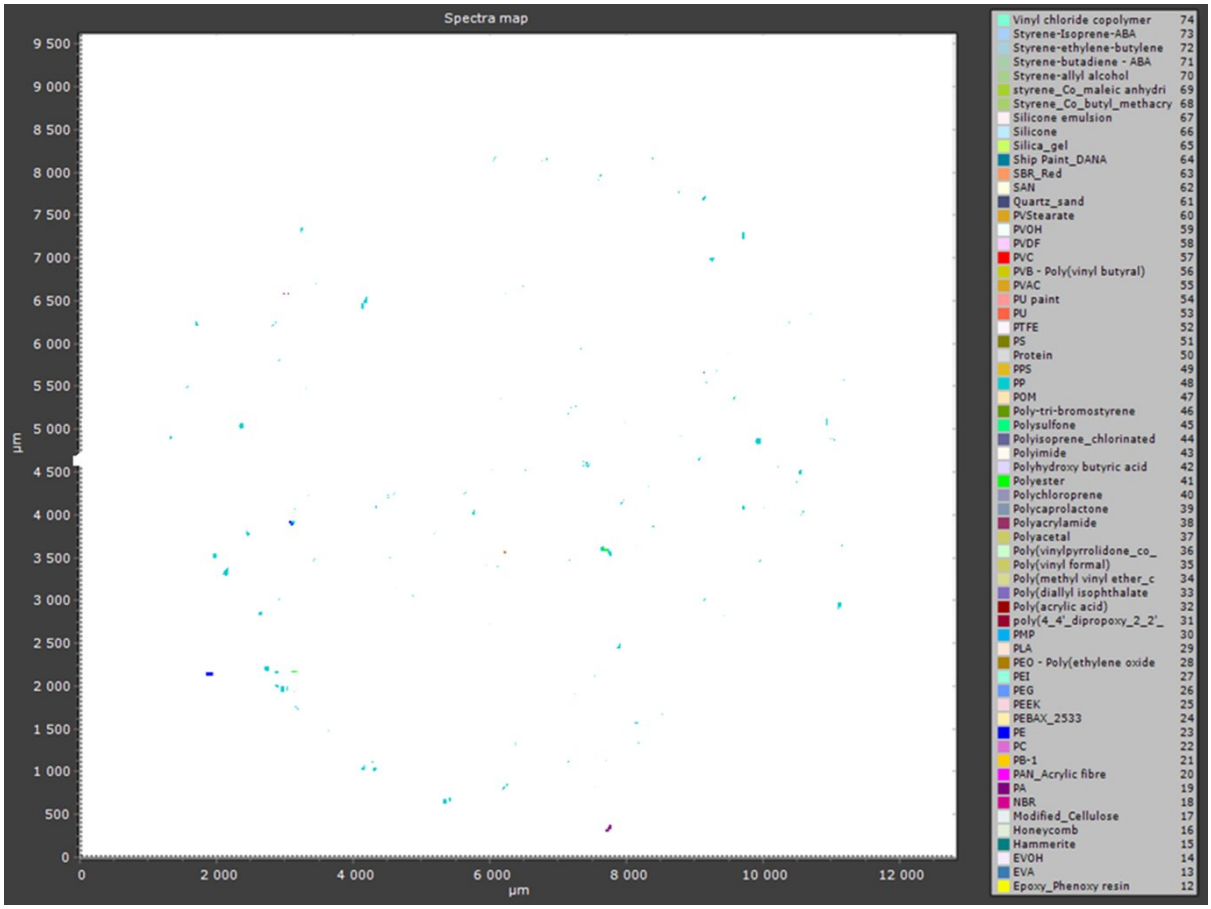

Figure 49B - Spectra map of sample 14B

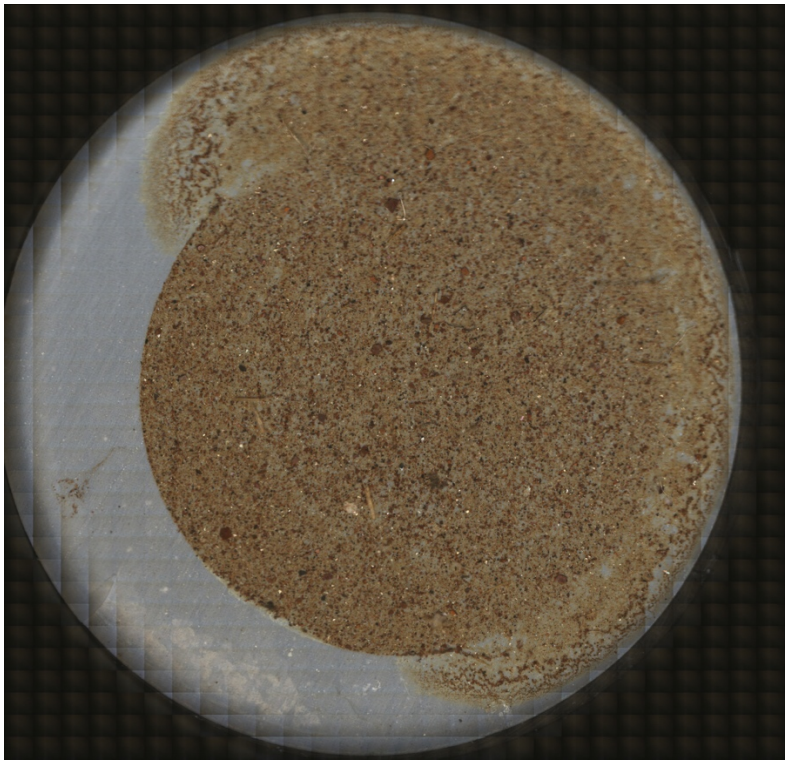

Figure 50B - Picture of analysis filter for sample 14C

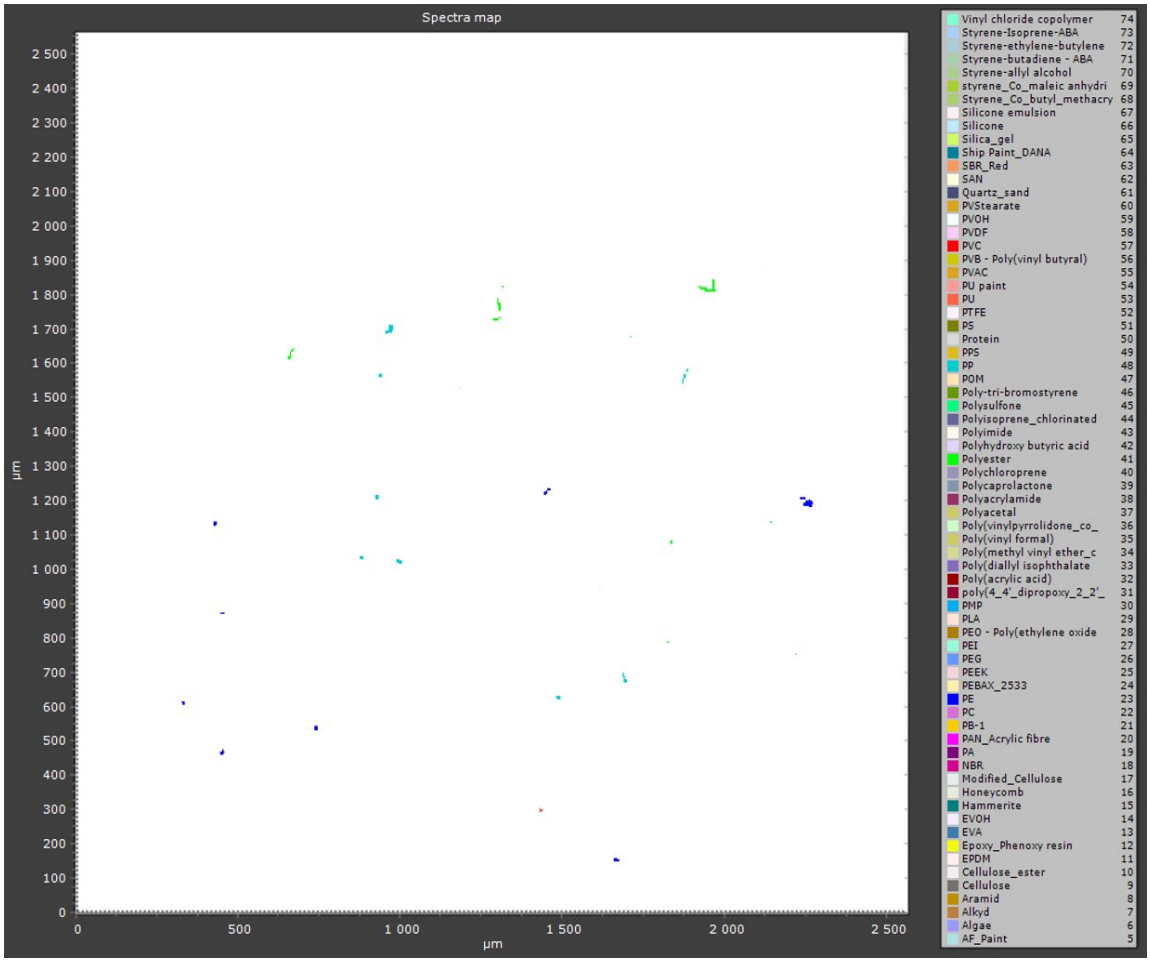

Figure 51B - Spectra map of sample 14C

QCL-IR - samples

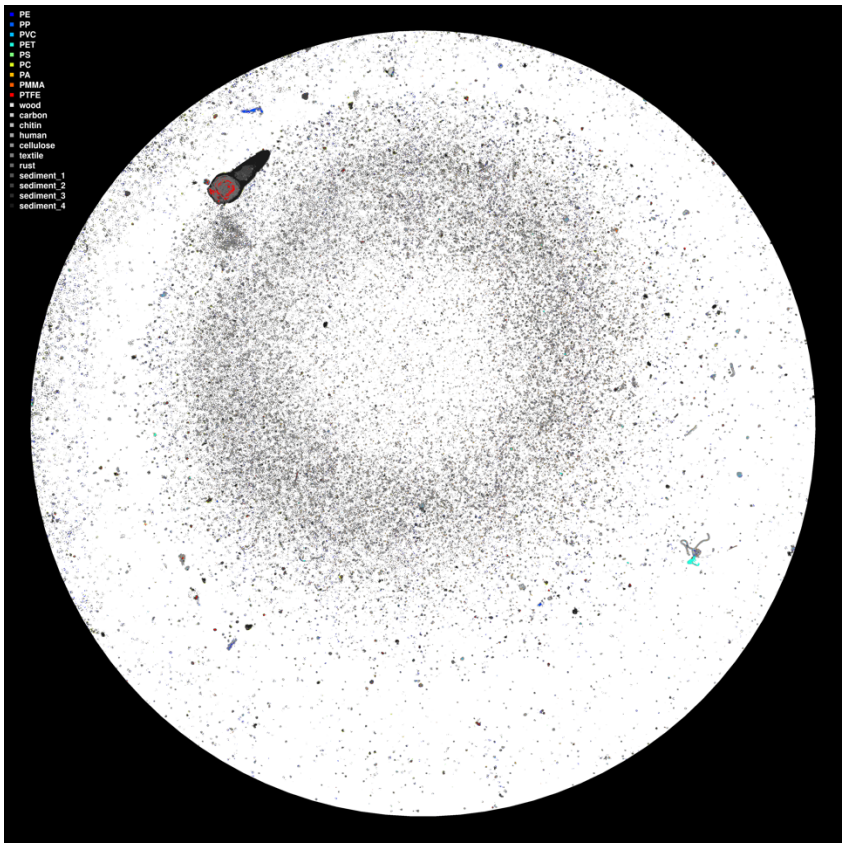

Figure 52B: Spectra map of sample 1C, analysis filter 1.

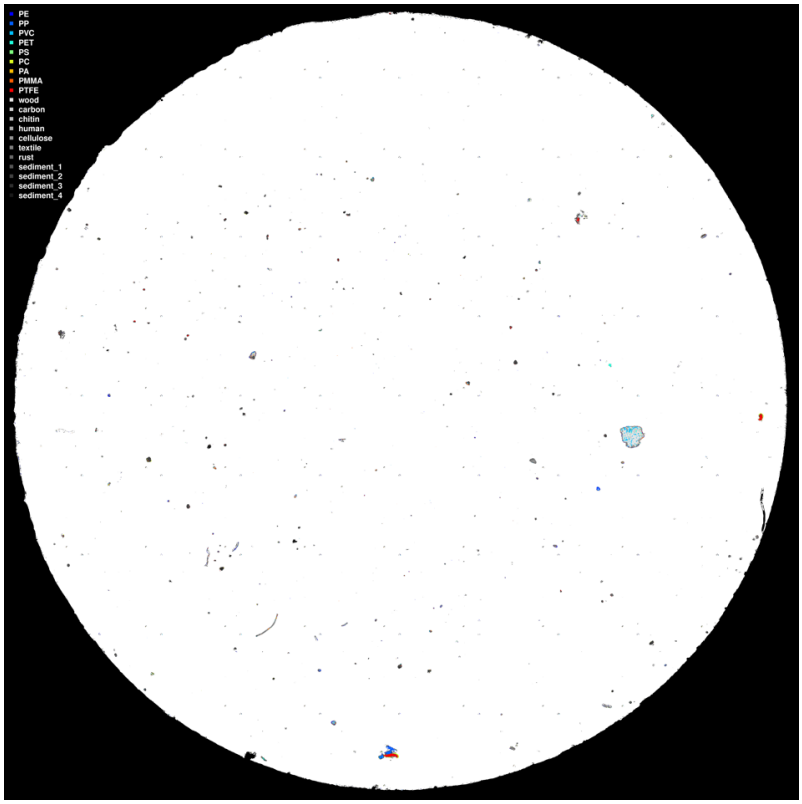

Figure 53B - Spectra map for sample 1C, analysis filter 2.

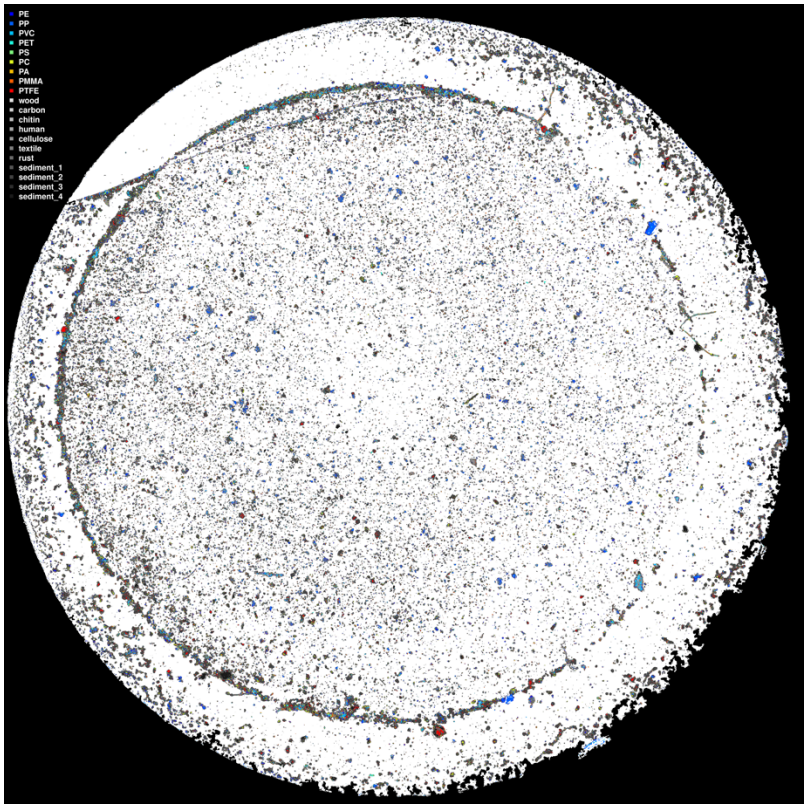

Figure 54B - Spectra map for sample 3A, analysis filter 1.

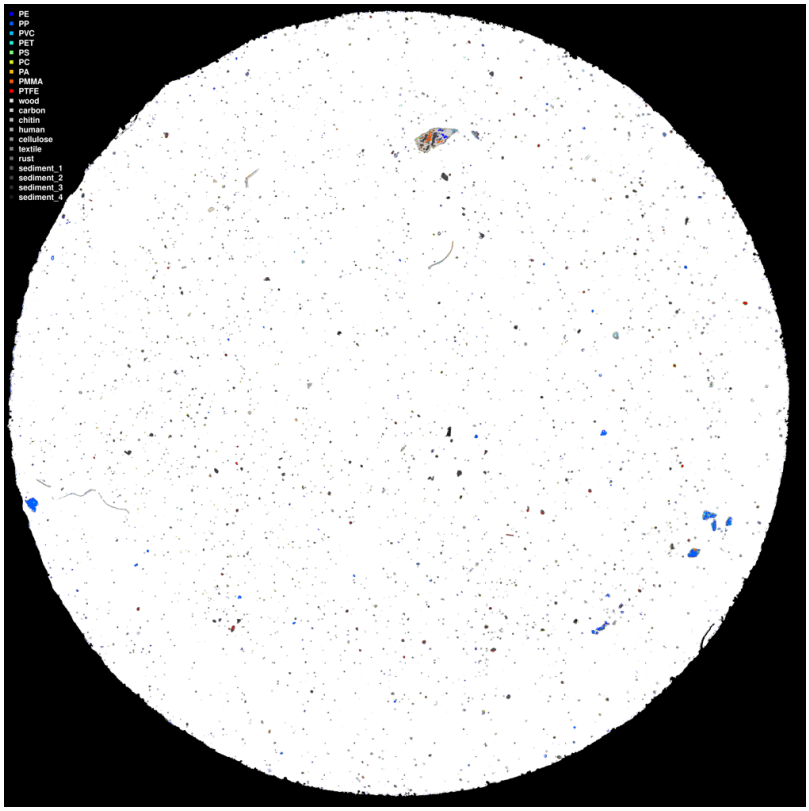

Figure 55B - Spectra map for sample 3A, analysis filter 2.

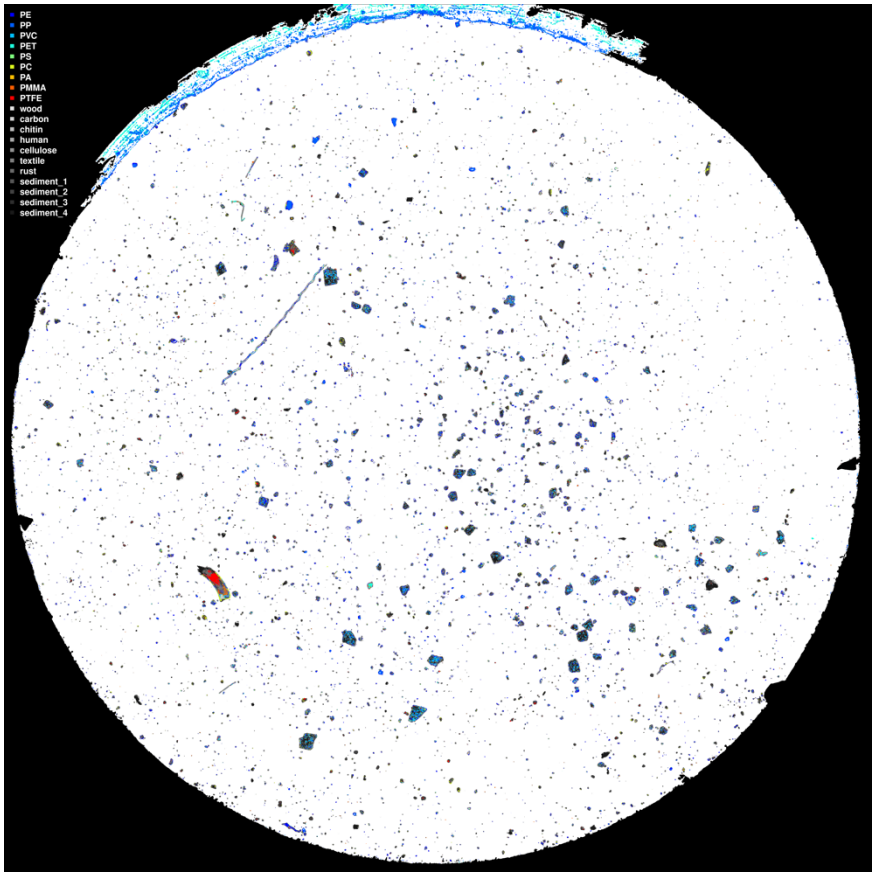

Figure 56B - Spectra map for sample 3B, analysis filter 1.

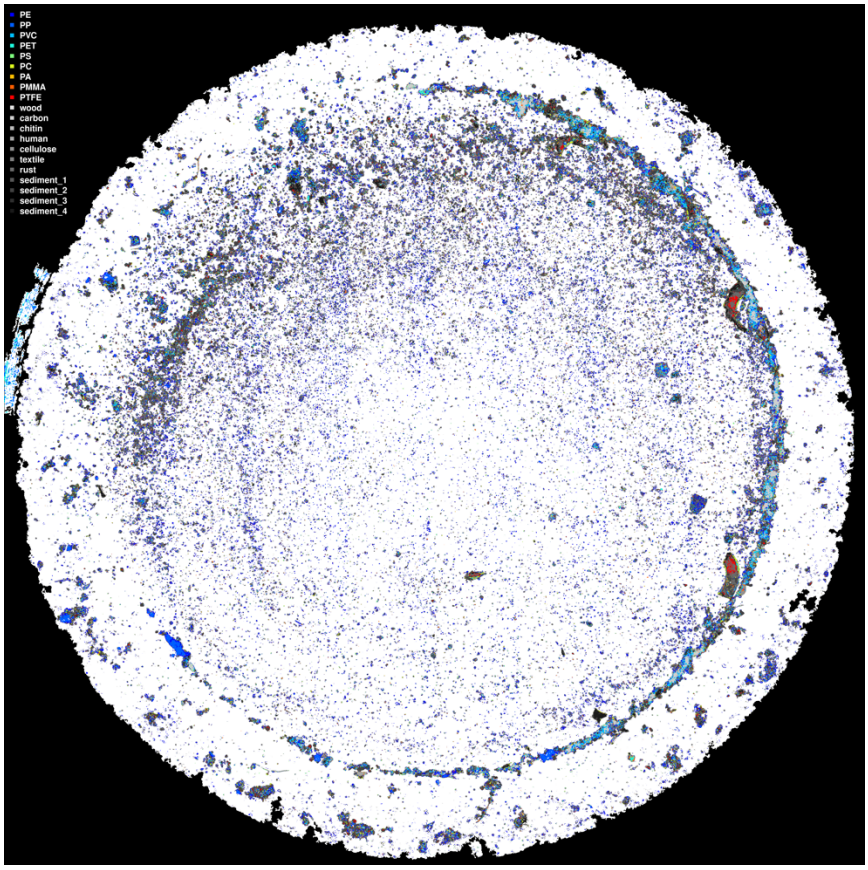

Figure 57B - Spectra map for sample 3B, analysis filter 2.

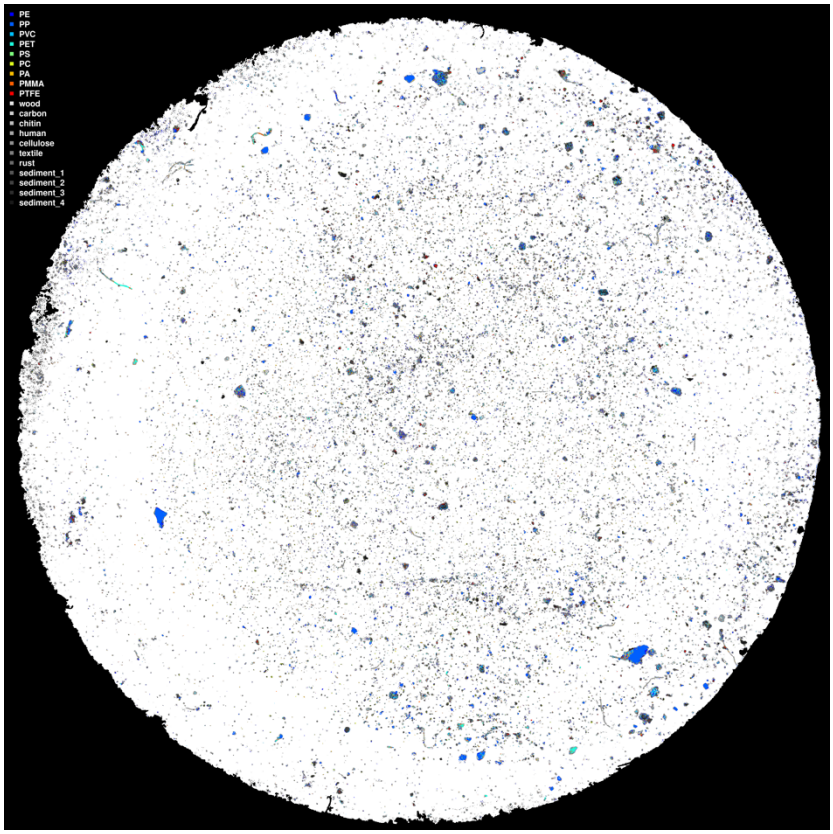

Figure 58B - Spectra map for sample 3C, analysis filter 1.

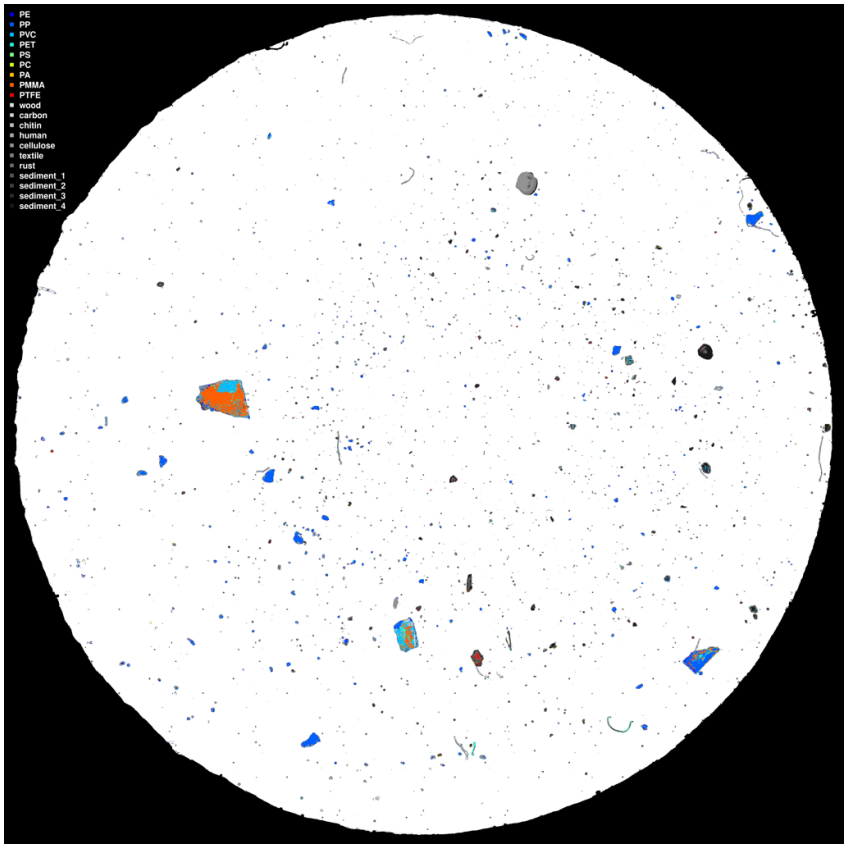

Figure 59B - Spectra map for sample 3C, analysis filter 2.

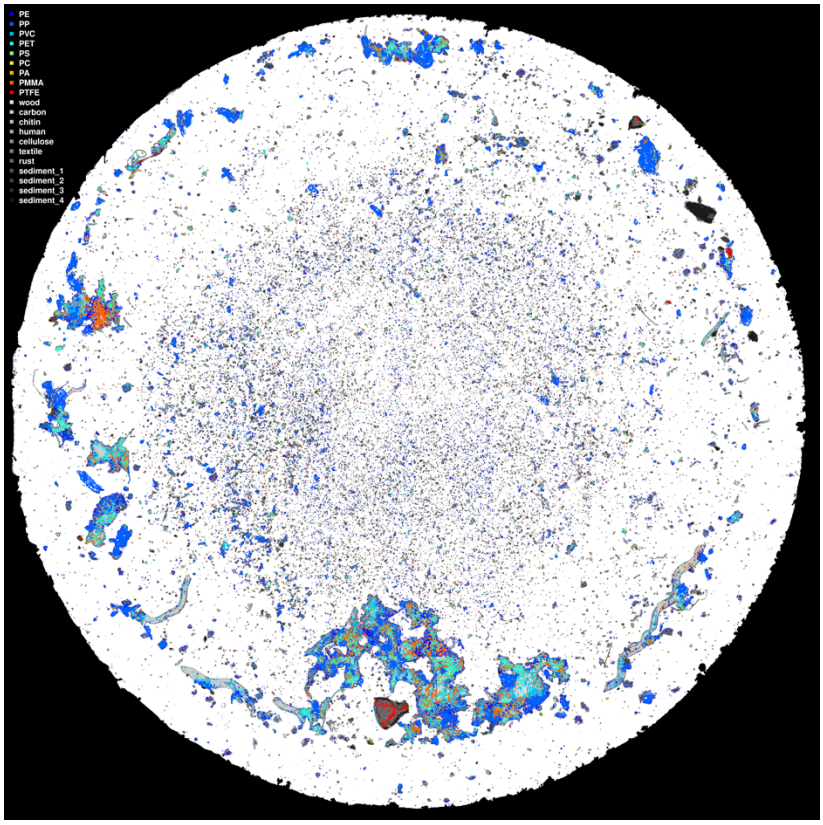

Figure 60B - Spectra map of sample 5B, analysis filter 1.

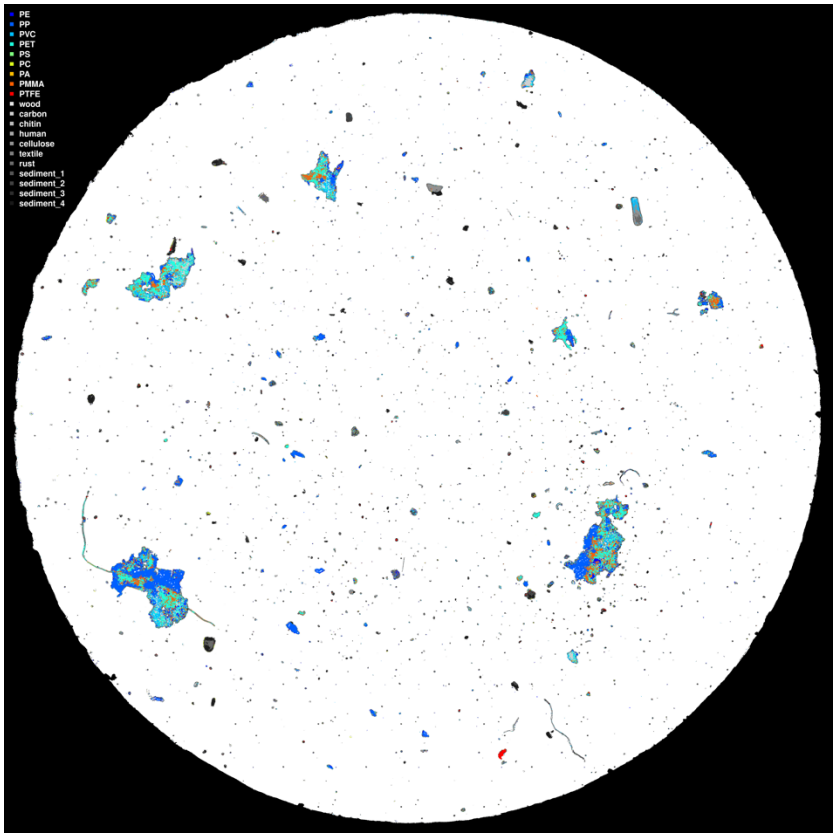

Figure 61B - Spectra map of sample 5B, analysis filter 2.

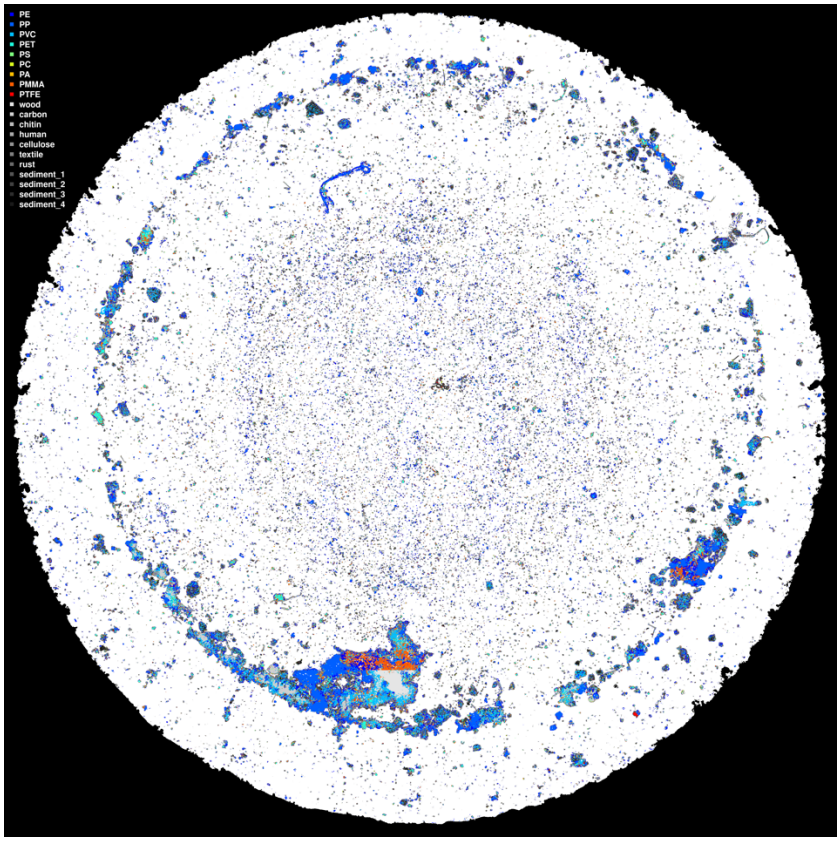

Figure 62B - Spectra map of sample 5C, analysis filter 1.

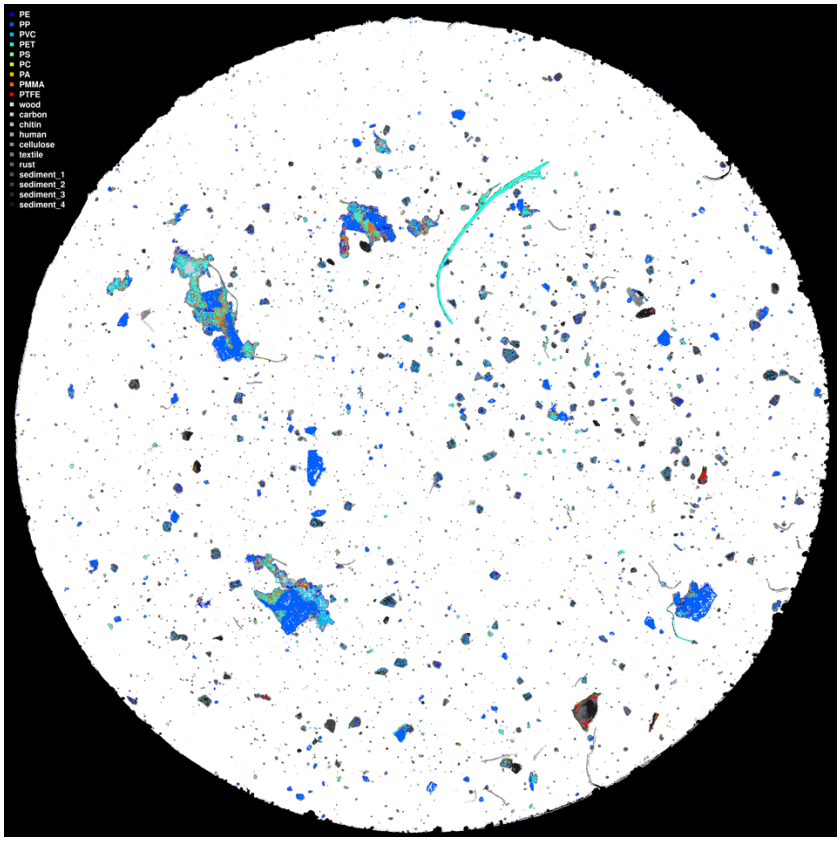

Figure 63B - Spectra map of sample 5C, analysis filter 1.

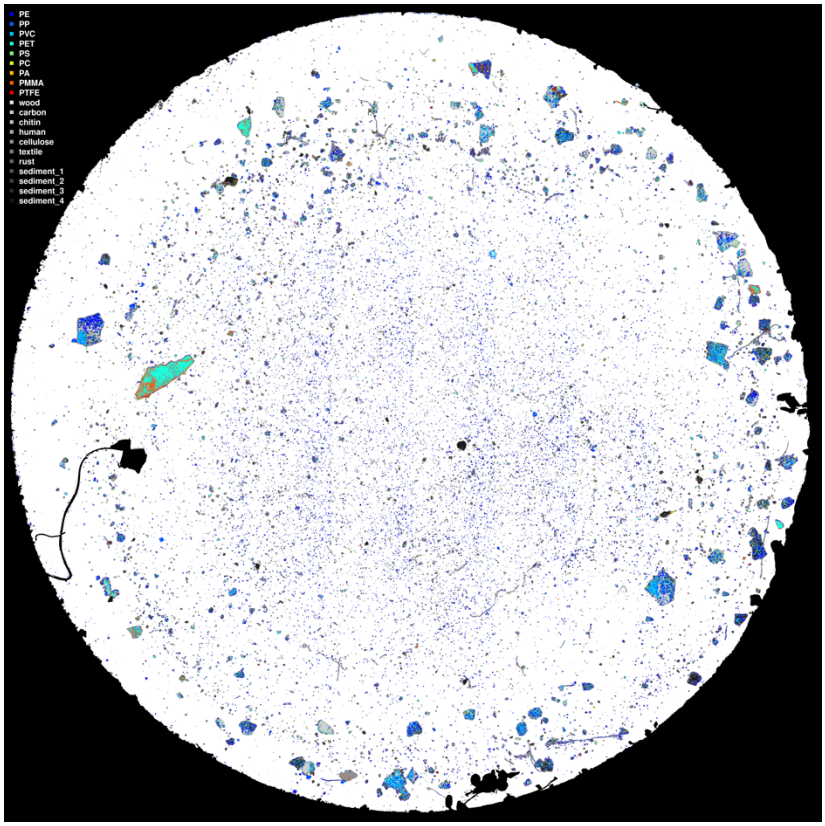

Figure 64B - Spectra map of sample 7A, analysis filter 1.

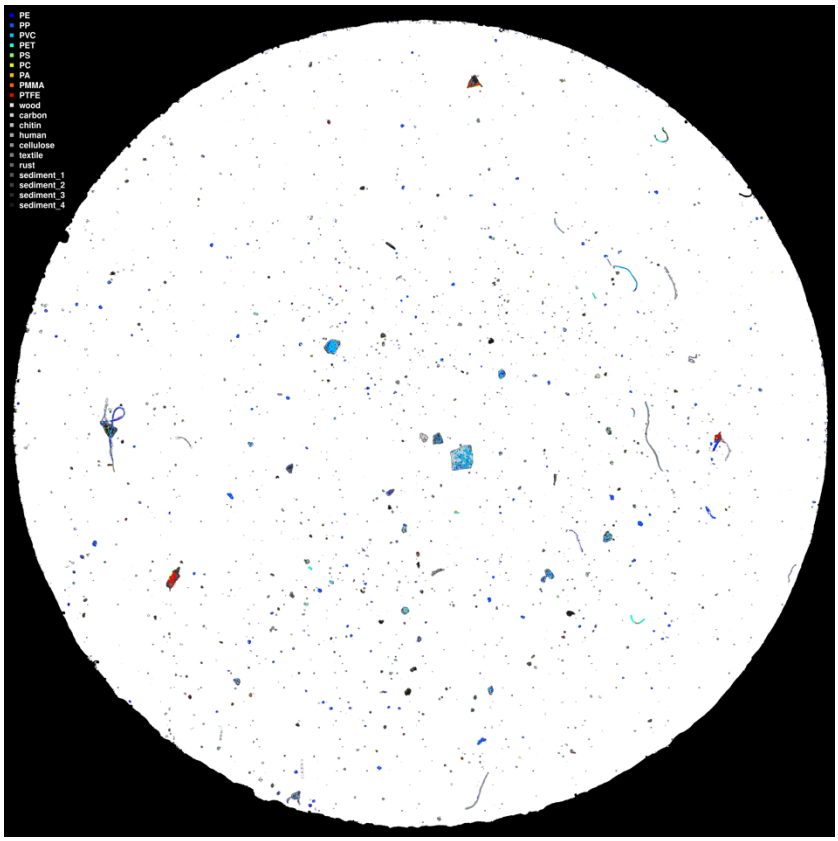

Figure 65B - Spectra map of sample 7A, analysis filter 2.

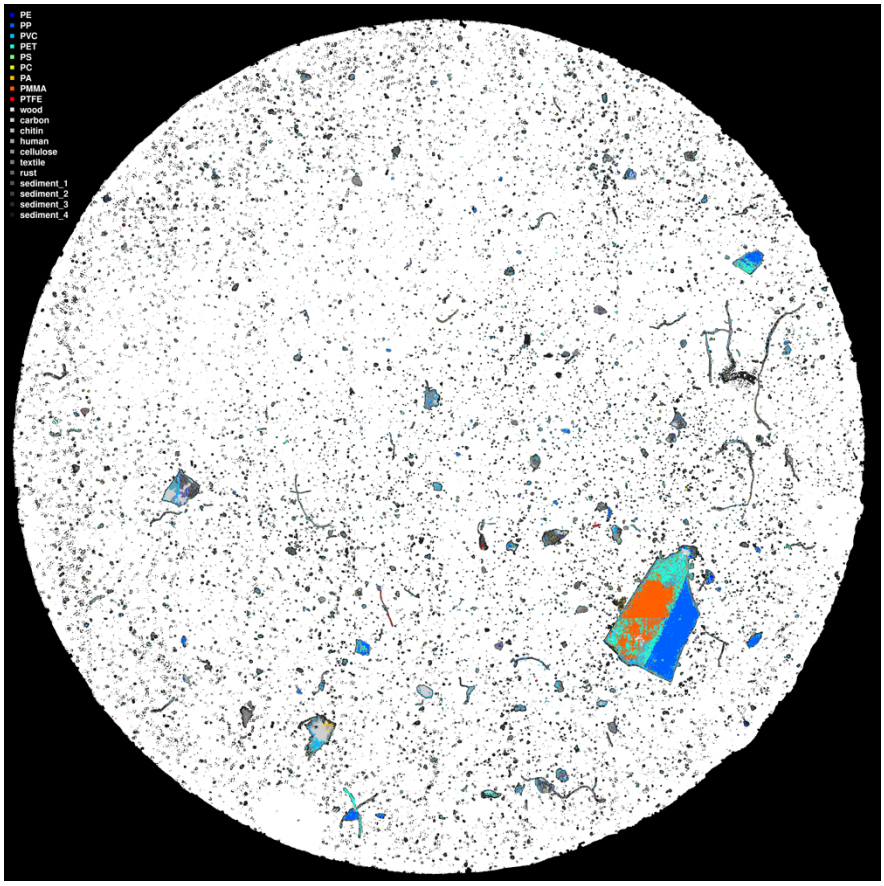

Figure 66B - Spectra map of sample 7B, analysis filter 1.

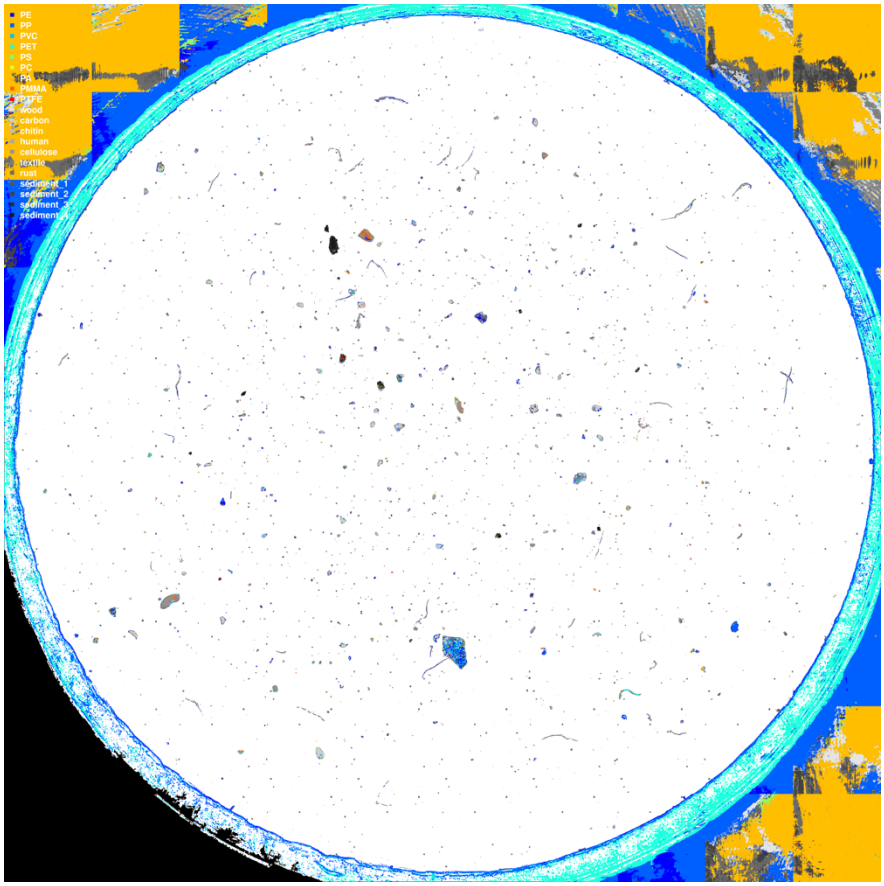

Figure 67B - Spectra map of sample 7C, analysis filter 1.

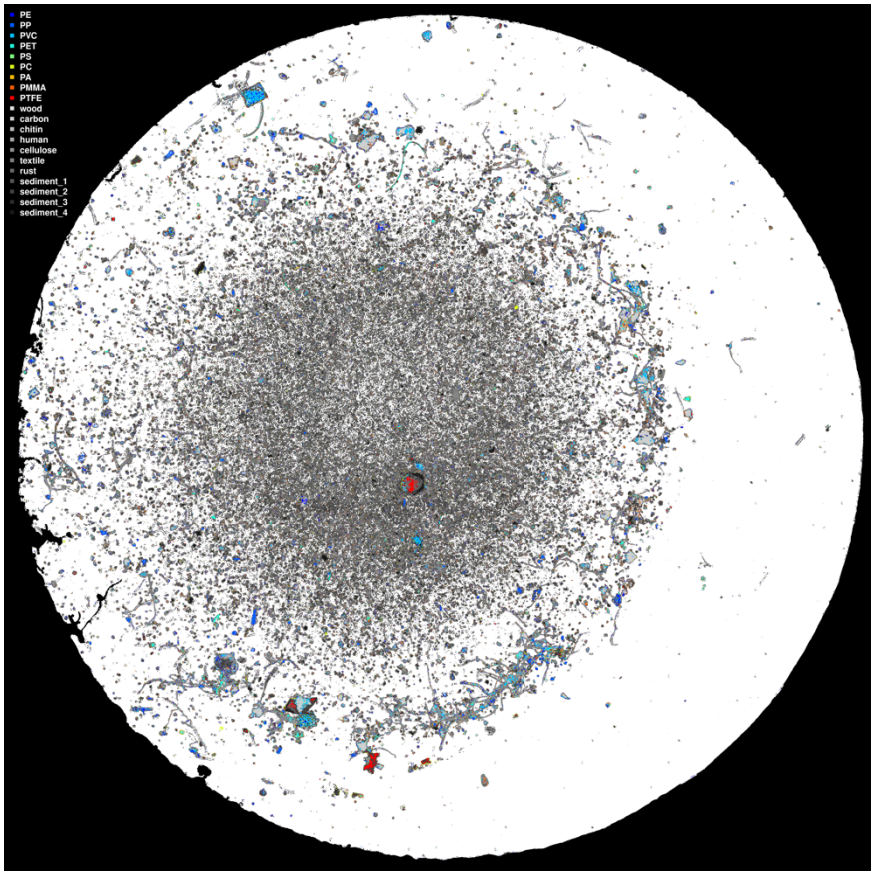

Figure 68B - Spectra map of sample 7C, analysis filter 2.

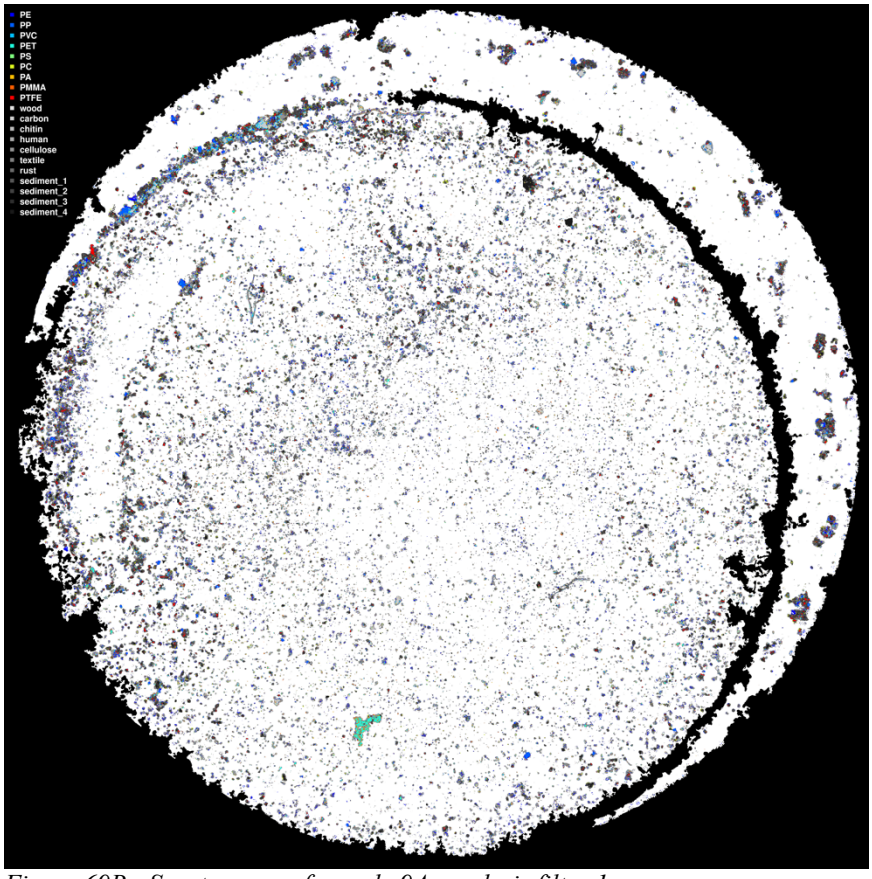

Figure 69B - Spectra map of sample 9A, analysis filter 1.

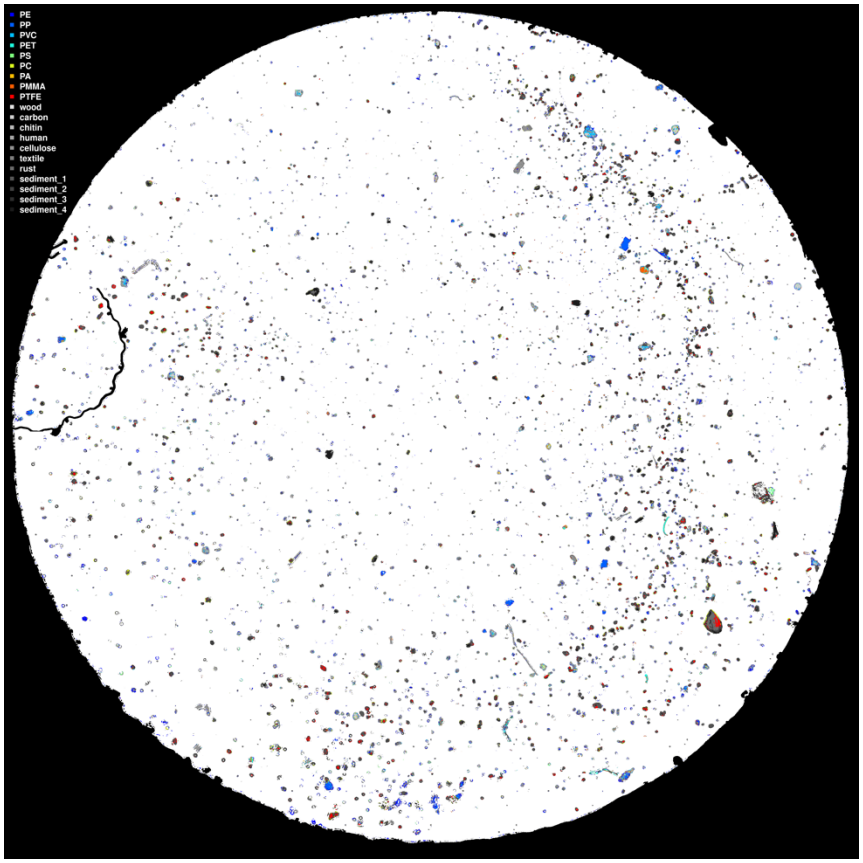

Figure 70B - Spectra map of sample 9A, analysis filter 2.

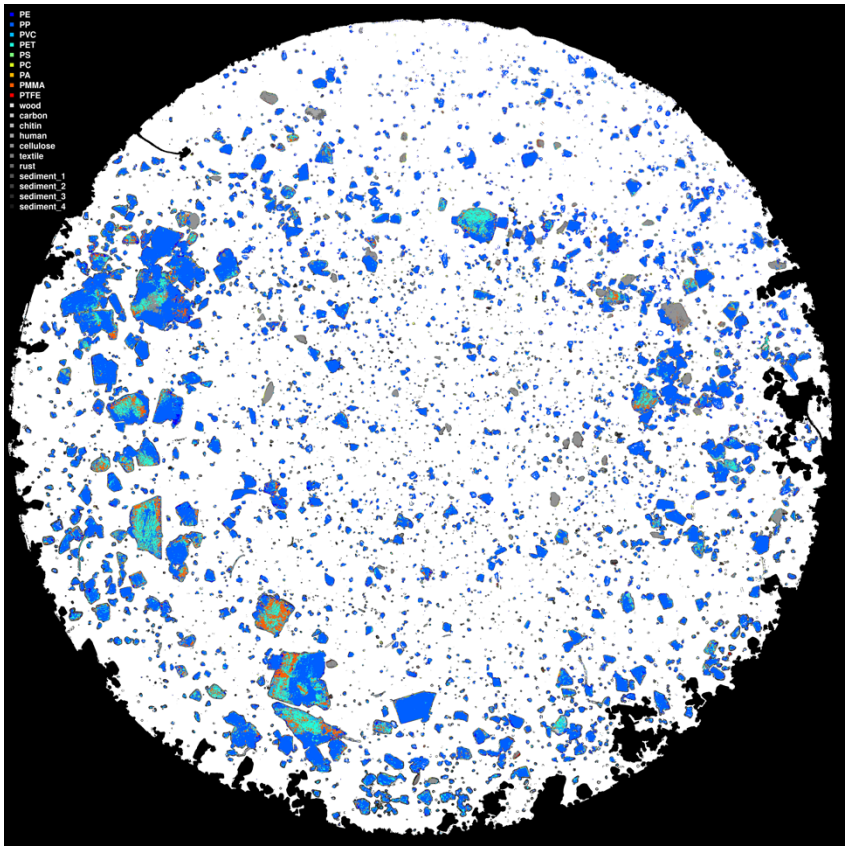

Figure 71B - Spectra map of sample 9B, analysis filter 1.

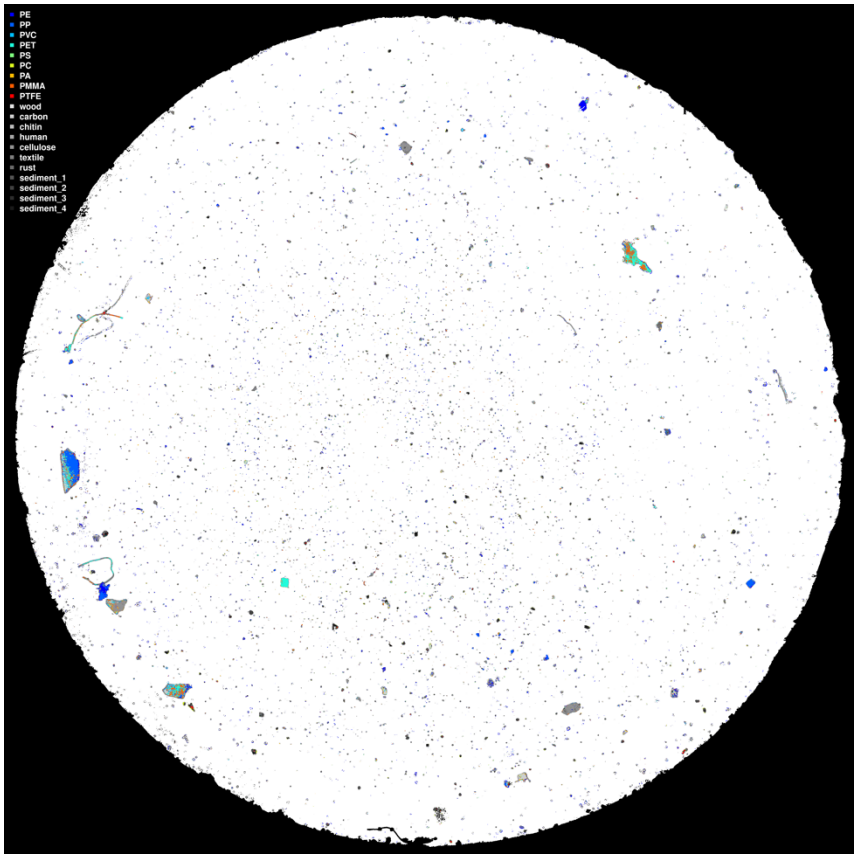

Figure 72B - Spectra map of sample 9C, analysis filter 1.

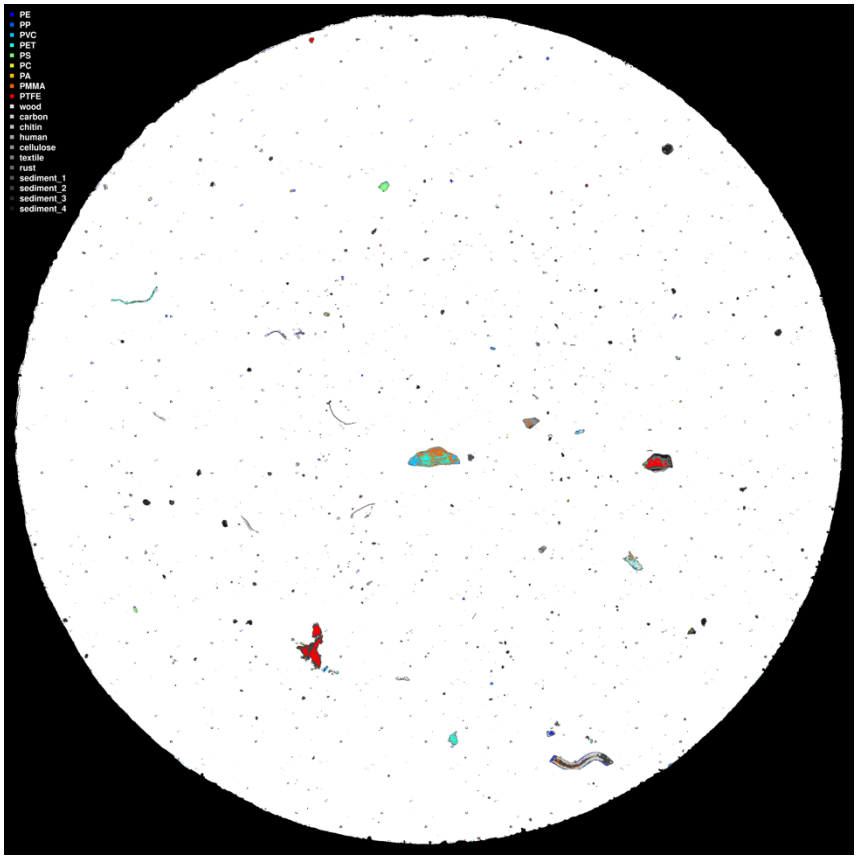

Figure 73B - Spectra map of sample 9C, analysis filter 2.

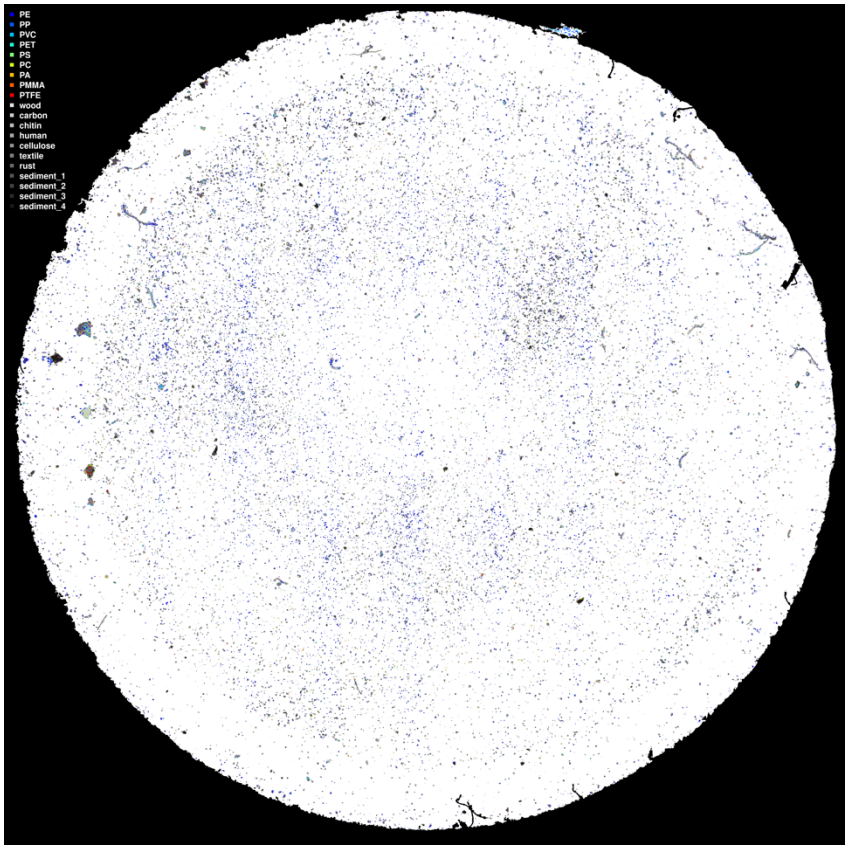

Figure 74B - Spectra map of sample 11A, analysis filter 1.

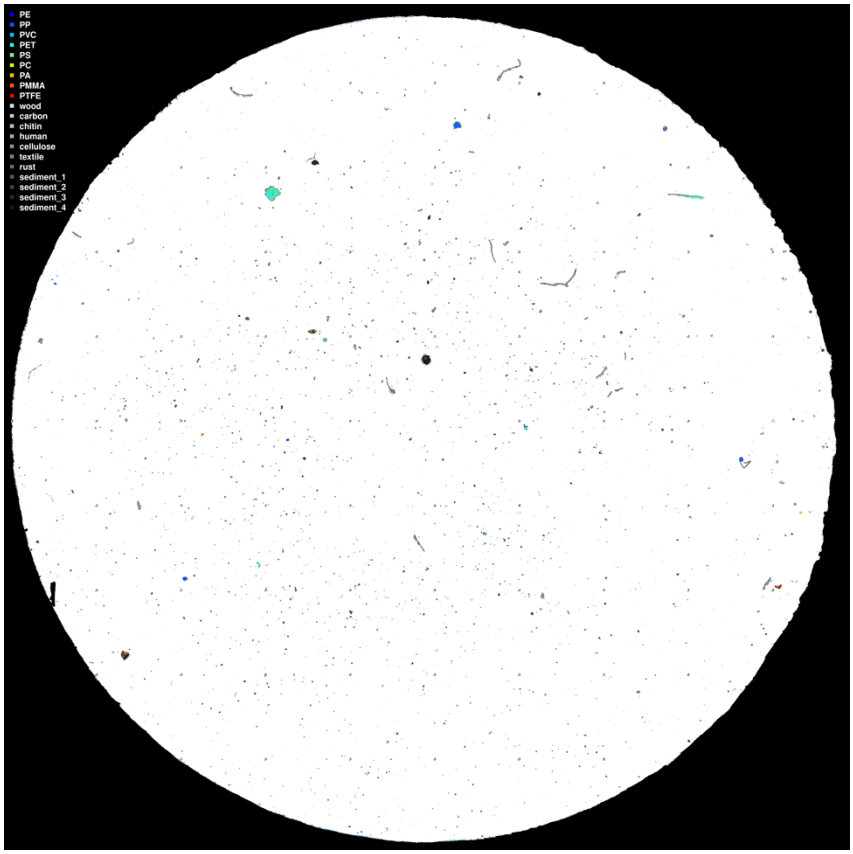

Figure 75B - Spectra map of sample 11A, analysis filter 2.

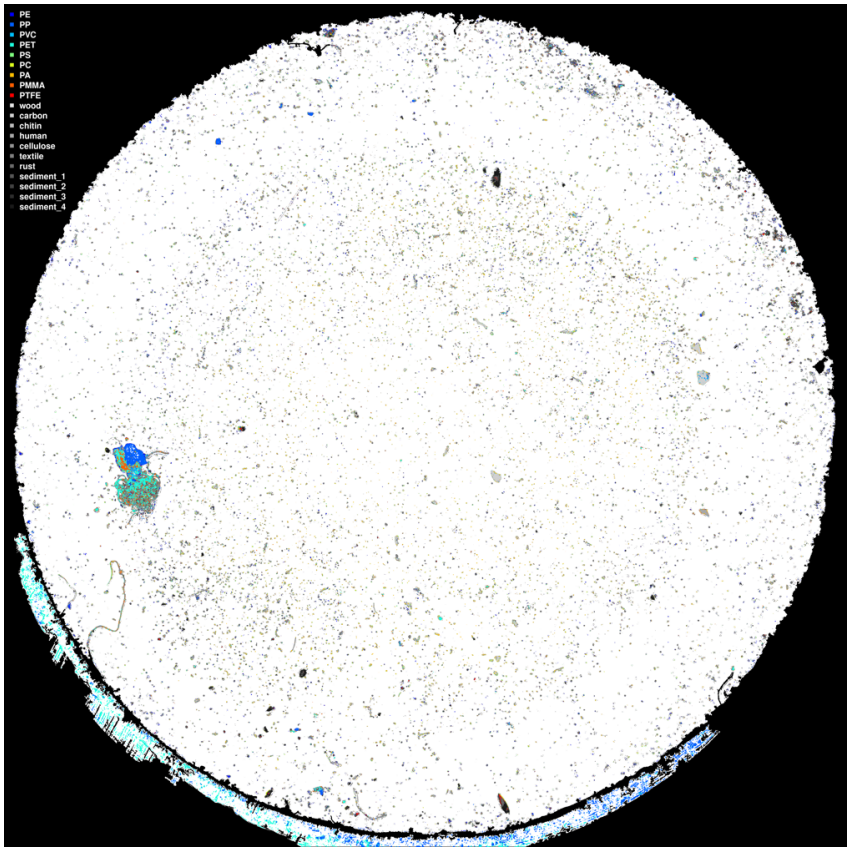

Figure 76B - Spectra map of sample 11B, analysis filter 1.

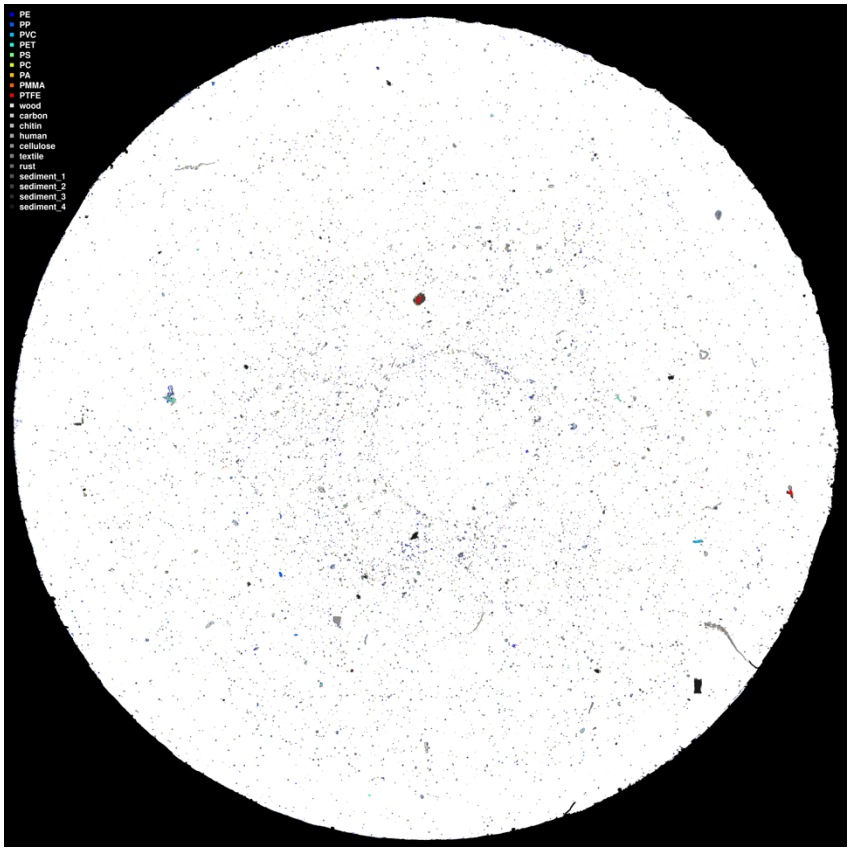

Figure 77B - Spectra map of sample 11C, analysis filter 1.

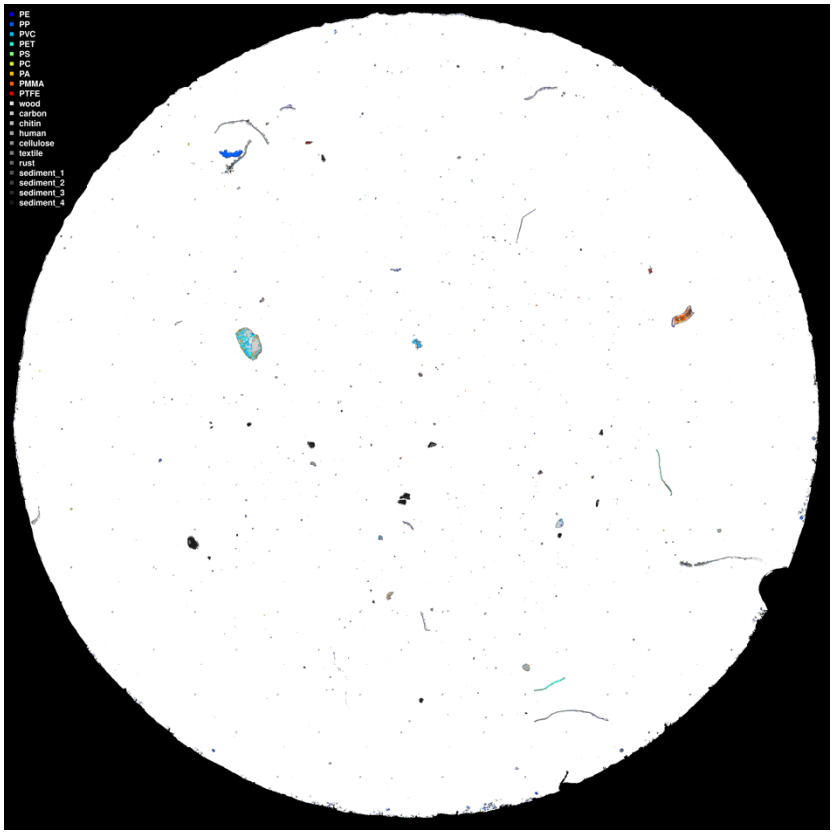

Figure 78B - Spectra map of sample 11C, analysis filter 2.

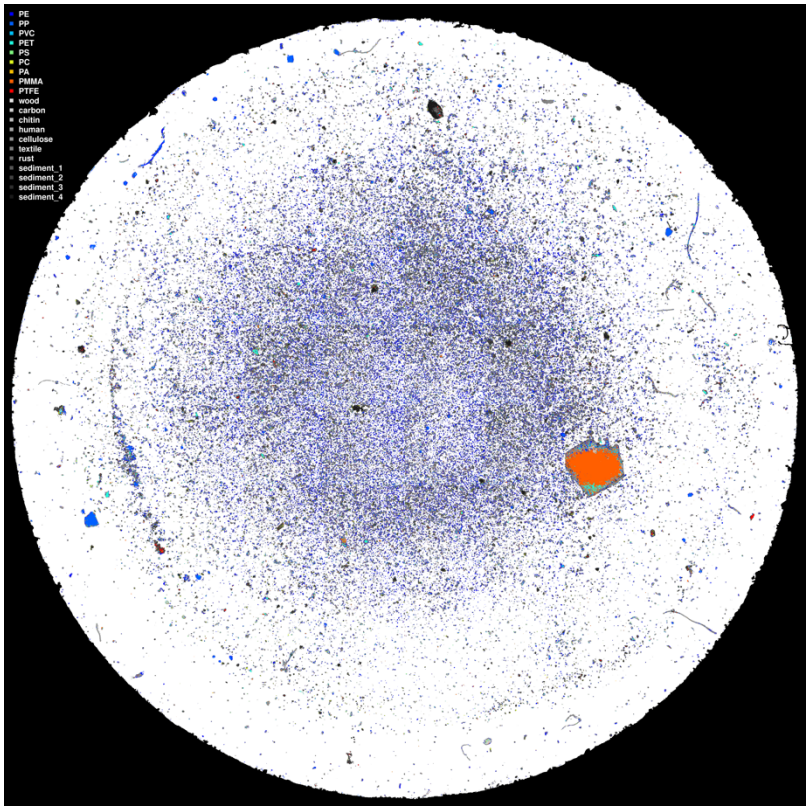

Figure 79B - Spectra map of sample 13A, analysis filter 1.

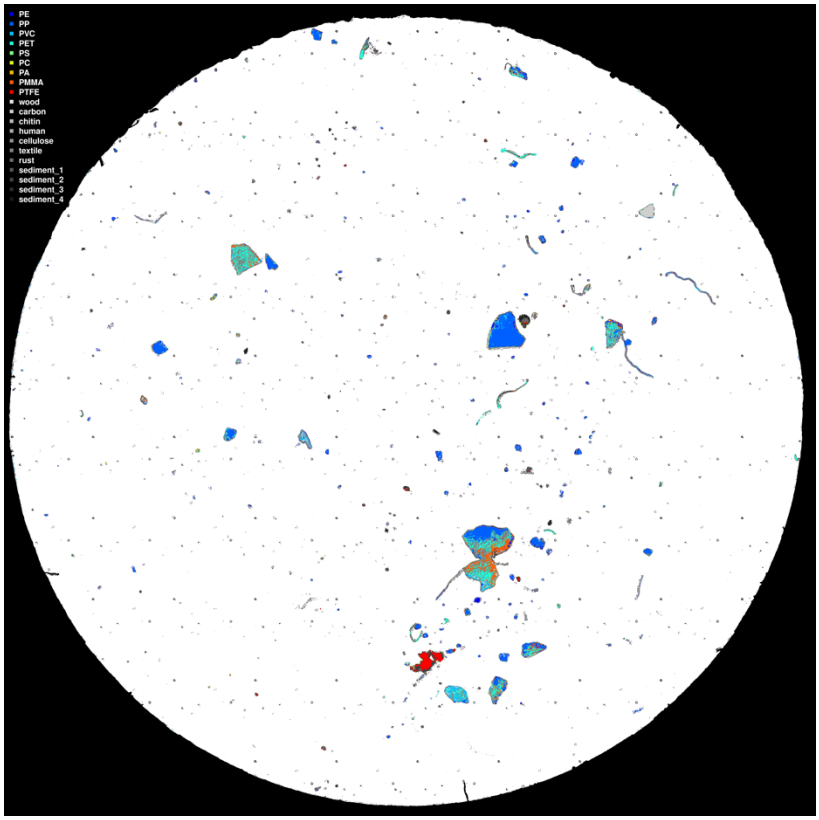

Figure 80B - Spectra map of sample 13A, analysis filter 2.

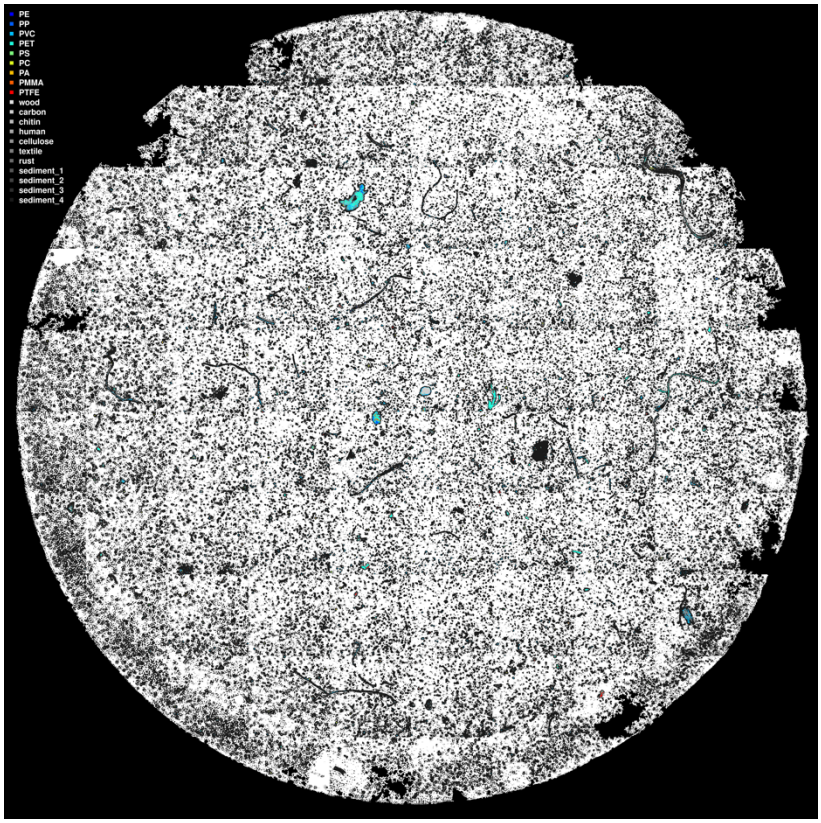

Figure 81B - Spectra map of sample 13B, analysis filter 1.

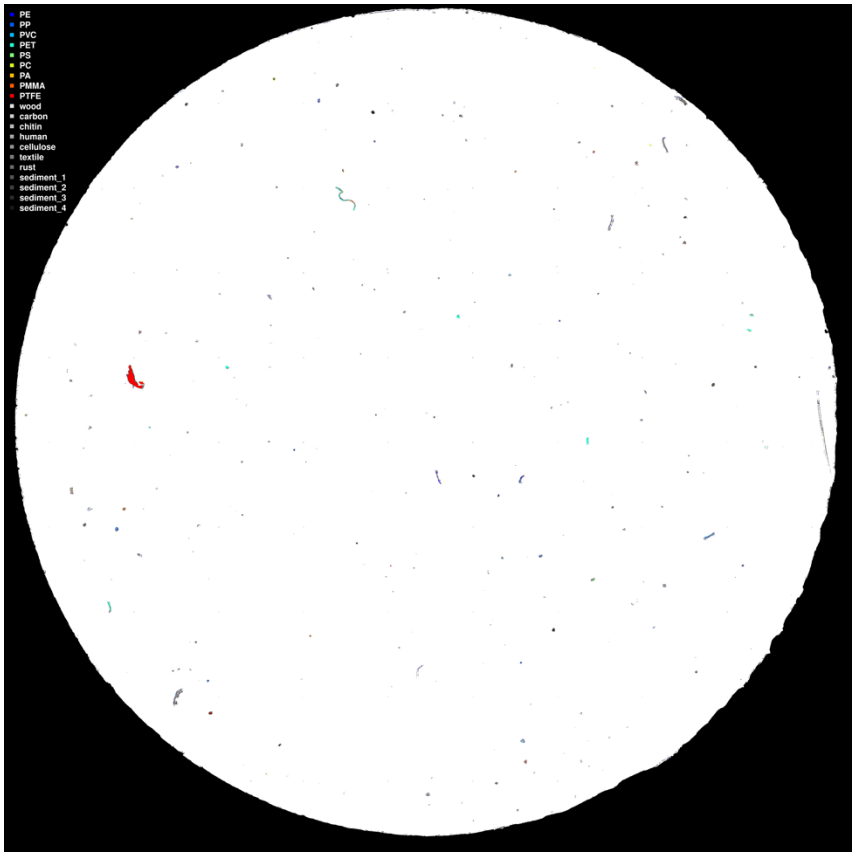

Figure 82B - Spectra map of sample 13B, analysis filter 3.

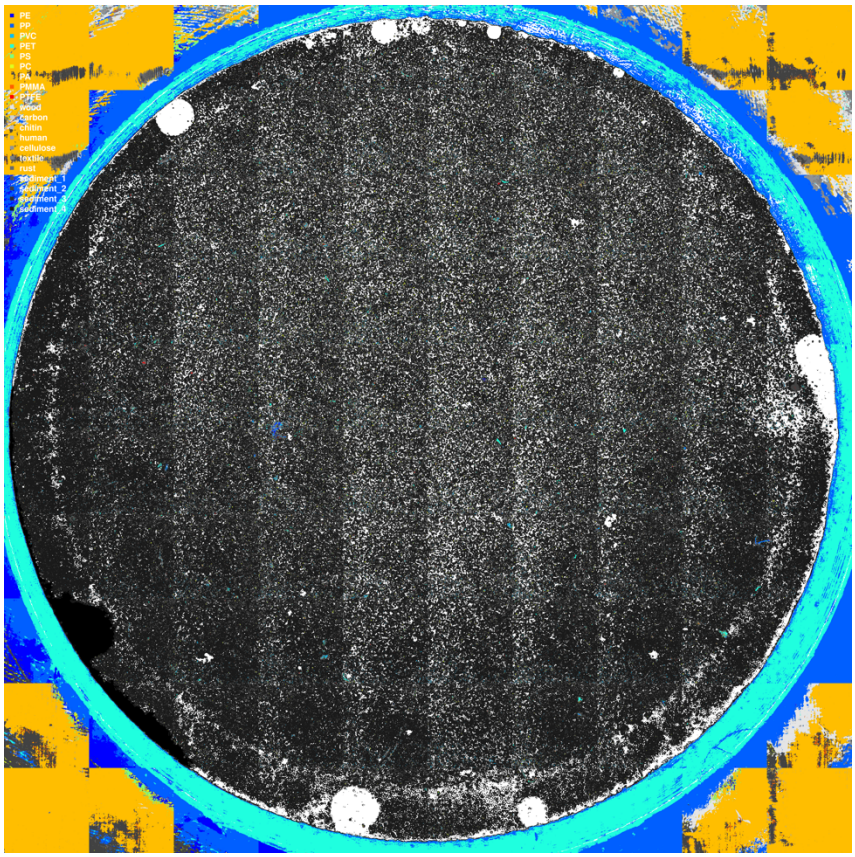

Figure 83B - Spectra map of sample 13C, analysis filter 1.

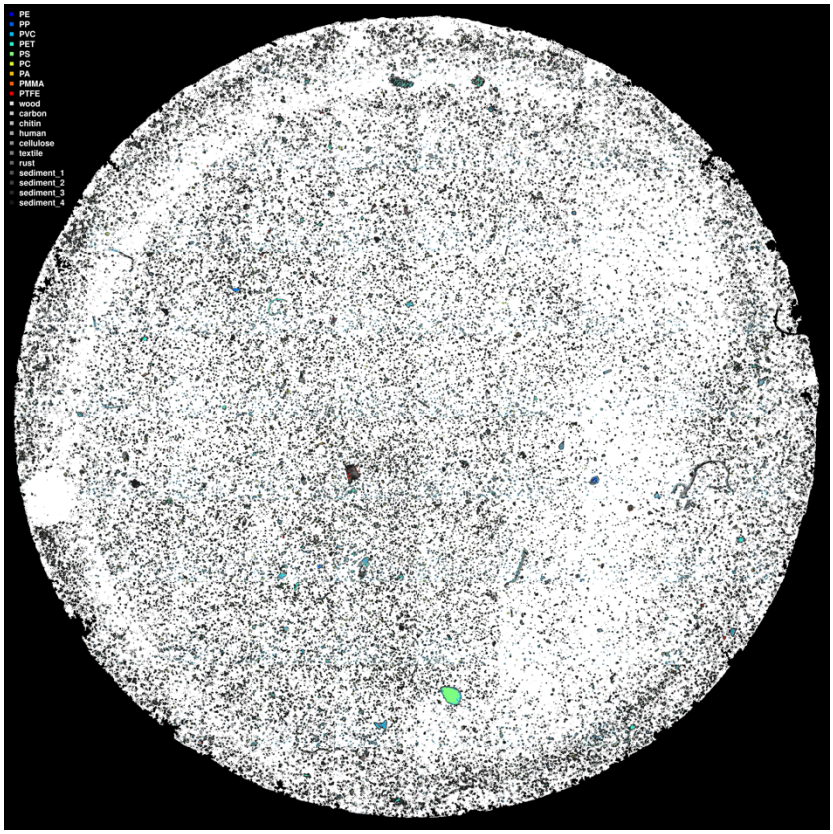

Figure 84B - Spectra map of sample 13C, analysis filter 2.

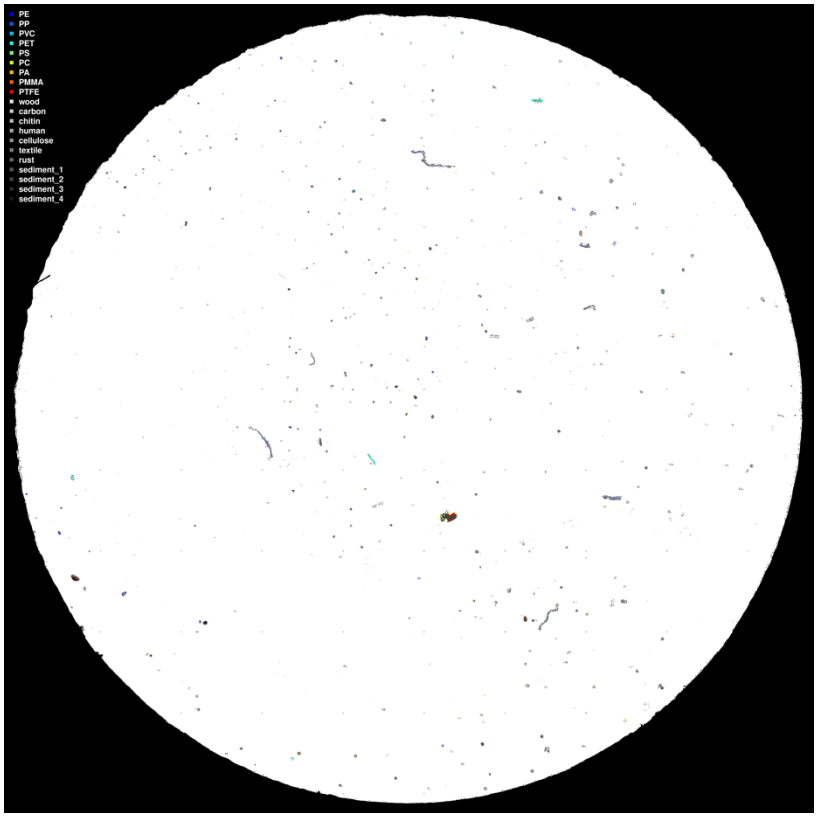

Figure 85B - Spectra map of sample 13C, analysis filter 3.